



MSU Graduate Theses

Summer 2018


Grapevine Vein Clearing Virus: Epidemiological Patterns and Construction of a Clone

Cory Von Keith

Missouri State University, Cory320@live.missouristate.edu

As with any intellectual project, the content and views expressed in this thesis may be considered objectionable by some readers. However, this student-scholar's work has been judged to have academic value by the student's thesis committee members trained in the discipline. The content and views expressed in this thesis are those of the student-scholar and are not endorsed by Missouri State University, its Graduate College, or its employees.

Follow this and additional works at: <https://bearworks.missouristate.edu/theses>

 Part of the [Cellular and Molecular Physiology Commons](#), [Molecular Genetics Commons](#), [Plant Pathology Commons](#), [Population Biology Commons](#), [Virology Commons](#), and the [Viticulture and Oenology Commons](#)

Recommended Citation

Keith, Cory Von, "Grapevine Vein Clearing Virus: Epidemiological Patterns and Construction of a Clone" (2018). *MSU Graduate Theses*. 3300.

<https://bearworks.missouristate.edu/theses/3300>

This article or document was made available through BearWorks, the institutional repository of Missouri State University. The work contained in it may be protected by copyright and require permission of the copyright holder for reuse or redistribution.

For more information, please contact bearworks@missouristate.edu.

**GRAPEVINE VEIN CLEARING VIRUS: EPIDEMIOLOGICAL
PATTERNS AND CONSTRUCTION OF A CLONE**

A Master's Thesis

Presented to

The Graduate College of

Missouri State University

In Partial Fulfillment

Of the Requirements for the Degree

Master of Science, Plant Science

By

Cory Von Keith

August 2018

Copyright 2018 by Cory Von Keith

GRAPEVINE VEIN CLEARING VIRUS: EPIDEMIOLOGICAL PATTERNS AND CONSTRUCTION OF A CLONE

College of Agriculture

Missouri State University, August 2018

Master of Science

Cory Von Keith

ABSTRACT

Grapevine vein clearing virus (GVCV) is a recently discovered virus belonging to the *Badnavirus* genus. Characteristic to its name, the virus is associated with a disease where symptoms manifest as pronounced vein-clearing, resulting in severe berry deformation and vine decline in susceptible grape varieties. Sustainable production of wine is dependent on healthy plants. The associated disease is mainly found in Midwest vineyards. Attempts were made in this thesis to provide evidence of causality of the virus to the associated disease and to infer the historical path and migration pattern of GVCV. Conclusions and discussions will provide grape producers with the latest information in designing management strategies to prevent the disease. The results support that GVCV is likely a native endemic virus, which has recently cultivated grapevines. This evidence is crucial in establishing quarantine protocols to prevent the spread of GVCV into new territories and to avoid pandemic in grape-growing regions worldwide.

KEYWORDS: Grapevine vein clearing virus, epidemiology, phylogeography, endemic, infectious clone, Koch's postulates, emergent, virus

This abstract is approved as to form and content

Dr. Wenping Qiu
Chairperson, Advisory Committee
Missouri State University

**GRAPEVINE VEIN CLEARING VIRUS: EPIDEMIOLOGICAL PATTERNS
AND CONSTRUCTION OF A CLONE**

By

Cory Von Keith

A Master's Thesis
Submitted to the Graduate College
Of Missouri State University
In Partial Fulfillment of the Requirements
For the Degree of Master of Science, Plant Science

August 2018

Approved:

Dr. Wenping Qiu

Dr. William McClain

Dr. John Heywood

Dr. Julie Masterson: Dean, Graduate College

In the interest of academic freedom and the principle of free speech, approval of this thesis indicates the format is acceptable and meets the academic criteria for the discipline as determined by the faculty that constitute the thesis committee. The content and views expressed in this thesis are those of the student-scholar and are not endorsed by Missouri State University, its Graduate College, or its employees.

ACKNOWLEDGEMENTS

First, and foremost, I would like to thank my family. I have put them through a significant amount of hell in their life, but they never gave up. They always pushed me to be better, and would not allow me to live beneath my potential. I love all of you.

I am incredibly thankful for the opportunity that the Darr College of Agriculture has provided me. Dr. Qiu, especially took a risk on a student who did not have the best undergraduate records and provided me with an opportunity to make up for past mistakes. His patience and wisdom will not be forgotten, and he has been a powerful role model in helping me to refine my academic pursuits.

Su Li and Sylvia, you have both been like sisters to me and I will cherish all the memories that we have made. Sylvia, I'm sure that you are expecting me to write some emotional nonsense about how we are the same person and I am glad that we found each other in life, but I won't do it.

I owe a significant amount of debt to undergraduate researchers that I tricked into helping me complete DNA extractions. You are not forgotten.

Rory, you have taught me that you can forget anything with enough liquid degeneracy.

I dedicate this thesis to Paul "Muad'Dib" Atreides.

TABLE OF CONTENTS

Literature Review.....	1
Wine industry.....	1
Epidemiology.....	4
Plant immunity.....	7
Viral taxonomy and classification	10
Viral lifecycle and cellular remodeling.....	13
Evolution of viruses	15
Endemic, emergence, epidemic, and pandemic	19
Badnaviruses	22
Grapevine vein clearing virus	24
Rationale	28
Chapter 1: Epidemiological patterns of GVCV	30
Introduction.....	30
Materials and Methods.....	36
Synopsis	36
Collection of samples.....	38
DNA extraction and PCR detection of GVCV	38
ORF II amplification and Sanger sequencing.....	39
Sequence alignment and recombination detection.....	39
Neighbor joining tree and molecular clock estimation	40
Test of selection	40
Test of suitability of ORF II as a candidate for phylogenetic reconstruction	40
BEAUti and the BEAST	41
SPREAD	42
Results	42
Viral detection and clock rate estimation.....	42
Test of selection	43
Test of phylogeny	43
Phylogeographic analysis.....	43
Discussion	44
Sampling and incidence suggest endemic nature.....	44
Implications of the 9bp-Indel.....	45
Molecular clock	46
Purifying selection	47
Maximum Likelihood phylogenetic analysis.....	47
Phylogenetic problems.....	48
Genetic diversity, host diversity, geographic diversity.....	50
Summary	50
Chapter 2: Construction of a Grapevine vein clearing virus clone.....	53
Introduction.....	53

Materials and Methods.....	55
Synopsis	55
Design	55
Construction.....	56
Transfer to binary vector and <i>Agrobacterium</i> transformation	59
Transfection of <i>Nicotiana benthamiana</i>	60
Sequencing of pGWB/GVCV	61
Results	61
Summary	61
Construction.....	61
Transfer to binary vector and <i>Agrobacterium</i> transformation	62
Sequencing.....	63
Second attempt.....	63
Discussion	63
References.....	65
Appendices	113
Appendix A. 2016 and 2017 Positive Samples and Locations	113
Appendix B. Codon Test of Positive Selection	116

LIST OF TABLES

Table 1. Number of samples collected over the previous years.	80
Table 2. Primer list.....	80
Table 3. Molecular clock rates of sequences and R ² values.....	80
Table 4. Restriction enzyme list used in construction of clone.....	81
Table 5. Table of plasmids and restriction enzymes used in the first step of clone construction.....	81

LIST OF FIGURES

Figure 1. Native range of <i>Vitis rupestris</i>	82
Figure 2. Native range of <i>Vitis riparia</i>	83
Figure 3. Native range of <i>Ampelopsis cordata</i>	84
Figure 4. Native range of <i>Vitis cinerea</i>	85
Figure 5. Native range of <i>Vitis vulpina</i>	86
Figure 6. Native range of <i>Vitis</i> Spp.....	87
Figure 7: Example of triplex PCR diagnostic to test for <i>Grapevine vein clearing virus</i>	88
Figure 8: Locations of <i>Grapevine vein clearing virus</i> -infected samples in from 2016 and 2017.....	89
Figure 9: Neighbor-joining tree of GVCV ORF II sequences.	90
Figure 10: Neighbor-joining tree of <i>Grapevine vein clearing virus</i> genomes.....	91
Figure 11: Neighbor-joining tree of <i>Badnavirus</i> genomes, that is used for estimation of molecular clock.....	92
Figure 12: Linear regression of evolutionary distance and time of GVCV based on ORF II sequences.....	93
Figure 13: Linear regression of evolutionary distance and time of <i>Grapevine vein clearing virus</i> based on the genome sequences..	94
Figure 14: Linear regression of evolutionary distance and time of <i>Badnaviruses</i> based on the genome sequences.....	95
Figure 15: Maximum Likelihood tree of GVCV based on ORF II sequences that collapsed to a 70% bootstrap cutoff value..	96
Figure 16: Screenshot from Tracer of ESS values and 95% HPD interval.	97
Figure 17: Screenshot from Tracer showing ESS values for the GTR gamma distribution for rates at each codon position are highlighted.	98

Figure 18: Divergence time and relative effective population size of <i>Grapevine vein clearing virus</i> estimated using ORF II sequence data.....	99
Figure 19: Maximum clade credibility tree of GVCV isolates, based on ORF II sequences, evolution through time.....	100
Figure 20: Maximum clade credibility tree of GVCV isolates, based on ORF II sequences, evolution through time.....	101
Figure 21: Maximum clade credibility tree of GVCV isolates, based on ORF II sequences, evolution through time.....	102
Figure 22: Maximum clade credibility tree of GVCV isolates, based on ORF II sequences, evolution through time.....	103
Figure 23: Genome arrangement of GVCV-CHA reference.	104
Figure 24: GVCV genome with overlapping PCR fragments.	105
Figure 25: Restriction enzyme digested fragments from PCR products.....	106
Figure 26: Fragments from Figure 3 ligated in correct orientation.....	106
Figure 27: pCR8/GVCV.	107
Figure 28: pGWB/GVCV.	108
Figure 29: Ligation of fragments “RsrII-SalI” and “SalI-AvrII” to make fragment “RsrII-AvrII” consisting of 7,286 bps.....	109
Figure 30: Ligation of “1.4 genome” into pGWB 401 to make pGWB/GVCV.....	110
Figure 31: Restriction digest of pCR8/1179 and pCR8/4804.....	111
Figure 32: Gel image of multiple pCR8/GVCV plasmids to check for contamination...112	

LITERATURE REVIEW

Wine industry

Wine has had a profound impact on the cultural development of the world. Evidence from archaeological findings suggest civilizations began producing wine at least 8,000 years ago (1, 2). “As a medicine, social lubricant, mind-altering substance, and highly valued commodity, wine became the focus of religious cults, pharmacopoeias, cuisines, economies, and society in the ancient Near East” (3). It is difficult to determine the influence wine has had on society, but it has left an impact that reverberates through many western cultures exemplified by the incorporation of wine into religious rituals such as the cults of Dionysus of ancient Greece and the eucharist of the Christian tradition. Today *Vitis vinifera*, or grapevine, is still a globally important crop. The fruit of the plant is consumed in the form of fresh fruit, dried fruit, juice, and wine. In 2016, the total global production of grapes was 75.8 million tons, of which over 47% was used to make wine. Wine alone had a global economic import value of \$32.85 billion and an export value of \$34.02 billion. The United States exports \$1.64 billion worth of wine while importing \$5.87 billion and consumes the most per capita of any other nation(4). The economic and cultural significance of wine will likely continue into the future due to the increase in global wine consumption.

Historically, Missouri has played an important role in the global wine and grape industry. In 2011 the total economic value of grapes grown in Missouri totaled \$2.88 billion (5). Wine contributes a large share to the economic value of Missouri-grown

grapes, with \$1.76 billion coming from the wine industry (6). While Missouri does not currently produce as much wine as many other states, the historical impact Missouri has had on the wine industry is significant. Before prohibition, Missouri commanded the largest market share of wine produced in the United States. Stone Hill Winery in Herman, MO, was the third largest winery in the world, producing world-renowned wines. While the economic impact of grapes and wine were and are significant, the contribution of Missouri to this industry goes beyond production. During the Great French Wine Blight, which destroyed over 40% of France's vines, Missouri's state entomologist, Charles Valentine Riley, proposed European *vinifera* varieties be grafted onto American varieties' rootstock (7). The American varieties were resistant to Grape Phylloxera, an insect which feeds on the roots and leaves of grapevines and causes serious economic damage. Missouri institutions continue to provide global support to the development of grapes, developing cultivars that are economically practical for a variety of reasons. Missouri State University is one of five national universities that are part of the National Clean Plant Network of Grapes. Alongside Cornell University, University of California-Davis, Washington State University, and Florida A&M, Missouri State University provides producers with certified disease free grape plants that can be used in vineyards (8).

Protecting the sustainability of the grape and wine industry is one goal of research institutions that focus on understanding horticulturally relevant traits in *Vitis spp.* Cold hardiness, root and branch architecture, and disease resistance are some of the primary traits under investigation to enhance the efficiency of vineyards. Grapevines are a perennial species that can live over 100 years, so understanding the genetic mechanisms

of these traits is necessary to help develop breeding programs that increase the efficiency of vineyards and reduce the amount of input costs required to return a profit. Disease resistance is communicated by vineyard owners to be of great importance as disease can have serious implications on the production of grapes and on the quality of wines. Disease causing organisms are divided into fungal pathogens, bacterial pathogens, and viral pathogens. Diseases resulting from fungal and bacterial pathogens are responsible for most loss of yield in grapevines annually, but these diseases can be treated with chemical inhibitors. Viral symptoms may be slow onset, but as there are no cures for viruses in plants the economic impacts can be quite severe to vineyards that may become infected with a virus.

Currently there are 64 known grapevine viruses that can infect *Vitis spp.* (9). Since virus-infected plants cannot be treated they are typically removed from a vineyard; prevention of viral spread into vineyards is the primary management strategy. Growers are advised to plant both resistant varieties and varieties that have been tested to be free of viral pathogens. These testing services can be provided by the National Clean Plant Network; positive economic impacts have been predicted to be \$50 million annually in the North Coast region of California (10) and could be in excess of \$16,014 per acre over a 25 year period in the Finger Lake region of New York (11). Viruses that escape detection in a vineyard become a reservoir of viral particles that can then infect other vines in a vineyard. The proximity of vines to one another can quickly cause an epidemic in a region where the only treatment is removal of infected individuals at a substantial economic cost.

Emerging viruses pose a unique threat to the sustainability of perennial crops. The long-lived nature of perennial plants allows for the potential accumulation of many viruses. Plants native to regions have natural immunities to endemic pathogens due to the historical co-evolution between the two organisms, but may still host these organisms. These endemic viral repositories act as a source of viral particles to infect agriculturally relevant crops that lack the resistance conferred by shared evolutionary history (12, 13). Emergent viruses are usually endemic to areas that escape detection until they jump into agriculturally important crops that the virus can use as an alternative host. Grapevine Vein Clearing Virus (GVCV) is an emergent virus that was first discovered in a vineyard of Missouri. The native Vitaceae vines act as a source of viral infection to the introduced *Vitis vinifera* vines which presumably lack a natural immunity.

Epidemiology

The disease triangle is an often-described model for the determinants of disease. There are three points to the triangle: the right host, the right pathogen, and the right environment. When all three conditions are met, a disease will flourish (14). Epidemiologists study a variety of methods using these three points. Methods can include disease causality, disease monitoring, disease transmission, and disease outbreak determinants. The primary goal of the epidemiologist is to study the spatial and temporal aspects of a disease moving through a population (15). These goals are shared by those who study plant epidemics (16). The eradication of disease is not a goal easily obtained when applied to plants. For humans, antibiotics, anti-fungals, and vaccines have led to a world where the leading cause of death in developed countries is heart disease. Viral

pathogens, such as small pox, have all but been eradicated from human populations through the use of vaccines and the concept of herd immunity. Plant diseases pose drastically different scenarios with the diversity of plant life that humans are reliant on for civilization. From the basics of food, to more abstract concepts of ecological carrying capacity, human civilization is dependent upon plants. Viral diseases in plants have no vaccines and there are not broad range antibiotics for plants, so tracking of disease and finding ways to limit spread are of major concern to agricultural producers. Once a plant contracts a virus, it has the virus until the death of the plant.

Plant epidemiology takes many of the tools used by those human disease researchers and applies them to plants. J. E. Vanderplanck is credited as a huge influence on the application of epidemiology towards plant diseases and outlined the foundations of the subject in his work, *Plant Diseases: Epidemics and Control*. Main concepts in his book include mathematical models of how outbreaks increase with time, how a rate of infection can be determined, definition and determination of a disease latency period, and how to properly control for disease (17).

The physiology is drastically different between plants and mammals, but the diseases are often similar bacteria, fungi, and viruses all attack both plants and mammals. The severity of diseases of plants are often a human concern. Agricultural commodities are often described in monetary value, but historically diseases can have a much higher value. *Phytophthora infestans* is the causative fungi of late potato blight. This disease caused the Irish Potato Famine and led to the starvation of over a million people. *Cryphonectria parasitica*, the causative agent of chestnut blight, ravaged the northeastern landscape of the United States by nearly driving the American Chestnut to extinction.

The disease saw over 8.8 million acres of canopy trees disappear in less than 50 years after the disease's emergence (18). The disease had a huge impact on not only local economies, but on the ecological community of a wide range of Appalachia. The loss of the American Chestnut led to the extinction of at least seven species of moth (19). Viral diseases have a range of symptoms and severity. While some viral pathogens slightly decrease yields, others can lead to total crop loss (20). *Cassava mosaic virus* is a *Begomovirus* that infects the cassava plant and is transmitted by whiteflies. Cassava is an important staple crop in the developing world and the disease has led to famine (21). The disease was relatively harmless until recently, when two of the dominant strains infected a single plant and recombined their genomes to produce a hyper virulent strain (21). The quick mutation rate of viruses and their ability to recombine, alter host genomes, transfer genes horizontally, and lack of treatment provide epidemiologists with a significant hurdle to overcome.

Bacteria and fungi were relatively well understood in their role of plant disease before viruses were discovered. Bacterial and fungal molds can be seen with the naked eye and their complex structures can be observed with an optical lens. The idea of infectious agents being responsible for disease has been around since at least 1546, but it did not take off until the late 1800's with pioneers like Robert Koch and Louis Pasteur taking the lead. Viruses escaped detection because of their small size; only the largest of the viruses can be detected with an optical lens, and then usually only when they are grouped together. It wasn't until it was shown that the tobacco mosaic disease could be transmitted after bacteria were filtered out, that the idea of the existence of smaller infectious agents was proposed. Soon after, the discovery of the electron microscope in

1931 led to the imaging of the first viral particles and the burgeoning field of virology took off. Virology was furthered with the boom of molecular biology in the 1980's.

Plant immunity

Pathogenic organisms are ubiquitous. The majority of life on the planet is in the form of viral, bacterial, and fungal organisms, most of which are microscopic. The close ecological history of these organisms with their host species has led to the evolution of defense mechanisms by plants (13, 22). While plants lack an adaptive immune system such as ours, their immune systems are innate and coded within their genetic makeup. The most widely accepted model is a system of plant immunity that has two basic levels. The first level is called pathogen associated molecular pattern (PAMP) triggered immunity (PTI). The second level of defense is termed effector triggered immunity (ETI). The zig zag imagery is used to explain the struggle between plants and their pathogenic organisms as they fight for survival. As PTI is overcome by pathogen effectors, the plant's second line of defense, ETI, kicks in until the pathogen overcomes the new immune response or is able to escape detection (22).

Pattern recognition receptors (PRRs) on the extracellular surface of plant walls recognize PAMPs structures or motifs. These structures are non-specific to pathogen species, but act as a basal defense against recognized pathogens. Common PAMPs include structures such as bacterial flagella and fungal haustoria. On recognition of PAMPs, PRRs send a signal cascade to express genes that confer broad range resistance to most invading pathogens. However, certain pathogens can overcome PTI, by using pathogen encoded components. Effectors are pathogen components that can provide

escape from PTI in a number of functional ways, but most contribute to the suppression of one or more components of PTI, named type III effectors. Type III effectors are gene products which allow the pathogen to overcome PTI and establish an infection (23).

Plants that share a common evolutionary history with pathogens that can overcome PTI have adapted a means of detecting effectors. Plants encode resistance genes (R-genes) which are able to recognize pathogen effectors, many of which encode nucleotide-binding leucine rich repeat (NB-LRR) proteins (22–24). Recognized effectors are called avirulence (Avr) proteins, and once detected send a signal cascade like that of PTI. The NB-LRR proteins can also indirectly recognize effectors by recognizing a change in the host protein that effectors target: ‘pathogen-induced modified self’ molecular pattern. This new response, ETI, often leads to cell death of the infected cell(s) by providing a hypersensitivity response (HR). ETI also induces production of signaling hormones, such as salicylic acid (SA) and jasmonic acid (JA), to signal neighbor cells of invasion to provide a systemic acquired resistance (SAR). This signaling also affects gene expression through transcription factors of the WRKY and TGA families to confer a more aggressive resistance to the invading foreign pathogen (22–24). Small RNA (sRNA) have been shown to also act as signaling molecules to control transcription in distant parts of the plant (25, 26). Continual selection pressure placed on pathogenic organisms by ETI eventually leads to the evolution of pathogens who are able to escape detection by ETI, or produce yet another set of effectors to limit the ETI response. The proximity of the pathogens and hosts in an area over time give rise to these complex co-evolutionary forces in a struggle for survival.

The PTI/ETI model of plant defense is not easily applied to viral pathogens. Few viral proteins or structures have been identified as PAMPs, instead plant immunity to viruses uses a different pathway. Plant RNA silencing pathways use small interfering RNA (siRNA) and micro RNA (miRNA) to confer resistance to viral pathogens. The siRNA pathway is triggered upon viral infection of a cell, and has been equated to PTI (27, 28). Most viruses in some stage of their lifecycle have a dsRNA component, and are recognized by the host cell machinery. This recognition of viral dsRNA is why the plant response it is equated to PTI. The dsRNA is recognized and cleaved by a host ribonuclease, Dicer (27, 28). Dicer like proteins (DCL) cut the RNA into siRNA consisting of between 20-25 nucleotides, and these siRNA are subsequently used to target other viral molecules by complementation with loading proteins called ARGONAUTES (AGOs). The AGO, siRNA, and DICER form a complex called the RNA induced silencing complex (RISC). RISC recognizes any template for which the siRNA binds to with perfect matching of base pairs, and results in cleavage into more siRNAs creating a feedback loop (27–30). siRNA can also be used in a transcriptional gene silencing pathway, the RNA induced transcriptional silencing (RITS). RITS loads siRNA onto complementary RNAs, but instead of cleavage, it methylates DNA and prevents transcription (31). While siRNA mediated RISC is a response to invading nucleic acids and the template for RISC is exogenous, miRNA are endogenous to the host and encoded in the genome. Similar in size, ~22 nt, miRNA have a different mechanism of silencing. miRNA can bind with incomplete complementarity and once bound, can either cleave the RNA, or prevent translation (31–33). miRNAs have a functional role outside of viral

suppression and immunity; they are complex transcriptional and translational control agents and can drastically alter the expression of genes within a cell (34, 35).

As bacteria and fungi have adapted effectors, viruses have adapted ways to mitigate the RISC. Viral silencing suppressors (VSRs) have adopted a variety of mechanisms to escape cleavage by DICER. Identified VSR's are numerous, with functions ranging from binding AGO proteins, sequestering siRNA, blocking DICER proteins, preventing methylation of DNA, or using RNA decoys to prevent maturation of siRNA (31). As efficient cellular parasites, viruses hijack cellular machinery to undergo their life cycle; they have demonstrated the production of their own miRNAs to alter host gene expression (32) and have demonstrated the hijacking of host miRNA to alter viral gene expression and replicative efficiency in a beneficial way (33).

Viral taxonomy and classification

Viruses are small organisms that are obligate parasites. They require a host cell to undergo replication and do not metabolize energy on their own and therefore contain genetic elements to remodel a host cell and genome (36). An individual viral unit is called a virion, and the structures of all virions have similarities. They all contain a capsid of a crystalline protein that encapsidates the genome and other necessary proteins and can conform into a variety of different shapes. Viruses can either be surrounded by a lipid membrane (enveloped) or can have a naked capsid shell (naked). The genome can either be RNA or DNA. Viral genomes range from 1000 bps to over 2,000,000 bps (37), so viruses employ a diverse range of efficient strategies to contain the necessary elements for host cell remodeling, genome replication, and virion assembly. Strategies include

polycistronic genes, genes in overlapping reading frames, ribosomal shunting and leaky scanning, and RNA modification. These strategies help ensure that the virus has all the necessary elements to infect and reprogram the host cell.

While viruses are undeniably similar, viral lineages are difficult to establish and their place on the evolutionary tree of life is debated (38). There are many hypotheses on the origin of viruses, resulting in an unclear understanding of where they belong on the tree of life (37, 38). Three dominant hypotheses persist: the virus-first hypothesis, the reduction hypothesis, and the escape hypothesis. As the name suggests, the virus first hypothesis proposes that viruses appeared before cells and the organism that became the Last Universal Common Ancestor (LUCA) (38, 39). The reduction hypothesis posits that early viruses were proto cells which were parasites of larger cells (38, 39), while the escape hypothesis states that viruses evolved from DNA or RNA that came from the genome of an organism (38, 39). All three hypotheses have problems that have not been resolved. Considering viruses are obligate parasites that need a plant cell to survive, the Virus-first hypothesis has doubters. If viruses were proto-cells, some scientists believe that we would find evidence of similar cells today and no such example exists. Viruses have capsids and other structures that are not found in any other domain of life, and the escape hypothesis cannot explain why these do not exist in any form in the three domains.

Historically, viruses have been classified by way of Baltimore classification. The Baltimore system groups viruses based on the arrangement of their genomes. There are seven groups: group I are dsDNA viruses, II include ssDNA viruses, III are dsRNA viruses, IV are (+)ssRNA viruses, V are (-)ssRNA viruses, VI contain ssRNA-RT

viruses, and group seven are the dsRNA-RT viruses. Recently, the International Committee on Taxonomy of Viruses (ICTV) has made an attempt to use the accumulation of molecular sequence data to group viruses into phylogenetically related families (40). Difficulty in resolving all of the relationships arises from the differing mutation rates of viruses from the same lineage (41, 42), the high rate of recombination (43, 44), genome reorganization and shuffling (45–47), and large, highly genetically variable population sizes (48–50). These problems in resolving phylogenomic relatedness of viral species have led to the use of protein folding analysis to place the viruses on the tree of life. This analysis is uniquely equipped to relate species of all domains of life, as it uses the similarities in the folding structures of proteins without needing amino acid or nucleic acid similarity. It posits that these proteins with similar folding structures are grouped into fold families (FF) and that these families can be placed into fold super families (FSF) (51). Grouping the genes of viruses into families and comparing them with other domains of life (archaea, prokaryote, eukaryote) has led to the discovery of common homology of some of these proteins and suggests viruses be placed on the tree of life into a fourth domain (51). This analysis has led researchers to view viruses as entities that branched off from the other three domains before ancient cells developed the machinery for metabolism (ribosomes) and became parasites of the other domains of life. This reasoning furthers that viruses branched off before the three domains of life because of their ubiquity in infecting all domains of life (38, 51).

Three further delineations exist in viruses from the traditional taxonomic nomenclature. Strain further separates viruses into a category segregating recognizably different phenotypic characteristics that remain stable in the population (52). A viral

variant is a virus of the same strain that has similar genetic sequences but no observed phenotypic variation (52, 53), and it has been proposed that a sequence that is $\leq 10\%$ divergent be considered a new variant (54). At the base level, isolate is used to describe any particular viral genome that has been isolated from a host (54).

Viral lifecycle and cellular remodeling

Viruses lack the ability to penetrate the cell wall of a plant on their own and need a way of entering a plant cell. This can be biotic or abiotic. Biotic vectors include insects, bacteria, fungi, and nematodes. Abiotic vectors include human cultural practices such as graft transmission and unsterile equipment for maintenance. All viruses, plant or other, behave similarly once inside the cell, but the mode of transmission can differ greatly.

Once inside the cell, the virus un-coats from its protein capsid. Some viruses are packaged with proteins that help in the beginning stages of viral infection, such as nuclear import of viral genomes (55). Once the viral nucleic acid is free of the protein coat, import into the host nucleus is achieved by a variety of strategies (56, 57), or the genome is localized to an area to begin its lifecycle. Inside the nucleus, the genome is processed by host machinery in the case of some RNA viruses (58), or begins its replicative and transcriptional lifecycle (59).

Viral proteins are transcribed by host ribosomes and the immediate remodeling of the cell begins to favor the assembly and maturation of virions. Systemic remodeling is achieved by mechanisms including viral and host protein interactions for formation of inclusion bodies (36, 60–62), expressional control of viral encoded miRNA (32), and hijacking of host miRNA for expressional control (33). Many of the remodeling

processes target host cell membranes and organelles to form miniature “virus factories” (36, 61, 62). Altered host organelles include golgi apparatus, mitochondria, endoplasmic reticulum, and chloroplasts (36). It is believed that these inclusion bodies or cellular localizations are strategies to bring the components of viral replication, assembly, and maturation into proximity. It is also believed that the localization and compartmentalization are a way to escape the host cell’s innate defenses (36).

Movement from cell to cell does not require an insect vector. Many viruses encode movement proteins (MP) that allow for efficient movement into adjacent cells to eventually establish a systemic infection. Most MP’s form complexes with plant plasmodesmata to widen the channel to allow for viral passage (63, 64). While some viruses pass as individual virions, others pass as “mobile viral factories”, transporting remodeled organelles with many virions to the next cell (62, 65).

Transport to other plants requires a vector; the majority of plant viruses are vectored by insects, including aphids and whiteflies which represent the transmission of the highest percentage (66). Many of these insect-vectored viruses have structural motifs which allow for efficient transmission by the associated vector, usually part of the viral coat protein (CP) (66). Insects can acquire and transmit viruses in four methods, circulative-persistent, circulative-propagative, non-circulative semi-persistent, and non-persistent (66). Insects vary in their uptake of viral particles based on the method of acquisition. Once transmitted to a new plant, the virus goes through the same cycle as above. This is how viruses spread through a region and establish epidemics.

Evolution of viruses

Viruses exist as quasispecies in their obligate host. Quasispecies are closely related viral genomes that oscillate around a consensus genome and continually undergo processes involved with genetic variation, competition between generated variants, and selection for the most fit variants in the host environment (67, 68). The quick molecular evolution rate of viral genomes and the short generation cycle lead to diverse populations where individuals compete to establish themselves in their host (69). Mechanisms of viral evolution that lead to high genetic variability include two main types: mutation and recombination (48, 49). Other processes include acquisition of host genetic elements (70) and re-assortment of genomes (48, 49). These processes give rise to a highly heterogenous population of viruses both within the host and geographically.

Viral mutation is a result of polymerase error. Viral genomes can either be RNA or DNA, as previously detailed, and are replicated by three classes of polymerase. The three polymerases introduce errors at different rates. RNA polymerases (RNAP) lack proofreading ability and introduce errors at the highest rate. DNA polymerases (DNAP) have proofreading ability to correct introduced errors, and have the lowest mutation rate. Reverse Transcriptase (RT) replicates by using an RNA template to synthesize a DNA strand, and introduces error rates like that of RNAPs due to the lack of proofreading machinery. RNA viruses mutate on the order of 10^{-3} - 10^{-5} changes per base per replication cycle, or about one error per round of replication (48, 49, 71–73). DNA viruses mutate on the order of 10^{-8} changes per base per replication cycle, or about 0.003

errors per round of replication (49, 74). Retroviruses and pararetroviruses which replicate by RT have similar rates to RNA viruses (49, 75).

Recombination results when segments of genomes from different genomes are switched during replication, and it can occur between variants from a quasispecies, or can occur from mixed infections of viral populations from different hosts meeting in a new host plant. The number of viral genomes that infect a cell is called the multiplicity of infection (MOI) (76), and the MOI of mixed infections can lead to recombination of evolutionarily distant variants. Current estimates place the MOI of viruses as a dynamic quantity that eventually reaches equilibrium, with values ranging from 2-13 genomes per cell (76). Rates of recombination also vary, depending on the family of virus. RNA virus recombination rates have been shown to be on the order of 10^{-5} recombination events per site per generation (77). *Cauliflower mosaic virus* (CaMV) is a pararetrovirus that replicates through RT, and it has been shown to have 10^{-4} to 10^{-5} recombination events per site per generation (78). It was also noted that all parts of the genome are equally likely to undergo a recombination event (78, 79).

Changes that occur to a viral genome eventually become distributed in a population through evolutionary processes that determine genetic structure. Two main processes drive the distribution of viral variants into the population, genetic drift and selection (80, 81). Genetic drift are the stochastic changes that determine the frequency of genetic alleles in a population. Selection is the process that some virologists argue is the driving factor behind genetic structure of viral populations. Selection can be broken down into two main types: positive and negative selection. Positive selection is when a mutation gives an organism an increase in fitness and the organism has a greater chance

of reproduction, therefore the frequency of the mutation is greater in the next generation. Negative selection, or purifying selection, results when a mutation decreases the fitness of an organism and the frequency of the mutation is less in the next generation. There is much evidence that viral pathogens have a surprising amount of purifying selection driving the population structure. As viral genomes are relatively small and condensed (73), it is reasonable to assume that mutational changes could be detrimental to fitness, even lethal. Coat proteins (CP) are highly conserved regions in most viruses (48, 49, 82–84), suggesting that changes severely impact viral fitness. Other gene products are also highly conserved (48, 49), and even non-coding regions in viruses remain conserved (85, 86), further validating the efficiency in packaging of genetic elements that are only necessary for the viral lifecycle.

The non-random nature of selection allows for the environment, the host, the vector, and other viral isolates to put evolutionary pressure on new replicated variants. The host can influence viral genomes through the interaction of the innate immunity and the RISC. Viruses that adapt to evade the plant defense will obviously have a higher number of progeny in the next generations. Adaptation of VSR's will be passed on to the next generation. The host range of the virus also directs the evolutionary flow of viral populations. Mutations that allow for an increase in host range will increase the viral population into a new host population. A vector's influence on the population structure comes from selecting only variants that have the necessary motifs, or gene products for successful acquisition and transition by the vector. The vector also stochastically acquires viral particles depending on their feeding pattern, and the population spreads into new plants from the few viral particles that were acquired (87).

It is worth mentioning that even variants that have lethal mutations can survive in mixed populations within a single host. Complementation occurs in a viral population when a variant that is evolutionarily fit provides a necessary gene product to the lethal mutant in *trans*. This allows for a larger population and population diversity in the host plant (88, 89). However, the large population size within a host is not representative of the allelic frequency in subsequent generations. The population will only have a small subgroup that determines the frequency of mutations in the future generations and this small number is termed the effective population size (N_e). The N_e of viruses is often many magnitudes smaller than the actual population size. HIV is a well-studied virus, and the actual population size in a host is predicted at 10^7 - 10^8 , while the N_e is estimated to be between 10^3 - 10^5 (90–92). These small sub-populations are the main determinants of population structure in the proceeding generations.

The high mutation and recombination rate, coupled with the processes of genetic drift and selection results in the quasispecies nature of viruses within a host. The host is a microcosm of geographic regions that each shape the population of the virus within. The population of viruses within a single plant can be highly variable from branch to branch in a large perennial plant. A single inoculation of *Plum pox virus* (PPV) into a *Prunus* spp. was observed over 13 years, and it was found that the viral populations segregated into distinct populations in different branches on the plant (93). Each sub-population evolved independently as they infected new tissues and organs (93). Population variability increases at each instance of infection with different viral genomes, and the junctions of where viral populations meet are areas of recombination between variants from different populations (48, 49, 76, 78, 79, 93).

Population bottlenecks occur quite frequently as a result of the random acquisition and transmission of viral isolates, selective sweeps in a host, mutation leading to a new species becoming a host, and the introduction into a new geographic region (12, 13, 48, 49). The resulting diminishment of populations leads to ‘founder effects’ and increases the population variability within the new host or region (94–97).

Populations within regions can be highly variable because of the aforementioned processes. Examples of high diversity with no geographic segregation are numerous, especially in *Badnavirus* (98–103). Other examples of high genetic diversity between populations where populations segregate based on geographic location also exist (104, 105). Host specificity of viruses also leads to diversity and divergence. Certain viral strains may prefer one host over another which will lead to further segregation of populations. This may eventually result in speciation. Examples in the literature suggest that viral populations are highly variable, but the genetic stability of the population does not change from year to year (106, 107). In summary, the distribution of allelic frequency, or haplotypes, of viruses tend to remain stable over many years, even though the variability of genomes is high. Populations can segregate based on geographic proximity or host specificity, or be well mixed with no host specificity.

Endemic, emergence, epidemic, and pandemic

Endemic viruses are the viral populations naturalized to a given region, where reservoirs of viral populations exist in indigenous plants. The ancient ecological relationship between endemic viruses and native plant populations has led to the evolution of reduced disease severity and little harm to indigenous plant communities

(12). Reduced disease severity is thought to be attributed to three main mechanisms. First, isolation of a host plant that is intermixed with other non-host plants in an ecosystem prevents a rapid spread of viral pathogens. Second, the interaction of vector insects with their predators in naturalized ecosystems leads to reduced transmission of viral pathogens. Lastly, the ancient relationship of viral pathogen with indigenous host plants lead to the evolution of a naturalized resistance as part of the innate immunity (13, 108).

Emergence of a virus occurs when an endemic virus increases host range, increases pathogenesis, and/or increases geographic distribution (13, 109). Emergence is usually noted when a new disease is observed on an agriculturally relevant crop. It has been calculated that 47% of emergent diseases are attributed to viral pathogens (13, 109). Epidemics of emerging diseases can result from changing agricultural practices or from altered viral biology. Agricultural practices that enhance the probability of emergence of indigenous viruses include agricultural intensification into native ecosystems, habitat fragmentation of indigenous ecosystems, loss of genetic diversity of crops (13, 110), and introduction of susceptible crop species to new regions (12, 13, 108–111). Biological changes that enhance the probability of emergence include expansion of natural host range (13, 112), founder events (13, 110, 113), new mutations (113, 114), and recombination or re-assortment (110, 113, 114).

Epidemics can quickly establish in crops that have little to no innate resistance due to lack of evolutionary history with the virus, and loss of resistance due to breeding programs focused on commercial qualities. As a result, viral populations can explode due to little selective constraint (13). The spread of a virus in susceptible crops is enhanced

due to the genetic uniformity of monoculture-style agriculture. Proximity of crops, lack of evolutionary history of resistance, and genetic uniformity can cause viral diseases to spread quickly amongst cropping systems. The economic impacts of viral diseases have varying effects from minor yield loss to total crop loss (20). For particularly severe viral diseases, epidemics can cause huge crop losses in a region (21).

Pandemics occur mostly from human spread of pathogen-infected vegetative material to other parts of the world (13, 115). Once a viral pathogen makes the jump into a new host, the quick evolution of the virus allows it to adapt to the new host, and the lack of innate immunity of the new host to the pathogen results in severe economic impacts. Bi-directional spread of viruses from infected crops to the indigenous plants of the new region can have profound impacts on ecology, as well as serving as a reservoir of viral pathogens to spread into other cropping systems (13). An example of quick spread of an indigenous virus into introduced crops, eventually leading to pandemic, can be seen in *Tomato yellow leaf curl* (TYLCV). TYLCV is an indigenous virus of the Mediterranean region and jumped into introduced tomatoes. A severe epidemic spread into the region causing serious losses to the countries of the Mediterranean. After vegetative material was spread internationally, TYLCV became a pandemic on the world stage (13, 116–118).

Studying the emergence of viral pathogens into agricultural systems is important to prevent crops losses, stop the establishment of epidemics, and prevent a global pandemic. Careful monitoring of agricultural systems of introduced crops to new areas of agricultural intensification can prevent the spread of unknown viruses into the global cropping system.

Badnaviruses

Grapevine vein clearing virus (GVCV) is a plant pararetrovirus belonging to the genus *Badnavirus* in the family *Caulimoviridae*. To date, 32 badnaviruses have been characterized across all continents excluding Antarctica (115). Most badnaviruses have a narrow host range, but overall badnaviruses can infect both monocots and dicots, with a majority infecting perennial plant species of temperate and tropic regions (119, 120). Symptoms in a plant can include but are not limited to: chlorotic spots, chlorotic streaks, yellow mosaic, deformed leaves, and vein clearing of the leaves (100). Tissues infected include parts from the entire plant. Transmissions of the viruses are primarily human and insect mediated, while a few species can transmit through seeds. Insects in the families Aleyrodidae, Aphididae, Cicadellidae, and Pseudococcidae are known *Badnavirus* vectors, with the majority borne by Pseudococcidae (mealybugs) (115). Humans are by far the most prolific vector of these viruses through agricultural practices, such as vegetative propagation and grafting (100).

Badnaviruses contain a circular double stranded DNA (dsDNA) genome that varies between 7200-9200 base pairs (bps). They replicate using an RNA intermediate from a viral encoded reverse transcriptase (RT), and in this way, resemble retroviruses. The genome is organized with as few as three open reading frames (ORFs) and as many as seven. The majority contain three (I-III) and are arranged without intergenic regions between them. ORF I is in a different frame as ORF II and III. ORF I ranges from 399 to 927 bps, ORF II ranges from 312 to 561 bps, and ORF III is much larger as it is a polyprotein, ranging from 5100 to 6000 bps. Upstream of the weak ORF I AUG start codon are multiple short ORFs (sORFs) (115, 121, 122). These sORFs are used in

formation of RNA secondary structures which brings a stronger AUG start codon within 10 nts of ORF I and drive translation through ribosomal shunting (123, 124). Several of the viruses with additional ORFs include ORFs on the minus (-) strand (115, 125, 126). Many of the functions of the ORFs remain elusive. ORF I is associated with the virion in ComYMV (127), ORF II has been shown to be nucleic acid binding in CSSV (128) and capsid binding in ComYMV (127, 129), and ORF III cleaves into four or five products including: a capsid protein, reverse transcriptase, aspartate protease, RNase H, and a protein thought to help in cell to cell movement. (115, 126, 129–131).

The lifecycle of badnaviruses is considered similar to *Cauliflower mosaic virus* (CaMV), the type virus of *Caulimoviridae*. From an active infection, a minichromosome of viral DNA is used for transcription of a polycistronic longer than full genome length terminally redundant RNA inside the host nucleus (132). This RNA is then exported into the cytoplasm where it is translated into the associated gene products of the ORFs through ribosomal shunting and leaky scanning (121, 123, 124). An inclusion body is formed inside the cytoplasm of the cell where the gene products are gathered. Assembly of the viral capsid occurs in this inclusion body where gene products are packaged into the capsid along with the longer than full length RNA (133). Reverse transcription produces a relaxed dsDNA circular genome of three discontinuous regions (132). Because of these gaps there is a propensity for recombination by template switching at this stage (134–136), adding to a higher virus population diversity (134, 137, 138). From here, the dsDNA is unencapsidated and imported into the nucleus of the host cell where the host's DNA polymerases close the nicks in the relaxed circular dsDNA genome and a minichromosome forms with host proteins to begin the cycle anew (132). While within

the nucleus of the host, the genome of the Caulimoviruses can become endogenized into the host genome without the machinery for active placement, thought to be due to the dsDNA genome (99, 139). It is believed that endogenization events for *Caulimoviridae* occur once every one million years (139). Badnaviruses include many examples of species becoming endogenized into host genomes that can escape detection until abiotic stressors allow for a badnavirus to become episomal, increasing the rate of infections (99, 140–142). This poses a significant problem for agriculturally relevant crops.

Grapevine vein clearing virus

Grapevine vein clearing virus (GVCV) was discovered by Dr. Wenping Qiu while working for the Center for Grapevine Biotechnology at the Missouri State Fruit Experiment Station in Mountain Grove. In 2004, a vineyard manager contacted Dr. Qiu when he was experiencing a severe disease on many of his ‘Chardone1’ grapevines. Dr. Qiu recognized the symptoms as virus-like and brought samples from diseased ‘Chardone1’ vines to his lab to test for pathogens. After initial tests showed negative for known viruses, his lab group extracted total RNA from the plant. The RNA was isolated to include only small RNAs (sRNA), and adapters were ligated to the RNA to form a library for next generation sequencing (NGS). The sequences of all sRNAs were compiled into a database and assembled into contigs, or short overlapping regions. These assembled contigs were then subjected to a viral BLAST search to look for any similar sequences that belonged to the NCBI GENBANK database. The BLAST search brought up numerous matches to viruses that belonged to the *Badnavirus* genus of the *Caulimoviridae* family and it was believed to be a new virus that was associated with the

disease in the vineyard (143, 144). In 2009, after the unknown sequence was discovered to belong to the *Badnavirus* genus, Dr. Qiu's lab group began designing degenerate primers that would work on conserved regions of the putative virus's genome. Through trial and error, primers were discovered to work and an entire genome was assembled through primer walking and Sanger sequencing (143). This genome was published in 2011 as the reference genome (NCBI Reference Sequence: NC_015784.2), named GVCV-CHA. At this point, the disease associated with the virus had only been reported in vineyards in Illinois, Indiana, and Missouri (143). Phenotypic characterization of the virus-associated symptoms include: translucent chlorotic veins, shoots that develop with shortened zig-zagging internodes, maturation of symptomatic leaves results in deformation and stunting, mosaic patterns on older leaves, and in later stages the vines become dwarfed with a reduced fruit yield and berry deformation (143).

The idea of a new virus emerging into the vineyards of the Midwest led researchers to look for a reservoir of the virus in native *Vitaceae* spp (Figures 1-6). In 2013 the virus was detected in two *Vitis rupestris*. Figure 2 shows the county distribution of this native plant. A year later, the second GVCV isolate genome was published in GENBANK (NCBI Accession: KJ725346.1), named GVCV-VRU 1 (103, 145). Concurrently in 2014, the relative amounts of GVCV particles in host tissue was determined through quantitative polymerase chain reaction (qPCR), and the host specificity was examined through graft transmission assays. It was found that GVCV accumulates in the petioles and that the cultivars 'Chambourcin' and 'Norton' could not acquire GVCV from grafting, whereas the native *V. riparia* could (146). In the same study it was shown that a phylogeny based on conserved regions of the RT and zinc finger

(ZF) domains of ORF III of 13 isolates was not concordant with either geography or host species (146). The following year, 2015, a second GVCV genome was published from *V. rupestris* (NCBI Accession: KT907478.1), named GVCV-VRU 2. This same year, researchers at the University of Missouri characterized the promoter region that would drive transcription of a pre-genomic RNA for GVCV and delineated it somewhere between nucleotides (nts) 7332 and 7672 of the GVCV-CHA reference genome, with transcription starting at nt position 7571 (147). In 2016 they used this knowledge to design a clone of GVCV-CHA to attempt to provide evidence of causality of the virus to the associated disease and for use in downstream applications (121). Back at Missouri State, the analysis of phenotypic and genetic variation from isolates GVCV-VRU 1 and GVCV-VRU 2 showed that symptoms can progress to necrosis in *V. rupestris*, isolates GVCV VRU 1 and 2 can produce mild mottle and leaf distortion when infecting ‘Chardonnay’, and that ORF II is the most divergent region of the genome with the presence or absence of an indel (103). The variation of ORF II was proposed to be used as a marker for distinguishing isolates due to the variability between 12-17% difference (103). While investigating native *V. spp.* in 2016, Qiu’s group noticed an unknown symptomatic vine growing in close proximity to native vines. A sample was taken and analyzed for the presence of GVCV and it was found to test positive. The plant was identified as *Ampelopsis cordata* of the *Vitaceae* family, and the new phenotypic symptoms of slight vein clearing and asymptomatic tissues were observed (148). Focus was shifted from sampling *V. rupestris* to *A. cordata* due to the low incidence rate of sampled *Vitis*. Collection and sequencing of four more genomes occurred in 2017. GVCV-AMP 1 and GVCV-AMP 2 (NCBI Accession: KX610316.1 and NCBI

Accession: KX610317.1) were isolated and sequenced from two wild *A. cordata* (148), while GVCV-AMP 3 and GVCV-CHA-2 were isolated and sequenced from a wild *A. cordata* and a cultivated *V. vinifera* ‘Chardone’ (Awaiting submission) that were within 10 feet of one another (122). Analysis of the 7 genomes, thus far sequenced, provided information on the secondary structure of the 5’ region of the pre-genomic RNA, and the highly conserved secondary structure of the intergenic region (IGR) between the seven isolates. The analysis indicates that a sORF is indeed in proximity to the start codon of ORF I, as is with other *Badnavirus* (121, 122). In the same study, a phylogenomic analysis of the seven genomes indicates that isolates GVCV-VRU 1 and 2 branch off from the other isolates to form a distinct clade (122). To determine in-host viral population variation and differences between viral populations of same host species from different spatial regions, three genomes were assembled using viral small RNAs (vsRNAs) in 2017. The results show that variation in a host is within 2% at the nucleotide level, and that populations between hosts more closely resemble each other based on spatial proximity, rather than host species (149).

Summarizing the information currently available, we see that GVCV exists as a diverse population that has a broad host range with the ability to infect *V. vinifera*, *V. rupestris*, *V. riparia*, and *A. cordata*. Phenotypic characteristics of disease symptoms vary among the hosts, and variation of isolates within a plant can be up to 2%. The isolates that have been phylogenetically analyzed do not seem to suggest common ancestry either within host species or within a spatial region, further indicating a diverse population. Phylogenomic analysis separates isolates in two distinct groups: those infecting *A. cordata* and *V. vinifera*, and those infecting *V. rupestris*. Attempts at providing

information for causality of the associated disease have been partially successful, and a pattern of population structure has not been observed.

Rationale

The following chapters contain two research projects that attempt to resolve some unanswered epidemiological questions for GVCV. First, is GVCV the sole causative agent for the progression of the disease complex? Does GVCV alone cause the disease noticed in vineyards, or is there a second pathogen that is required for the disease to progress? Second, do isolates of GVCV cluster in a geographic pattern, and what is the route of transmission into vineyards? Is the virus historically endemic to the region, recently jumping into vineyards where it is causing serious economic loss, or has the virus been introduced into our region and spread into the wild plants from the vineyards? Both questions, when answered, will provide invaluable knowledge to grape producers in the region.

Looking back at the disease triangle of epidemiology, one cornerstone is the pathogen. Correct identification of the pathogen is paramount in developing strategies to mitigate damage in a vineyard. Successful treatment and prevention are not possible if the pathogen is miss-identified. To answer this question, Koch's postulates are used to determine a link of causality between the disease and the virus. Infectious clone construction of GVCV and inoculation of clean plants using *Agrobacterium* mediated transfection into disease-free grapevines was the method used to provide evidence of causality. Construction of this clone will also allow future researchers the ability to

answer further questions dealing with the virus's phenotype, genome structure, and pathology.

Determining the contemporary distribution of GVCV in the region will help provide insight into the historical movement of GVCV. This can help answer questions relating to the origin of the epidemic in the region, prediction of the rate of spread into other regions, and establishing the predicted N_e population size. This information will allow growers to reduce the incidence and spread of GVCV into their vineyards.

Furthermore, if GVCV is found to be endemic in the region, quarantine of plants from this region into other regions will prevent economic losses in more intensive wine producing regions, such as California or France. Clean vine testing services such as the National Clean Plant Network should be utilized to prevent the spread of infected plant tissues to other regions.

CHAPTER 1: EPIDEMIOLOGICAL PATTERNS OF GVCV

Introduction

Molecular evolutionary analyses rely on mathematical models to predict the probability that two given nucleotide sequences are related. Simply enough, it uses the proportion of different nucleotides to the number of nucleotides that are the same to determine the number of differences between two related nucleotide sequences, known as the Hamming distance (150–152). The inferences that can be made using molecular sequence data are numerous, including estimation of effective population sizes, prediction of emerging disease epidemics, inferring past migration events, and most notably, resolving ancestry between two organisms.

The Wright- Fisher model assumes an idealized population that allows for a number of methods to be applied to population genetics and phylogenetic inference (80, 81, 150–154). The idealized population of the Wright-Fisher model can be summed into three simplified assumptions: the population in question has a constant population size, there are discrete generations between ancestors and progeny, and there is a random and complete mixing of alleles (80, 81, 152, 153). The model traditionally deals with the frequency of allelic genes in a diploid population, but it can be adapted for use of haploid organisms, such as viruses (92, 152, 153). From hence forward, alleles will refer to the alternative copies of nucleotides: adenine, thymine, cytosine, and guanine (A,T,C,G).

Allelic frequencies can be determined in a population by sampling individuals in a population and the inferences of population structure can be estimated by applying models of sequence evolution. Sequences evolution is caused by mutational change to

genes (such as point mutations, recombination, indels, and gene duplication) combined with migration, natural selection, and genetic drift (80, 81, 150–152). Current theories of sequence evolution attribute a stronger affect to genetic drift as the driving factor in evolution than selection (92, 150–153), but selection does play a role, especially in determining fit variants of viral population (48, 49).

Genetic drift is the stochastic changes in allele frequencies in a population over time (80, 81, 150, 151, 153). The strength of genetic drift is inversely proportional to the effective size of the population (N_e). N_e is the population size equivalent to the mathematical quantity that works in an idealized model which predicts the same value of a particular trait as the observed natural population (92, 150, 154), more simply it can be thought of as the number of individuals that attribute genetic diversity to the overall population. N_e is often much smaller than an actual population size as the number of individuals that contribute to offspring for the next generation is a subset of the whole population. As N_e increases, the strength of genetic drift decreases, and it takes longer for an allele to become fixed in the population, increasing allelic diversity (155, 156).

Some processes of evolution behave in a regular pattern that can be observed in a population of the same species. Mutational changes in viruses, such as nucleotide substitutions, occur as a result of the error of polymerases during genome replication. The changes are observable and can be estimated as changes to a genome per generation. Applying discrete generations to calendar times, we can get a molecular clock which is the change of nucleotides per site per year (151, 157). This task is easier for haploid organisms such as viruses, when it is likely that the generations are discrete and it can satisfy more appropriately the assumption of the Wright-Fisher model.

Adding the mutational rate to the process of genetic drift, we constantly have additions of new alleles to the population. Small N_e sizes with a slow mutation rate have a low allelic diversity, whereas large N_e with a high mutation rate have a high allelic diversity. Due to the mutation rate constantly substituting nucleotides, the allelic diversity is always changing. As a consequence of genetic drift fixing alleles over time, large populations with a high mutation rate are adding alleles to the population before drift can fix them. This results in high allelic diversity, or genetic variation within a population.

Evolutionary nucleotide substitutions do not occur with the same frequency at every nucleotide position. DNA sequences are not all coding and can include non-coding regions, repetitive elements, exons, or introns. Functional constraint is placed more heavily on coding regions, as these regions are the instructions for the amino acid sequence in proteins. A change to this region has the potential to be fatal to an organism if the mutation causes an amino acid change. Furthermore, the position of the nucleotide in a coding region has different rates of evolution. The first and second position of a codon add more functional constraint to the codon than the third codon because of the degeneracy in the DNA code, and because of this degeneracy a mutation may be silent or non-silent. A silent mutation is a change to a nucleic acid, but the change results in the same amino acid. Non-silent mutations are changes to the nucleic acid results in a different amino acid. Purifying selection results in the survival of organisms who have not changed the function of their proteins by changes to their amino acids. Further complicating the situation, a change to an amino acid may not change the function of the protein as some amino acids have similar function. Selection only purifies those changes

which are lethal or result in significantly diminished fitness to an organism (150–152, 157)

Neutral mutation, combined with genetic drift, has been shown to have a stronger effect on sequence diversity than selection (150, 151, 157–159). However, pure neutral mutation is rarely the case. Instead, mutations lead to a slight decrease in fitness of an organism. Genetic drift and the accumulation of mutational alleles that add a slightly deleterious effect to the population leads to a process known as Muller's Ratchet.

Muller's Ratchet is the accumulation of deleterious mutations in a population as the result of drift and it leads to extinction or less fit populations over time (160). The concept was initially introduced as a way to explain the evolution of sex as a means to introduce recombination and have the re-assortment of alleles introduced back into the population (160). Muller's ratchet has been observed for viruses in vitro where serial transmissions in a laboratory lead to loss of fitness (161–163).

Molecular phylogenetics attempts to resolve the ancestry or relatedness of observed sequences. There are multiple models that deal with sequence evolution and distance between two related species, but most evolutionary models are a modification of the neutral theory and mutational changes of two related sequences (150–153, 157).

These substitution models utilize transitional rate matrices to determine the probability that a nucleotide will change from one state to another (i.e. A to T), and are a sophistication from a simple proportion of nucleotide sites that are different. Some models apply a uniform probability to substitution rates (159), others consider the transition/transversion bias (164), and more complex models account for the transition/transversion bias and the GC content bias (158). Further complexity is added

when one considers that the evolutionary rate from site to site is not the same, as is the case in the first and second nucleotide of a codon. This can be modelled by changing the shape parameter of the probability distribution to the gamma distribution (150, 151, 165).

The phylogenetic tree is a fundamental graph for the imaging and study of evolutionary relationships. Trees can either be rooted, or unrooted. Rooted trees show a direction of evolution between the related sequences while unrooted trees only show the relationship between sequences. Methods used to build trees include distance methods, maximum parsimony methods, and maximum likelihood methods. Distance methods draw trees based on the genetic distance between related sequences, maximum parsimony methods compare four or more sequences and the topology of the tree is picked for the minimum amount of evolutionary changes to the sequences, and maximum likelihood methods maximize the likelihood of observing a given set of sequences for specific substitution models for each possible topology of the tree and the most likely topology is selected (150).

Rooted trees made by any of the methods can be used to infer time trees, or trees where branch lengths correspond to units of calendar time (152). For large population sizes (N), the Wright-Fisher model gives rise to a distribution of time trees, called the coalescent tree distribution (152–154). Coalescent theory attempts to resolve past evolutionary processes that affect a population from contemporary sequence data (153, 154). The coalescent distribution is the distribution of probabilities that two random members of a current generation from a population share a common ancestor (152–154). The probability can then be determined for the number of discrete generations it took for the sequences to diverge from their common ancestor common ancestor (153, 154).

Establishment of the time to most recent common ancestor (TMRCA) is a powerful tool that coalescent theory can infer from contemporaneous sequence data.

Phylogeography is an approach that merges phylogenetics and biogeography (166), and has become more popular with advances in the models of coalescent theory and computation (167). Phylogeography can address questions of geographical origins and expansions and the effect of complex factors such as climate change and human involvement on geographic dispersal (152). For fast-evolving pathogens, such as viruses, a ‘mugration’ model of Phylogeography can be adopted. Mugration is the modeling of the migration processes using a substitution model of analyzed sequences (168, 169). Locations of where the sequences were collected are used to estimate the migration rates between pairs of locations (152). This approach has been used on a variety of quickly evolving viruses, such as influenza A H5N1, to determine the origin and paths of global spread (170). It has also been implemented for dog rabies (171), *Rice ellow mottle virus* (RYMV) (172), and *Potato Virus Y* (PVY) (173). While the majority of examples of phylogeographic methods are used in studying human or mammalian viruses, the adoption into the study of plant viruses is burgeoning.

Grapevine vein clearing virus (GVCV) is thought to be a recently emerging virus in the *Badnavirus* genus of the Caulimoviridae family which severely impacts the sustainability of grape production in the Midwest (122, 143, 145, 146, 148). Previous studies have found alternative hosts for GVCV in the native *Vitaceae* of the Midwest (145, 148). Phylogeographic models were implemented to address the question of the effective population size, if GVCV is endemic to the region, and the historical pattern of spread of GVCV. Taken together, we can predict the N_e of GVCV by estimating the

mutation rate, resolving the phylogenetic relationship of organisms, and working backward to determine how many generations it would take to find a common ancestor for the sampled isolates. In essence, the allelic diversity of the sequences analyzed will be used to predict the N_e by determining the discrete generations that took place to get the observed sequence variation. Applying the estimated molecular clock will convert generations to calendar time, the discrete geographic coordinates of the sampled isolates will be fixed points in a continuous landscape, the resolution of phylogenetic relationship between the isolates sampled from the discrete positions will give the likely route and rate of spread through the region. A diffusion model based on a modified Brownian motion will predict the areas, where it is likely the virus can be found. If the TMRCA is sufficiently old, it is likely the virus is endemic to the region. This information is crucial for stakeholders, as it will allow them to predict patterns of spread into their vineyards from the wild populations of *Vitaceae*, and can potentially help prevent a pandemic scenario into other wine producing regions where GVCV has not been detected.

Materials and Methods

Brief synopsis. Inference of the historical spread of *Grapevine vein clearing virus* (GVCV) from the wine producing regions of Missouri and Arkansas was attempted using a tip-dated Bayesian phylogeographic approach. ORF II was proposed to be used for phylogenetic analysis because of the high sequence divergence for providing higher resolution between isolates (103, 122). The summary of methods used were to sample from wild *Vitaceae* populations, test for GVCV, build a dataset of non-recombining sequences, determine the best substitution model for phylogenetic analysis, set up tip-

dating analysis by testing evolutionary change and determining the molecular clock, perform Bayesian evolutionary analysis, determine effective population size (N_e) and time to MRCA, and finally overlay evolutionary changes onto a continuous landscape to infer historical spread of GVCV through the region.

Samples were collected from native *Vitaceae* plants for two years, and previous samples collected by former researchers were also incorporated into the data set. Samples were collected without regard to symptoms from pre-designated regions in proximity to wine producing regions, and in regions remote from wine production. Plants were identified visually in the field, samples were collected, and discrete geographic coordinates were recorded on mapping software. Tissue samples were brought back to the lab where a portion was used for DNA extraction, and the remainder frozen for long term storage. An Excel file containing all samples with geographic coordinates was created. Polymerase chain reaction (PCR) detection of GVCV nucleic acids was performed on all samples. Positive samples were selected to PCR amplify the open reading frame (ORF) II region. Amplified products were extracted and sequenced. Sequences were aligned to the reference genome GVCV-CHA's ORF II and compiled into a FASTA file. All sequences were aligned in MEGA 7 and an alignment file was exported to RDP4 to test for recombination. Recombinant sequences were removed from the FASTA file. The new FASTA file was aligned in MEGA 7 and a neighbor joining tree without bootstrap values was inferred. The tree was uploaded to TEMPEST to determine if sequences fit a clocklike behavior to calculate a molecular clock rate. The FASTA file containing all sequences was compiled and uploaded with the molecular clock rate to the program BEAUti to set evolutionary model parameters. The generated

file was uploaded to the program BEAST to perform a Bayesian evolutionary analysis using a continuous time Markov Chain Monte Carlo (MCMC) method. The generated file was uploaded into TreeAnnotator and DensiTree, and a maximum clade credibility (MCC) tree was visualized and trimmed. The tree was uploaded into the program SPREAD along with geographic coordinates of each sample. The diffusion of GVCV through the region was imaged on Google Earth using the SPREAD algorithm.

Collection of samples. Sampling from *Ampelopsis cordata* was preferentially chosen due to the previously sampled incidence rate (148). County maps for native *Vitaceae* plants were consulted for sampling from appropriate locations (Figures 1-5). Young shoots were collected from observed plants and placed in pre-labeled plastic bags containing a moist paper towel to prevent desiccation of leaves. Naming convention started with year sampled, followed by genus, and ending with a four-digit numerical code (i.e. 16AMP0001). A discrete geographic coordinate point using Decimal Degrees was marked and stored on the iPhone app, GaiaGPS. Samples were stored on ice in the field until they were brought back to the lab for long term storage. Three replicates of samples were weighed in amounts of ~45mg of fresh tissue, flash frozen in liquid nitrogen, and stored in -80°C until extraction.

DNA extraction and PCR detection of GVCV. DNA was extracted from the samples by using the Synergy™ 2.0 disruption tubes, BeadBug™, and silica columns according to the Synergy™ manufacturer protocol. DNA concentration and quality were analyzed on the Thermofisher 2100 Nanodrop. DNA concentration was diluted to 10 ng/μl and all samples were stored at -20°C.

PCR was performed using a triplex primer set containing two GVCV primer sets and one plant specific primer set for a DNA positive internal control. Primer sets used were 1101 F and 1935 R, 4363F and 4804 R, and 16s F and 16s R; a list of primer sequences is located in Table 2. Samples showing a band for either GVCV primer set were determined to have the virus.

ORF II amplification and Sanger sequencing. GVCV primers flanking the ORF II region, 963 F and 1634 R (Table 2), were used to amplify the gene sequence of all positive samples. PCR amplicons were extracted from 1% agarose gel using the MinElute™ DNA Purification kit supplied by Qiagen. DNA quality and quantity were analyzed on the Thermofisher 2100 Nanodrop.

DNA samples were prepared with primers 963 F and 1634 R and sent to Nevada Genomics for Sanger sequencing. Sequences were provided by Nevada Genomics in the form of a chromatograph that includes the nucleotide sequence and a phred quality score of the likelihood the correct base was called. The chromat file was imported to the CodonCode Aligner software package and the sequences were aligned to the GVCV-CHA genome (GenBank Accession: KX610317.1). Only sequences where phred scores were above 20 were kept, corresponding to a 99% accuracy of base-calling. All gene sequences were compiled into a FASTA file.

Sequence alignment and recombination detection. The FASTA file of all compiled sequences was imported to MEGA 7 (174). Alignment of all the sequences was performed using the default parameters of the CLUSTAL W algorithm (175). Manual inspection of the alignment output was performed to correct any discrepancies from the reference genome. The alignment file was saved as a Nexus file.

The alignment file was imported to RDP4, a recombination detection program (176). Recombination algorithms were used to detect potential recombination events. Sequences were considered recombinant if five of the algorithms detected a recombination event. Recombination sequences were removed from the positive sequence file, due to the confounding effects of recombinant sequences on accurate phylogenetic analysis (177).

Neighbor joining tree and molecular clock estimation. The new FASTA file was uploaded to MEGA 7 and the alignment was performed as previously described. A phylogenetic analysis of the aligned sequences was performed by using a neighbor-joining distance tree under the prior assumptions of a Timura-Nei substitution model using a gamma distributed rate variation with a five-shape parameter. The tree was exported as a Newick tree and saved to a file. This process was repeated for all GVCV genomes currently sequenced and for 56 *Badnavirus* genomes acquired from Genbank.

The Newick tree files were imported into TempEst to estimate the molecular clock rate. The program estimates the clock rate by regressing the branch lengths of the Newick tree on the dates of the collection of the sampled sequences (178). The mutation rate is the number of mutations per nucleotide site, per year for the given sequence data.

Test of selection. The aligned ORF II sequences were tested for evidence of purifying or positive selection at each codon by using the adaptive Branch-Site Random Effects Likelihood (aBSREL) method in MEGA 7 (179).

Test of suitability of ORF II as a candidate for phylogenetic reconstruction. The aligned ORF II sequences with the removed recombination sequences were used to construct a Maximum Likelihood tree with 1000 bootstrap replicates to test for

phylogenetic signal from the ORF II region. The Tamura-Nei substitution model and a uniform rate between sites were the parameters used to reconstruct phylogeny.

BEAUti and the BEAST. The Nexus files of all alignments (ORF II, GVCV, *Badnavirus*) were imported into BEAUti (180). The years of collection were set as the tip dates. A trait partition was imported to use discrete geographic coordinates in a continuous landscape and linked to each sample for the ORF II sequence data. The substitution model used a general time reversible (GTR) transition rate matrix (181) using rate heterogeneity set to a five-parameter gamma probability distribution for each site (1+2+3) with unlinked substitution rates. The location traits were set to determine routes of historical transmission using a Brownian random walk model for the ORF II sequence data. The clock model used was an uncorrelated relaxed lognormal clock, using the estimated clock rate from Tempest. A coalescent constant population size was used to determine the tree shape parameters. Ancestral states were reconstructed for the location partitions to simulate the geographic spread of GVCV. The Markov Chain Monte Carlo (MCMC) tree construction was set to 10 million iterations and tree samples were taken every 10,000 iterations. A BEAST file was generated using these parameters. BEAST performed the Bayesian evolutionary analysis through sampling trees (BEAST) from the generated file, and built two files for analysis (180).

The data were analyzed on Tracer to determine the 95% highest posterior density (HPD) interval and the effective sample size (ESS) values for each dataset. The tree data were uploaded to FigTree and used to find the tree with the highest posterior probability and build a Maximum clade credibility (MCC) tree. The MCC was imaged on DensiTree

to determine relative divergence dates between isolates, and to image the direction of the evolutionary relationship.

SPREAD. The MCC of the ORF II sequences linked to traits of physical locations was uploaded to SPREAD (182). Visualization attributes will be set to image the predicted transmission history of GVCV on a continuous landscape. A kmz file was created and uploaded to Google Earth (<http://earth.google.com>) and a time-lapse of GVCV movement through the region will be created.

Results

Viral detection and clock rate estimation. A total of 488 wild plants were sampled and 134 tested positive for GVCV. The number of samples and those that tested positive for GVCV are listed in Table 1. In this study, two new *Vitis* spp., *Vitis cinerea* and *Vitis vulpina*, were found to be natural hosts of GVCV., An example of the triplex PCR for detecting GVCV is presented in Figure 7. Distributions of natural boundaries of each species are shown in Figures 4 and 5. A list of positive samples with geographic coordinates is in Appendix A, and a map of all GVCV-positive vines is presented in Figure 8. The ORF II regions of all 134 GVCV isolates were sequenced and were compiled into a FASTA file along with the ORF II sequences previously determined. A total of 143 sequences were aligned without a root and imported to RDP4. Recombination events were detected in 7 sequences by five of the algorithms in RDP4 and were removed from the sequence file. The 56 *Badnavirus* sequences from Genbank were compiled into a FASTA file without a root and aligned. The seven sequenced genomes from GVCV were also compiled into a FASTA file and aligned. The Neighbor-

Joining trees are presented in Figures 9-11. The Neighbor-Joining trees of each dataset were imported to TEMPEST and the molecular clock rate was estimated by regressing tip dates to genetic distance. Screenshots of the linear regression of samples evolutionary distance to sampling dates can be found in Figures 12-14. The clock rates and R^2 values are listed in Table 3. The slope of the line is the molecular clock rate that was used in subsequent analysis.

Test of selection. The analysis of selection for each codon of ORF II showed that 18 codons out of 114 went through purifying selection with the majority being under no selective constraint. This suggests that ORF II is not a conserved region, as the literature suggests, and that its structure and function can be widely adaptable. A table of the dN/dS ratio with P-values can be found in Appendix B.

Test of phylogeny. *Gooseberry vein banding associated virus* (GVBaV) (GenBank Accession: NC_018105.1) was added to the non-recombinant ORF II sequences and used as a root to provide a direction of evolution. Phylogenetic analysis using a Maximum Likelihood tree showed evidence of an unresolved tree with many polytomies coming from the central branch. Figure 15 shows the lack of resolution of the phylogenetic relationship. Phylogeographic analysis was pursued even though there was a lack of supported phylogenetic relationship to provide future researchers with a look into the methods used for a more suited molecular sequence.

Phylogeographic analysis. The sequence file was further trimmed to include the 125 non-recombinant sequences from 2016 and 2017 for the phylogeographic analysis. Highest posterior density (HPD) ranges and effective sample size values (ESS) were low for phylogenetic reconstruction and the uncorrelated-relaxed clock rate, and high for the

substitution model used. An example can be seen in Figures 16 and 17. Continuation of the analysis was conducted to provide a method for future researchers to follow with a better suited molecular sequence dataset. All results from here will be statistically unsupported but are relevant for future researchers.

The estimated time to the most recent common ancestor (TMRCA) of GVCV and GBVBaV based on ORF II sequences is approximately 270 years ago. The TMRCA of GVCV isolates occurs at a population explosion event occurring between 15-30 years ago, where the relative effective population size (N_e) jumped by order of a magnitude. A graph showing the estimated historical N_e changing through time is shown in Figure 18.

The Maximum clade credibility tree of GVCV and ORF II is shown in Figure 19. A common haplotype in GVCV is the presence or absence of a 9-bp indel in ORF II, a common genomic feature of GVCV; 35 out of 125 sequences contained the indel. Figure 20 highlights the isolates with the indel and shows the relative geographic positions and placement on the tree. Figure 21 highlights the isolates from *Vitis* spp. on the MCC tree. Augusta and Herman, MO were two of the most heavily sampled areas. Figure 22 shows their relative positions on the MCC. All highlighted samples show their relative geographic locations in their real world. Inference of the transmission history of GVCV was unsuccessful, but future attempts will be made to resolve some key issues.

Discussion

Sampling and incidence suggest endemic nature. The sampling of native plants in the *Vitaceae* family revealed two new hosts for GVCV, *V. cinerea* and *V. vulpina*. There are now five known wild hosts to GVCV. *A. cordata* has a higher incidence rate of

GVCV than *Vitis* spp. Approximately 33% of sampled *A. cordata* test positive for GVCV, whereas 14% of sampled *Vitis* spp. were infected with GVCV (Table 1). As mentioned in the literature review, it is common for a naturalized wild host of a virus to have mild or absent symptoms due to the co-evolutionary relationship of the pathogen with the plant (12, 13, 112–114). We rarely observe distinct GVCV-associated symptoms on *A. cordata*, they are usually very mild. Conversely, the GVCV associated disease progresses from vein clearing to necrotic spots in the leaves of *V. rupestris* (103, 145). It is likely that GVCV is endemic to the region and has evolved to infect *Vitis* spp. as a new host, first in wild plants, and then into cultivated *Vitis* spp. The distribution of *A. cordata* overlaps with many *Vitis* spp. in the Midwest (Figures 1 to 5). If GVCV is endemic to the region and is recently emergent, it is imperative to establish the borders of the virus in wild populations, and to investigate potential alternative hosts. Figure 6 shows the range of all *Vitis* spp. in North America. There is a logical route of migration for GVCV to spread into alternative hosts, and discovery of the insect vector will help predict the rate of spread, as sequence data could not resolve issues of past demographics.

Implications of the 9bp-Indel. The 9bp-indel in ORF II at nt position 262 is likely a deletion. It is interesting to note that isolates from both *V. spp.* and *A. cordata* have the 9bp-indel, further suggesting that GVCV is not host specific in the *Vitaceae* family. Viral genetic diversity is known to be large, but generally stable from year to year if looking at number of haplotypes in the population (48, 49, 117). If the indel is used as a haplotype, then we can see that 19 out of 40 sequences (47.5%) sampled from 2016 contain the indel, while 19 out of 86 sequences (22%) from 2017 contain the indel. This

does not fit the haplotype population stability from year to year as is suggested (48, 49, 117). Perhaps this could be due to the difference in sampling regions from the two years. 2016 had the majority of samples from Arkansas and southern Missouri, while 2017 primarily focused on central and northern Missouri. This could provide evidence of a historical movement of the virus from the south, as the indel seems to be a deletion. This is, however, speculation. Further sampling from the boundaries of the *A. cordata* range could provide insight into the segregation of isolates based on geography.

Molecular clock. The molecular clock rates were estimated for ORF II, GVCV genomes, and *Badnavirus* genomes by linear regression of tip-dates (sample dates) to evolutionary distance between sequences. This is a simplistic method to estimate a rate, but it proves to be fairly accurate (183). It is worth noting the clock rates determined that the older sequences were more divergent from the root, suggesting that the virus is de-evolving over time. This is shown by the negative slope of the line generated in TEMPEST. The clock rates are shown in Table 3. GVCV and *Badnavirus* genomes were used to determine if the magnitude of the clock was correct, as the evolutionary relationship between whole genomes can be resolved easily. All clock rates were of the same magnitude, so the clock rate used for the analysis was ORF II. The R^2 values were low for the *Badnavirus* and ORF II clock estimate, but were the same magnitude as the GVCV genome rate (47, 71, 72). Interestingly, the rates predicted fit more closely with the mutation rate of RNA viruses, rather than DNA viruses. This is not surprising as Badnaviruses replicate through the RNA intermediate using reverse transcriptase (RT).

Purifying selection. Purifying selection was found to act on only 18 out of 114 codons of ORF II, starting at codon 63 and increasing in density. The test of positive selection showed no signal. It is likely that the putative protein has great adaptability in function as little constraint is placed on this gene sequence, not surprising considering it is the most variable region. As discussed earlier, the ORF II of Badnaviruses has been shown to be nucleic acid binding and capsid binding in two species (128, 129). The function of GVCV's ORF II is unknown, but it is likely multi-functional, as viral proteins usually serve multiple purposes (73).

Maximum Likelihood phylogenetic analysis. Before a phylogeographic approach could be attempted, it was necessary to test if the sequence data could accurately resolve the phylogenetic relationship between isolates. A maximum likelihood (ML) tree was constructed with 1000 bootstrap sampling. The tree could not be satisfactorily resolved. When the bootstrap cutoff value was set to 70, there were very few resolved clades and the tree had many polytomies. The tree took a characteristic star shape, and is indicative of a population explosion in coalescent theory, or suggests low phylogenetic information in the data set (152–154). Population explosion would make sense, if the endemic virus recently evolved to broaden its host range and increased its reproductive fitness (12, 13, 109, 110, 118).

Unfortunately, this lack of phylogenetic reconstruction prevents the accurate inferences that the analysis was attempted to address. However, the analysis still provided researchers with a method if more data were collected, and perhaps find a path through a complicated task.

Phylogenetic problems. The only clear conclusion from this data set is that ORF II is an unsuitable gene candidate to determine phylogenetic relationships of the sampled isolates. The test of selection showed that the majority of the mutations to the dataset occurred from neutral mutations and that there was minimal selective constraint on the gene region, suggesting that the use of substitution models should resolve the phylogeny. The gene sequence contains 384-393 nts and is the most highly variable region in the GVCV genome (103, 122, 145). It is generally accepted that 200 nts is the lowest value for giving confidence values that can completely resolve the phylogenetic relationship between isolates (184). It is likely that the high variability in the gene sequence and the low amount of genetic characters, prevent the current models from resolving the relationship between the isolates. There are a number of explanations beyond this rationale that could hinder accurate analysis in the future and that will also be discussed.

Recombination events have a drastic detriment to the inference of phylogenies and can make the phylogeny difficult to resolve even with a few sequences in a large dataset (177, 185). *Caulimovirus* as a family are known to be highly recombinant, as is described in the literature review, which is why the program RDP4 was used to remove recombinant sequences. The software could have missed detection of recombinant sequences and could cause problems.

Badnavirus species have been shown to endogenize in their hosts genome (99, 140–142). Endogenized viral elements (EVE) will have the potential to have the same or similar sequences as episomal forms, but will mutate at a much slower rate (139, 186, 187). The magnitude of Badnaviruses molecular clock was estimated to be in the

magnitude of 10^{-3} , while the host plant can range from 10^{-8} - 10^{-12} , depending on where the EVE is located (150, 151). If GVCV is endogenized, it could be an extinct variant that is an ancestor to the extant species. This would cause many problems in phylogenetic reconstruction.

Time tree imbalances can come from incomplete sampling and oversampling from one year when using heterochronous data. When using a tip-dated phylogenetic analysis, imbalances in sampling areas and lack of significant heterochronous separation can lead to biases in the estimation of past timescales (188, 189). This is likely a problem that occurred for the Bayesian tip-dated analysis. The speciation event of 300 years that was predicted between GVBaV and GVCV is likely grossly underestimated, as GVBaV is considered endemic to Europe (190). Further evidence imbalances causing problems for this analysis is the estimated time to the population explosion of GVCV between 15-30 years ago. The area covered in sampling is large and the sequence diversity is high, so this is likely also grossly underestimated as a time of origin for the diversity we see today.

The sequence likely lacks the length of characters that models need to resolve the phylogeny, especially considering the observed variability in the region. Whole genome sequences, more discerning sampling times (days, month, year), and continued sampling from other regions would likely resolve any issues with the analysis. If whole genome sequences were not used, then it would benefit to use a less diverse region of the genome along with ORF II for phylogenetic analysis, most likely a region that undergoes significant purifying selection and is therefore conserved between isolates. The RT region would be an excellent candidate of this as it has been shown to undergo selective

constraint (146), and is used by the ICTV for taxonomic purposes of new *Badnavirus* species (40). Further confounding the temporal analysis is the use of years, and not more discerning sampling times. More complete sampling using days, months, years may help more accurately resolve the timescales of ancestor states at nodes. A more thorough sampling of regions, extending to the boundaries of the known distribution of *A. cordata* could provide a better picture of geographic division between haplotypes.

Genetic diversity, host diversity, geographic diversity. From the analysis so far, it seems that GVCV isolates are not segregated by preference of host. There are six examples where isolates from *Vitis* spp. are closely related to isolates from *A. cordata*; five of the isolates have complete identity between their ORF II sequences. Figure 15 shows the ML tree with related isolates. Two complete sequences were isolated from a *V. vinifera* ‘Chardonel’ and an *A. cordata* that were 6 meters away from each other and their genomes were 99.8% similar (122), suggesting that the isolates came from the same ancestor. If one were to look at the phylogeographic analysis (that is not statistically supported), it seems that the population is highly mixed in the regions sampled and there are no discernible delineations of populations segregating into distinct geographic regions. Figures 19-21 show a few noteworthy categories of viral isolates related to the geographic landscape: 9-bp indel, *Vitis* spp., and the regions of Herman and Augusta.

Summary

The discovery of the disease in vineyards in 2009 was prompted by the unique and severe symptoms on a hybrid grape ‘Chardonel’. It is unlikely that the disease was

unnoticed in vineyards in Missouri before, as Midwest has a 150-year history of viticulture. It is also unlikely that the disease was unnoticed if it came from another region such as California or France, where the viticulture is well developed. The fact that there is no evidence of these symptoms appearing in the literature before the recent emergence further suggests this is a newly emergent disease. The incidence of GVCV in *A. cordata* and the asymptomatic nature of the disease makes it likely that the virus is endemic to the Midwest. Wild isolates were found in Missouri, Oklahoma, and Arkansas for this sampling period, and cultivated isolates were found in the vineyards of Illinois and Indiana by previous researchers (143, 146). The broad-range of GVCV indicates that the virus has been established in the region for some time, and the presence of GVCV in vineyards of Illinois and Indiana suggests spreading of the virus. Unfortunately, the accurate inference of the historical rate of spread was unsuccessful. If stakeholders believe it to be of importance, future researchers should address the problems with the current analysis and use more robust sampling techniques, longer and more conserved molecular sequences, and a more specific date for tip-date phylogenies.

Surprisingly, GVCV has been found in Brazil, likely arriving in the country from rootstocks from the Midwest region (191). It is known that humans are a notorious vector of viral diseases and can establish pandemics by transporting infected plants globally (12, 13, 109, 116, 117). It would be a sound management practice to understand the natural boundaries of GVCV to establish an effective quarantine protocol in afflicted regions. This would prevent the virus from spreading into more intensive grape producing regions and could mitigate future outbreaks. *Vitis vinifera* is the preferred grape for wine production in most of the world for its superior berry flavor. The virus induces a strong

response and the disease progression is severe in this species. Death of a vine can occur within seven years (143). Regions such as California and France overwhelmingly produce wine made from *V. vinifera* could potentially be devastated by the virus.

Identification of the vector or potential vectors of GVCV is important in understanding how it spreads into vineyards without the aid of humans. The rate of spread of GVCV is dependent on the migration pattern of the vector. Vector transmission is likely as the virus spreads naturally in the wild without human interference. There have been five identified *Vitaceae* species that have been found to host GVCV in the wild. The range of all *Vitis* spp. can be seen in Figure 6. It is also important to determine the potential alternative hosts of GVCV to see if the virus can migrate into other regions without human involvement. Inference of the historical spread would be important for stakeholders in other regions to predict how the virus may spread across the continent. Unfortunately, the phylogeographic analysis of historical transmission was unsuccessful, so it is unknown how the virus has spread through the region naturally, although it is likely that human involvement has mixed the populations as GVCV was only detected in 2009.

CHAPTER 2: CONSTRUCTION OF A GRAPEVINE VEIN CLEARING VIRUS CLONE

Introduction

Grapevine vein clearing virus (GVCV) was isolated from a grapevine that was affected by an associated disease of vein clearing and vine decline. Transmission studies using vegetative grafting of infected vines onto clean vines, and sRNA sequencing and genome reconstruction provide evidence that GVCV is associated with the disease (149, 192). However, evidence of definitive causality of GVCV as the sole infectious agent of the associated disease is lacking. To provide evidence of causality of infectious agents to associated diseases, pathologists employ Koch's postulates.

Koch's Postulates are four criteria that must be met before an organism can be declared as the causative agent of a disease. These criteria are: the organism is observed in all cases of the disease, the organism can be isolated from a diseased host and a pure culture can be obtained, a pure culture of the organism introduced to a healthy host will produce disease symptoms, and the isolation of the organism from the inoculated host must be the same organism as the original inoculum (193). This task is relatively simple when studying diseases caused by fungi or bacteria, as the cultures can be isolated on growth media. Viruses are considerably more difficult, as they are obligate parasites and need a host cell to undergo a full life cycle. The small size of viruses adds to this difficulty. Molecular techniques have made isolation of pure viral particles easier and has facilitated the explosion in research on viral pathogens.

Viral genomes must be reconstructed at the molecular level to construct a clone of a virus that satisfies the requirement of a pure culture. This is done in a variety of ways. Polymerase chain reaction (PCR) is used to amplify entire viral genomes and these are inserted directly into transfection vectors (194), viral genomes fragments are amplified by PCR and assembled into transfection vectors (195), and viral genomes are assembled piecewise and blasted into cells using particle bombardment (196). These are three of the most common ways to introduce pure viral cultures into healthy hosts.

Viral clones are said to be infectious if the clone undergoes a full replication life cycle and virions can be observed in infected tissues. The clone must contain all necessary components of the genome to undergo successful replication, independent of components from sources not found in the wild-type virus. If the clone is infectious, the disease symptoms appear on healthy plants which have been transfected, virions are observed, and then Koch's postulates are said to be fulfilled for a viral organism.

GVCV is a double stranded DNA virus that replicates through a terminally redundant, longer than full length genome RNA intermediate (121, 147). The DNA is thought to begin replication from the RNA intermediate at the first tRNA^{met} binding site and then the reverse transcriptase (RT) switches template to the second tRNA^{met} to make the DNA molecule (130, 132). Once the DNA template strand is synthesized, host DNA polymerase replicates the second strand (123, 132). As a member of the *Badnavirus* genus, there are numerous examples of successful cloning techniques. Many techniques utilize a terminally redundant longer than full length DNA construct introduced by *Agrobacterium* spp. (197–199). These protocols use 1.4 genome lengths of viral DNA to construct their clone to provide terminally redundant ends for the switching of the RT to

the redundant tRNA^{met} binding site. The promoter region of GVCV was shown to be between nts 7332 and 7672 (147). Design of the clone took into consideration that previous attempts of the clone with 1.2 genome lengths was insufficient to provide evidence of causality or replication (121). Identification of the promoter, knowledge of the replication strategy of Badnaviruses, and successful attempts in the literature were considered for construction.

Materials and methods

Synopsis. Construction of the clone utilizes a design of 1.4 genome length terminally redundant GVCV fragment introduced into the shuttle vector pCR8/GW/TOPO. The 1.4 genome length is assembled from two PCR amplicons that were cut with unique type IIb restriction enzymes for directional cloning. Three fragments were digested from the two amplicons and assembled into the correct conformation for a longer than full length genome that is in the correct reading frame. Once assembled into pCR8/GW/TOPO, the clone was introduced into the destination vector pGWB401 to be transformed into *Agrobacterium tumefaciens* strain ‘GV3101’. *Agrobacterium* mediated transfection of healthy susceptible plants was monitored to test for the presence of GVCV’s associated disease symptoms and molecular tests will provide evidence for successful replication of the clone construct.

Design. The GVCV-CHA reference genome (Figure 23) (NCBI Reference Sequence: NC_015784.2), the entry vector pCR8/GW/TOPO, and the destination vector pGWB401 sequences were downloaded from Addgene (<https://www.addgene.org>).

FASTA files were uploaded into the program SerialCloner 2.6 (http://serialbasics.free.fr/Serial_Cloner.html). The program identified all unique single cut restriction sites in all genomes. Manual inspection of restriction sites revealed three restriction enzyme (RE) recognition sequences that were unique to GVCV, contained overhangs for directional cloning, used the same reaction buffers, and had similar reaction conditions. Figures 23 and 24 show the genome arrangement of GVCV and the RE sites used, respectively. The three unique restriction sites were Sal I (GTCGAC), Rsr II (CGGWCCG), and Avr II (CCTAGG) are listed in Table 4. A list of all RE used is located in Table 4. A multiple cloning site (MCS) was designed to contain all three restriction sites in the order Sal I, Rsr II, and Avr II with an overhang of an A at the 3' end of each strand (GTCGACCGGWCCGCCTAGGA). To construct the MCS, two oligonucleotides were ordered from Eurofins. The oligonucleotides were reverse-complimentary and annealed together by adding 25µl of 100µM of each into a 1.5 microcentrifuge tube, heated to 94° C, and then slowly cooled to room temperature. The MCS was labeled, "MCS/SalI-AvrII", and stored at -20°C until ready for use.

Construction. PCR Primers were designed to amplify two overlapping fragments of the GVCV genome that contained the chosen RE sites (Figure 2). Two sets of primers were identified with similar T_m. Primer sequences of 4363 F and 1179 R, and 697F and 4804R are listed in Table 1. PCR amplified two fragments of 4,570 bp, and 4,187 bp, respectively. The fragments were directly inserted into pCR8/GW/TOPO and the new plasmids were labelled pCR8/4808 and pCR8/1179. The two plasmids were transformed into One Shot™ Top 10 Chemically Competent *Escherichia coli* using the standard

protocol included with the pCR8/GW/TOPO vector. A 90 μ l solution of transformed bacteria was plated on Lysogeny Broth (LB) agar plates mixed with 100 μ M spectinomycin and incubated at 37°C overnight to isolate single colonies. Successful plasmid transformation was confirmed by colony PCR using the GVCV specific primers listed above. Positive colonies were grown in 5 ml LB broth with 5 μ l of 100 μ M spectinomycin added to prevent contamination from ubiquitous bacteria. Liquid cultures were incubated at 37°C for 16 hours. 700 μ l of liquid culture solution was prepared for long term storage at -80° C by adding 300 μ l of 50% glycerol. Plasmids were isolated using the Qiagen QIAprep Spin Miniprep kit following the manufacturer protocol. DNA quality and concentration was determined using the ThermoFisher Nanodrop 2000.

Three RE digests using the overlapping PCR fragments were performed with two sets of REs in each reaction. An image of fragments produced is presented in Figure 25. RE digests were performed according to the NEB protocols. Reaction one used pCR8/1179 as a template and was digested with Sal I and Rsr II to produce two fragments of sizes 3,893 bps and 3,439 bps. Reaction two also used pCR8/1179 as a template and was digested with Sal I and Avr II to produce two fragments of sizes 3,429 bps and 3,903 bps. Reaction three used pCR8/4804 as a template and was digested with Rsr II and Sal I to produce two fragments of sizes 3,853 bps and 3,072 bps. The three reactions were terminated by adding 10 μ l of 6x Purple Loading dye, supplied by NEB. Reactions were loaded into a 1% agarose gel and fragment sizes were determined by electrophoretically separating fragments and comparing to a DNA ladder of known fragment sizes (1Kb plus NEB). The fragment of 3,893 bps, corresponding to GVCV DNA from position 4,643 to 786, was isolated from reaction one and labelled “SalI-

RsrII". The fragment of 3,429 bps, corresponding to GVCV DNA from position 4643 to 323, was isolated from reaction two and labelled "Sall- AvrII". The fragment of 3,853 bps, corresponding to GVCV DNA from position 786 to 4,643, was isolated from reaction three and labelled "RsrII- Sall". All fragments were isolated using the Qiagen MinElute Gel Extraction Kit by following the manufacturer's protocol, analyzed on the Nanodrop, and stored in 1.5 microcentrifuge tubes at -20°C.

MCS/Sall-AvrII was removed from cold storage and inserted into pCR8/GW/TOPO following the manufacturer's protocol; the new plasmid construct was named "pCR8/MCS". One Shot™ Top 10 Chemically Competent *E. coli* were transformed with pCR8/MCS and incubated as previously described. RE digest of pCR8/MCS with Sall and HpaI were used to confirm successful transformation. Successful transformations were added to liquid cultures and incubated as previously described. pCR8/MCS in *E. coli* was stored in -80°C as previously described. pCR8/MCS was isolated from liquid culture, analyzed on the Nanodrop, and stored as previously described.

Fragments RsrII-Sall and Sall-AvrII were ligated using alkaline bovine T4 ligase. The reaction was set up using 500ng of each fragment, 2µl of T4 ligase buffer, and 1 µl of T4 ligase. The reaction was incubated at 16°C overnight. The fragment was confirmed to be 7,286 bp, corresponding to nucleotide positions 786 and 323 of the GVCV-CHA genome. The fragment was excised from a 1% agarose gel and labeled, "RsrII-AvrII". pCR8/MCS was digested with Rsr II and Avr II as previously described and the new fragment was ligated into the digested pCR8/MCS to make a new plasmid named, "pCR8/RsrII-AvrII". The reaction used 1000ng pCR8/MCS and 500ng of fragment RsrII-

AvrII, while using the same amounts of other reagents as previously described. The new plasmid was transformed into Top 10 *E. coli*, incubated, confirmed positive by colony PCR, isolated, and stored as previously described.

pCR8/RsrII-AvrII was subjected to a RE digest using Rsr II and Avr II, as previously described. The fragment was separated on a gel, excised, purified, and analyzed on the Nanodrop. Fragment Sall-RsrII was removed from storage and ligated to the purified RsrII-AvrII fragment using reaction conditions similarly described and named, “1.4 GVCV”. The orientation of each fragment from Figure 25 is shown as the final construct in Figure 26. Concurrently, pCR8/MCS was digested with Sal I and Avr II and the 1.4 GVCV fragment was ligated into pCR8/MCS to become pCR8/GVCV and is shown in Figure 27. pCR8/GVCV was transformed into competent *E. coli*, incubated, confirmed positive by colony PCR, isolated, and stored as previously described. Further confirmation of the construct was performed by RE digest with a double cutter RE BsrGI. This RE flanks the region of the 1.4 length GVCV insert and provides a fragment of 11,245 bps. The fragment was viewed on a 0.5% agarose gel, excised, purified, and analyzed on the Nanodrop. The fragment was labeled, “BsrGI GVCV”.

Transfer to binary vector and *Agrobacterium* transformation. An LR recombination reaction using Gateway™ technology was used to transfer the 1.4 genome insert from pCR8/GW/TOPO into pGWB 401. Reaction conditions were according to the manufacturer protocol. Concurrently, the pGWB 401 plasmid was digested with a double cutter, BsrGI that was previously used to excise the 1.4 genome length from the pCR8/GW/TOPO backbone. The BsrGI GVCV fragment was ligated into the pGWB 401 backbone using reaction conditions as previously describe. The 1.4 genome length of

GVCV in the gateway binary vector 401 is named pGWB/GVCV. Aliquots of 1µl of each reaction were transformed into competent *E. coli* and successful recombinant plasmids were selected for on a LB agar with 50µM Kanamycin. Colony PCR using M13 F and GVCV specific primer 1179 R (Table 1) was used to test for successful transformations. Liquid cultures were taken of positive colonies and a sample was stored at -80°C. Plasmid pGWB/GVCV, shown in Figure 28, was then transformed into competent *Agrobacterium* 'GV3101', plated on rifampicin and kanamycin selective LB agar plates, and incubated in the dark at 28°C for 48 hours. Colony PCR using GVCV internal primers was used to select against false positive transformations. *Agrobacterium* that tested positive for pGWB/GVCV were grown in LB broth in the same conditions and a sample was stored at -80°C.

Transfection of *Nicotiana benthamiana*. *Nicotiana benthamiana* were grown from seed and tested for the presence of GVCV while pGWB/GVCV transformed *Agrobacterium* were grown to OD600. Transfections of 20 *N. benthamiana* plants were done by syringe infiltration. The transfected plants were placed in insect-proof tents to prevent the potential for recombinant GVCV DNA to escape, and the plants were grown in standard greenhouse conditions. Control plants that were not inoculated were also placed in insect-proof tents and grown in the same conditions. Progression of any disease symptoms was monitored for a month. At the end of the month, standard PCR detection using a triplex PCR was used to test for replication of GVCV.

Transfections into susceptible grapevine 'Chardonnay' will proceed only in when there is successful replication in the *N. benthamiana* alternative host. Syringe infiltration

and vacuum infiltration are used to test if pGWB/GVCV can successfully lead to a persistent infection in grapevines while also producing the associated disease symptoms.

Sequencing of pGWB/GVCV. Sequencing of the construct was done at Nevada Genomics, using M13 primers, and GVCV specific primers in a primer walking strategy. Samples were prepared using 500ng of pGWB/GVCV with the desired primers and shipped. Sequences were provided by Nevada Genomics in the form of a chromatograph that includes the nucleotide sequence and a phred quality score of the likelihood the correct base was called. The chromat file was imported to the CodonCode Aligner software package and the sequences were aligned to the theoretical sequence of the 1.4 genome length clone built on Serial Cloner. Only sequences where phred scores were above 20 were kept, corresponding to a 99% accuracy of base-calling.

Results

Summary. The first attempt at construction of the pGWB/GVCV fragment proved unsuccessful. There was evidence at each stage that the construction was successful, but upon sequencing of pGWB/GVCV, it became clear that there were false positives along the way. The process was attempted again, but a detailed look at each step for the first attempt provides evidence for possible error.

Construction. PCR fragments 1179 and 4804 were amplified using a high-fidelity polymerase. The respective bands were purified and inserted into pCR8/GW/TOPO, and transformed into *E. coli*. The plasmids were isolated from liquid *E. coli* and digested with the aforementioned REs, and these digested fragments were purified from an agarose gel to produce fragments for ligation. The ligation of the

fragments RsrII-SalI and SalI-AvrII to make fragment RsrII-AvrII at 7,286 bps is shown in Figure 29. The ligated fragments were excised from the gel, purified, and transformed into RE digested pCR8/MCS.

pCR8/ RsrII-AvrII was digested with the corresponding REs, the band was purified from the gel to isolate fragment “RsrII-AvrII”, and it was ligated to fragment “SalI-RsrII” to make the fragment “1.4 GVCV”. pCR8/MCS was digested with REs Sal I and Avr II, and the fragment “1.4 GVCV” was ligated to the pCR8/GW/TOPO backbone to create plasmid pCR8/GVCV.

Transfer to binary vector and *Agrobacterium* transformation. An LR clonase reaction was attempted using the manufacturer’s protocol, but was unsuccessful, producing strange banding patterns when imaged on a gel. The traditional method of cloning was pursued. BsrG I restriction sites were placed in the Gateway plasmids by the manufacturers to provide an avenue of traditional cloning. These sites flank the TOPO site where the LR reaction would insert the “1.4 GVCV”, so the BsrG I enzyme was used to digest pCR8/GVCV and pGWB 401 to transfer the GVCV insert into the binary vector for *Agrobacterium* mediated transfection. Bands were purified from the gel, and ligated to form pGWB/GVCV as shown in Figure 30.

pGWB/GVCV was transformed into competent *A. tumefaciens* ‘GV 3101’ and selection of successfully transformed bacteria utilized antibiotic selection plates. Colony PCR provided evidence that two of five tested colonies had the correct plasmid. Liquid cultures of *A. tumefaciens* ‘GV 3101’ were grown to an OD of 600 and used to infiltrate leaves of *N. benthamiana* by syringe, while a sample of pGWB/GVCV was sent for

sequencing. GVCV like symptoms were noticed, but PCR assays never detected viral nucleic acids after 2 months of incubation.

Sequencing. Nevada Genomics sequencing did not show GVCV DNA between the M13 primers that flanked the insert site. The sequence that was recovered was uploaded to BLAST and a BLASTN search was queried against the GenBank database. The hits all corresponded to Gateway cloning vectors, suggesting that the ligations were backbone within backbone.

Second Attempt. A second attempt was made at construction of the clone, since it is unclear where error was introduced. The process was started from scratch, beginning with the PCR amplification of the overlapping fragments 1179 and 4804. The PCR amplification was successful and the fragments were gel purified and introduced to pCR8/GW/TOPO to make pCR8/1179 and pCR8/4804. Figure 31 shows a successful RE digest of both plasmids. The gel was switched to a 0.5% agarose solution and ran for two hours to separate bands that were similar in fragment length. This is believed to be the step that introduced error, and will be discussed further in the discussion section. Continuation of the construction of the clone follows the methods previously described is currently under way.

Discussion

The failure of the first attempt at construction was likely researcher's error. The band sizes of the first RE digest are similar for each of the three fragments used to construct the clone, and the backbone of the pCR8/GW/TOPO vector from where they were excised. Table 5 lists the REs used and the expected band sizes that would be

imaged on a gel. It is likely that the similar sizes of the fragments, the 1% agarose gel, and the inadequate time for separation all contributed to the failure to separate the bands in the initial attempt at construction. Figure 31 shows the separation of the bands of the digested pCR8/1179 and pCR8/4804 plasmids on a 0.5% agarose gel run at 2 hours. It is obvious that the bands were too similar in size to fully separate on the first attempt, so a test for contamination of the pCR8/GVCV plasmid was performed. Figure 32 shows the plasmids used for construction loaded into a 0.5% gel with no RE. There should be only one band, whereas there are two. It is possible that the first attempt made a chimeric plasmid of backbone and GVCV inserts. Considering they have similar sizes and the same restriction sites, if the bands of the pCR8/GW/TOPO backbone and GVCV fragments were purified together, then there could be ligation of backbone to GVCV and tests using restriction enzymes and GVCV specific primers would provide false positives. The insert's 5' and 3' ends were pCR8/GW/TOPO sequences, so the colony PCR assays must have detected a GVCV sequence that was flanked by backbone sequences. This unique failure provided positive results until the construct was fully built into pGWB/GVCV.

The construction of the second attempt will proceed with much more care. Gel times will be longer to allow full separation of bands, especially of similar lengths, and sequencing will be done at regular intervals instead of at the end, as it is a definitive method for confirmation of construct makeup. Greater care will also be taken in making sure the resolution of the ladder is good enough for determining the size of detailed bands, instead of looking at relative regions. The methods and designs are sound and should provide the correct construct if proper care is taken in each step.

REFERENCES

1. **Cavaliere D, McGovern PE, Hartl DL, Mortimer R, Polsinelli M.** 2003. Evidence for *S. cerevisiae* fermentation in ancient wine. *J Mol Evol* 57:S226–S232.
2. **McGovern PE, Fleming SJ, Katz SH.** 2003. The origins and ancient history of wine: food and nutrition in history and anthropology. Routledge.
3. **McGovern P, Jalabadze M, Batiuk S, Callahan MP, Smith KE, Hall GR, Kvavadze E, Maghradze D, Rusishvili N, Bouby L.** 2017. Early Neolithic wine of Georgia in the South Caucasus. *Proc Natl Acad Sci* 114:E10309–E10318.
4. **(OIV) IO of V and W.** 2012. Statistical Report on World Vitiviniculture 2012.
5. **NASS U.** 2011. USDA National Agricultural Statistics Service. Acreage Report.
6. 2015. Missouri Wines. Industry.
7. **Simms C.** 2017. The grape depression. *New Sci* 236:60–62.
8. 2015. National Clean Plant Network. Natl Clean Plant Centers.
9. **Meng B, Martelli GP, Golino DA, Fuchs M.** 2017. Grapevine Viruses: Molecular Biology, Diagnostics and Management. Springer.
10. **Fuller KB, Alston JM, Golino DA.** 2015. The economic benefits from virus-screening: A case study of grapevine leafroll in the North Coast of California. *Am J Enol Vitic ajev-2014*.
11. **Gómez MI, Atallah SS, Martinson TE, Fuchs MF, White GB.** 2010. Economic analysis of the financial impact of the grape leafroll virus (GLRV) in the Finger Lakes region of New York. Charles H. Dyson School of Applied Economics and Management, College of Agriculture and Life Sciences, Cornell University.
12. **Cooper I, Jones RAC.** 2006. Wild plants and viruses: under-investigated ecosystems. *Adv Virus Res* 67:1–47.
13. **Jones RAC.** 2009. Plant virus emergence and evolution: origins, new encounter scenarios, factors driving emergence, effects of changing world conditions, and prospects for control. *Virus Res* 141:113–130.
14. **Scholthof K-BG.** 2007. The disease triangle: pathogens, the environment and society. *Nat Rev Microbiol* 5:152.
15. **Rothman KJ, Greenland S, Lash TL.** 2008. Modern epidemiology.

16. **Madden L V, Hughes G, Bosch F.** 2007. The study of plant disease epidemics. American Phytopathological Society (APS Press).
17. **Van der Plank JE.** 2013. Plant diseases: epidemics and control. Elsevier.
18. **Holmes TP, Aukema JE, Von Holle B, Liebhold A, Sills E.** 2009. Economic impacts of invasive species in forests: past, present, and future. *Ann N Y Acad Sci* 1162:18–38.
19. **Paillet FL.** 1982. The ecological significance of American chestnut (*Castanea dentata* (Marsh.) Borkh.) in the Holocene forests of Connecticut. *Bull Torrey Bot Club* 457–473.
20. **Bos L.** 1982. Crop losses caused by viruses. *Crop Prot* 1:263–282.
21. **Legg JP, Fauquet CM.** 2004. Cassava mosaic geminiviruses in Africa. *Plant Mol Biol* 56:585–599.
22. **Jones JDG, Dangl JL.** 2006. The plant immune system. *Nature* 444:323.
23. **Chisholm ST, Coaker G, Day B, Staskawicz BJ.** 2006. Host-microbe interactions: shaping the evolution of the plant immune response. *Cell* 124:803–814.
24. **Baker B, Zambryski P, Staskawicz B, Dinesh-Kumar SP.** 1997. Signaling in plant-microbe interactions. *Science* (80-) 276:726–733.
25. **Lu S, Sun Y, Amerson H, Chiang VL.** 2007. MicroRNAs in loblolly pine (*Pinus taeda* L.) and their association with fusiform rust gall development. *Plant J* 51:1077–1098.
26. **Xin M, Wang Y, Yao Y, Xie C, Peng H, Ni Z, Sun Q.** 2010. Diverse set of microRNAs are responsive to powdery mildew infection and heat stress in wheat (*Triticum aestivum* L.). *BMC Plant Biol* 10:123.
27. **Ding S-W, Li H, Lu R, Li F, Li W-X.** 2004. RNA silencing: a conserved antiviral immunity of plants and animals. *Virus Res* 102:109–115.
28. **Ding S-W.** 2010. RNA-based antiviral immunity. *Nat Rev Immunol* 10:632.
29. **Lewsey MG, Murphy AM, MacLean D, Dalchau N, Westwood JH, Macaulay K, Bennett MH, Moulin M, Hanke DE, Powell G.** 2010. Disruption of two defensive signaling pathways by a viral RNA silencing suppressor. *Mol plant-microbe Interact* 23:835–845.

30. **Zvereva AS, Pooggin MM.** 2012. Silencing and innate immunity in plant defense against viral and non-viral pathogens. *Viruses* 4:2578–2597.
31. **Csorba T, Kontra L, Burgyán J.** 2015. Viral silencing suppressors: tools forged to fine-tune host-pathogen coexistence. *Virology* 479:85–103.
32. **Skalsky RL, Cullen BR.** 2010. Viruses, microRNAs, and host interactions. *Annu Rev Microbiol* 64:123–141.
33. **Guo YE, Steitz JA.** 2014. Virus meets host microRNA: the destroyer, the booster, the hijacker. *Mol Cell Biol* MCB-00871.
34. **Ambros V.** 2004. The functions of animal microRNAs. *Nature* 431:350.
35. **Bartel DP.** 2004. MicroRNAs: genomics, biogenesis, mechanism, and function. *Cell* 116:281–297.
36. **Laliberté J-F, Sanfaçon H.** 2010. Cellular remodeling during plant virus infection. *Annu Rev Phytopathol* 48:69–91.
37. **Campillo-Balderas JA, Lazcano A, Becerra A.** 2015. Viral genome size distribution does not correlate with the antiquity of the host lineages. *Front Ecol Evol* 3:143.
38. **Nasir A, Kim KM, Caetano-Anollés G.** 2012. Viral evolution: primordial cellular origins and late adaptation to parasitism. *Mob Genet Elements* 2:247–252.
39. Villarreal LP. 2005. *Viruses and the evolution of life.* ASM press.
40. **Carstens EB.** 2012. Introduction to virus taxonomy. *Virus Taxon Ninth Rep Int Comm Taxon Viruses*,(eds King, AMQ, Adams, MJ, Carstens, EB, Lefkowitz, EJ) 3–20.
41. **Felsenstein J.** 1978. Cases in which parsimony or compatibility methods will be positively misleading. *Syst Zool* 27:401–410.
42. **Huelsenbeck JP, Ronquist F, Nielsen R, Bollback JP.** 2001. Bayesian inference of phylogeny and its impact on evolutionary biology. *Science* (80-) 294:2310–2314.
43. **Padidam M, Sawyer S, Fauquet CM.** 1999. Possible emergence of new geminiviruses by frequent recombination. *Virology* 265:218–225.
44. **Jetzt AE, Yu H, Klarmann GJ, Ron Y, Preston BD, Dougherty JP.** 2000. High rate of recombination throughout the human immunodeficiency virus type 1

genome. *J Virol* 74:1234–1240.

45. **Burke GR, Walden KKO, Whitfield JB, Robertson HM, Strand MR.** 2014. Widespread genome reorganization of an obligate virus mutualist. *PLoS Genet* 10:e1004660.
46. **Fraile A, Alonso-Prados JL, Aranda MA, Bernal JJ, Malpica JM, García-Arenal F.** 1997. Genetic exchange by recombination or reassortment is infrequent in natural populations of a tripartite RNA plant virus. *J Virol* 71:934–940.
47. **Steinhauer DA, Holland JJ.** 1987. Rapid evolution of RNA viruses. *Annu Rev Microbiol* 41:409–431.
48. **García-Arenal F, Fraile A, Malpica JM.** 2001. Variability and genetic structure of plant virus populations. *Annu Rev Phytopathol* 39:157–186.
49. **García-Arenal F, Fraile A, Malpica JM.** 2003. Variation and evolution of plant virus populations. *Int Microbiol* 6:225–232.
50. **Roossinck MJ.** 1997. Mechanisms of plant virus evolution. *Annu Rev Phytopathol* 35:191–209.
51. **Nasir A, Caetano-Anollés G.** 2015. A phylogenomic data-driven exploration of viral origins and evolution. *Sci Adv* 1:e1500527.
52. **Van Regenmortel MH V.** 2007. Virus species and virus identification: past and current controversies. *Infect Genet Evol* 7:133–144.
53. **Fauquet CM, Stanley J.** 2005. Revising the way we conceive and name viruses below the species level: a review of geminivirus taxonomy calls for new standardized isolate descriptors. *Arch Virol* 150:2151–2179.
54. **Kuhn JH, Bao Y, Bavari S, Becker S, Bradfute S, Brister JR, Bukreyev AA, Chandran K, Davey RA, Dolnik O.** 2013. Virus nomenclature below the species level: a standardized nomenclature for natural variants of viruses assigned to the family Filoviridae. *Arch Virol* 158:301–311.
55. **Sherman MP, Greene WC.** 2002. Slipping through the door: HIV entry into the nucleus. *Microbes Infect* 4:67–73.
56. **Krichevsky A, Kozlovsky S V, Gafni Y, Citovsky V.** 2006. Nuclear import and export of plant virus proteins and genomes. *Mol Plant Pathol* 7:131–146.
57. **Whittaker GR, Helenius A.** 1998. Nuclear import and export of viruses and virus genomes. *Virology* 246:1–23.

58. **Goodin M, Yelton S, Ghosh D, Mathews S, Lesnaw J.** 2005. Live-cell imaging of rhabdovirus-induced morphological changes in plant nuclear membranes. *Mol plant-microbe Interact* 18:703–709.
59. **Menissier J, De Murcia G, Lebeurier G, Hirth L.** 1983. Electron microscopic studies of the different topological forms of the cauliflower mosaic virus DNA: knotted encapsidated DNA and nuclear minichromosome. *EMBO J* 2:1067–1071.
60. **Kawakami S, Watanabe Y, Beachy RN.** 2004. Tobacco mosaic virus infection spreads cell to cell as intact replication complexes. *Proc Natl Acad Sci* 101:6291–6296.
61. **Bak A, Gargani D, Macia J-L, Malouvet E, Vernerey M-S, Blanc S, Drucker M.** 2013. Virus factories of Cauliflower mosaic virus are virion reservoirs that engage actively in vector-transmission. *J Virol* JVI-01883.
62. **Beauchemin C, Boutet N, Laliberté J-F.** 2007. Visualization of the interaction between the precursors of VPg, the viral protein linked to the genome of turnip mosaic virus, and the translation eukaryotic initiation factor iso 4E in planta. *J Virol* 81:775–782.
63. **Cheng C-P, Tzafrir I, Lockhart BE, Olszewski NE.** 1998. Tubules containing virions are present in plant tissues infected with Commelina yellow mottle badnavirus. *J Gen Virol* 79:925–929.
64. **Niehl A, Heinlein M.** 2011. Cellular pathways for viral transport through plasmodesmata. *Protoplasma* 248:75–99.
65. **Schoelz JE, Angel CA, Nelson RS, Leisner SM.** 2015. A model for intracellular movement of Cauliflower mosaic virus: the concept of the mobile virion factory. *J Exp Bot* 67:2039–2048.
66. **Fereres A, Raccach B.** 2015. Plant virus transmission by insects.
67. **Eigen M.** 1993. Viral quasispecies. *Sci Am* 269:42–49.
68. **Domingo E, Sheldon J, Perales C.** 2012. Viral quasispecies evolution. *Microbiol Mol Biol Rev* 76:159–216.
69. **Schneider WL, Roossinck MJ.** 2001. Genetic diversity in RNA virus quasispecies is controlled by host-virus interactions. *J Virol* 75:6566–6571.
70. **Becker Y.** 2000. Evolution of viruses by acquisition of cellular RNA or DNA nucleotide sequences and genes: an introduction. *Virus Genes* 21:7–12.
71. **Drake JW, Holland JJ.** 1999. Mutation rates among RNA viruses. *Proc Natl*

- Acad Sci 96:13910–13913.
72. **Drake JW.** 1993. Rates of spontaneous mutation among RNA viruses. *Proc Natl Acad Sci* 90:4171–4175.
 73. **Belshaw R, Pybus OG, Rambaut A.** 2007. The evolution of genome compression and genomic novelty in RNA viruses. *Genome Res* 17:0.
 74. **Drake JW.** 1991. A constant rate of spontaneous mutation in DNA-based microbes. *Proc Natl Acad Sci* 88:7160–7164.
 75. **Guimarães KMC, Silva SJC, Melo AM, Ramos-Sobrinho R, Lima JS, Zerbini FM, Assunção IP, Lima GSA.** 2015. Genetic variability of badnaviruses infecting yam (*Dioscorea* spp.) in northeastern Brazil. *Trop Plant Pathol* 40:111–118.
 76. **González-Jara P, Fraile A, Canto T, García-Arenal F.** 2009. The multiplicity of infection of a plant virus varies during colonization of its eukaryotic host. *J Virol* 83:7487–7494.
 77. **Tromas N, Zwart MP, Poulain M, Elena SF.** 2014. Estimation of the in vivo recombination rate for a plant RNA virus. *J Gen Virol* 95:724–732.
 78. **Froissart R, Roze D, Uzest M, Galibert L, Blanc S, Michalakakis Y.** 2005. Recombination every day: abundant recombination in a virus during a single multi-cellular host infection. *PLoS Biol* 3:e89.
 79. **Chenault KD, Melcher U.** 1994. Phylogenetic relationships reveal recombination among isolates of cauliflower mosaic virus. *J Mol Evol* 39:496–505.
 80. **Wright S.** 1931. Evolution in Mendelian populations. *Genetics* 16:97.
 81. **Fisher RA.** 1999. The genetical theory of natural selection: a complete variorum edition. Oxford University Press.
 82. **Altschuh D, Lesk AM, Bloomer AC, Klug A.** 1987. Correlation of co-ordinated amino acid substitutions with function in viruses related to tobacco mosaic virus. *J Mol Biol* 193:693–707.
 83. **Rajamäki M, Merits A, Rabenstein F, Andrejeva J, Paulin L, Kekarainen T, Kreuze JF, Forster RLS, Valkonen JPT.** 1998. Biological, serological, and molecular differences among isolates of potato A potyvirus. *Phytopathology* 88:311–321.
 84. **Deom CM, Naidu RA, Chiyembekeza AJ, Ntare BR, Subrahmanyam P.** 2000. Sequence diversity within the three agents of groundnut rosette disease. *Phytopathology* 90:214–219.

85. **Sanz AI, Fraile A, Gallego JM, Malpica JM, García-Arenal F.** 1999. Genetic variability of natural populations of cotton leaf curl geminivirus, a single-stranded DNA virus. *J Mol Evol* 49:672–681.
86. **Kurath G, Heick JA, Dodds JA.** 1993. RNase protection analyses show high genetic diversity among field isolates of satellite tobacco mosaic virus. *Virology* 194:414–418.
87. **Moury B, Fabre F, Senoussi R.** 2007. Estimation of the number of virus particles transmitted by an insect vector. *Proc Natl Acad Sci* 104:17891–17896.
88. **SYu M, Fedorkin ON, Schiemann J, Baulcombe DC, Atabekov JG.** 1997. Complementation of a potato virus X mutant mediated by bombardment of plant tissues with cloned viral movement protein genes. *J Gen Virol* 78:2077–2083.
89. **Malysenko SI, Kondakova OA, Taliansky ME, Atabekov JG.** 1989. Plant virus transport function: complementation by helper viruses is non-specific. *J Gen Virol* 70:2751–2757.
90. **Brown AJL.** 1997. Analysis of HIV-1 env gene sequences reveals evidence for a low effective number in the viral population. *Proc Natl Acad Sci* 94:1862–1865.
91. **Rouzine IM, Coffin JM.** 1999. Linkage disequilibrium test implies a large effective population number for HIV in vivo. *Proc Natl Acad Sci* 96:10758–10763.
92. **Kouyos RD, Althaus CL, Bonhoeffer S.** 2006. Stochastic or deterministic: what is the effective population size of HIV-1? *Trends Microbiol* 14:507–511.
93. **Jridi C, Martin J-F, Marie-Jeanne V, Labonne G, Blanc S.** 2006. Distinct viral populations differentiate and evolve independently in a single perennial host plant. *J Virol* 80:2349–2357.
94. **Mayr E.** 1999. Systematics and the origin of species, from the viewpoint of a zoologist. Harvard University Press.
95. **Kurath G, Dodds JA.** 1995. Mutation analyses of molecularly cloned satellite tobacco mosaic virus during serial passage in plants: evidence for hotspots of genetic change. *RNA* 1:491–500.
96. **Kurath G, Palukaitis P.** 1989. RNA sequence heterogeneity in natural populations of three satellite RNAs of cucumber mosaic virus. *Virology* 173:231–240.
97. **Provine WB.** 1989. Founder effects and genetic revolutions in microevolution and speciation: an historical perspective. *Genet Speciat Found Princ* 43–76.

98. **Eni AO, Hughes J d'A, Asiedu R, Rey MEC.** 2008. Sequence diversity among badnavirus isolates infecting yam (*Dioscorea* spp.) in Ghana, Togo, Benin and Nigeria. *Arch Virol* 153:2263–2272.
99. **Umber M, Filloux D, Muller E, Laboureau N, Galzi S, Roumagnac P, Iskra-Caruana M, Pavis C, Teycheney P, Seal SE.** 2014. The genome of African yam (*Dioscorea cayenensis-rotundata* complex) hosts endogenous sequences from four distinct badnavirus species. *Mol Plant Pathol* 15:790–801.
100. **Bhat AI, Sasi S, Revathy KA, Deeshma KP, Saji K V.** 2014. Sequence diversity among badnavirus isolates infecting black pepper and related species in India. *VirusDisease* 25:402–407.
101. **Yang IC, Hafner GJ, Revill PA, Dale JL, Harding RM.** 2003. Sequence diversity of South Pacific isolates of Taro bacilliform virus and the development of a PCR-based diagnostic test. *Arch Virol* 148:1957–1968.
102. **Geering ADW, McMichael LA, Dietzgen RG, Thomas JE.** 2000. Genetic diversity among Banana streak virus isolates from Australia. *Phytopathology* 90:921–927.
103. **Beach SJ.** 2015. Genetic Diversity of Grapevine Vein Clearing Virus Orf Ii and Characterization of a New Isolate.
104. **Rocha CS, Castillo-Urquiza GP, Lima ATM, Silva FN, Xavier CAD, Hora-Júnior BT, Beserra-Júnior JEA, Malta AWO, Martin DP, Varsani A.** 2013. Brazilian begomovirus populations are highly recombinant, rapidly evolving, and segregated based on geographical location. *J Virol* JVI-00155.
105. **Tsompana M, Abad J, Purugganan M, Moyer JW.** 2005. The molecular population genetics of the Tomato spotted wilt virus (TSWV) genome. *Mol Ecol* 14:53–66.
106. **Hillman BI, ANZoLA J V, Halpern BT, Cavileer TD, Nuss DL.** 1991. First field isolation of wound tumor virus from a plant host: minimal sequence divergence from the type strain isolated from an insect vector. *Virology* 185:896–900.
107. **Blok J, Mackenzie A, Guy P, Gibbs A.** 1987. Nucleotide sequence comparisons of turnip yellow mosaic virus isolates from Australia and Europe. *Arch Virol* 97:283–295.
108. **Jones RAC.** 2006. Control of plant virus diseases. *Adv Virus Res* 67:205–244.
109. **Anderson PK, Cunningham AA, Patel NG, Morales FJ, Epstein PR, Daszak**

- P. 2004. Emerging infectious diseases of plants: pathogen pollution, climate change and agrotechnology drivers. *Trends Ecol Evol* 19:535–544.
110. **Fargette D, Konate G, Fauquet C, Muller E, Peterschmitt M, Thresh JM.** 2006. Molecular ecology and emergence of tropical plant viruses. *Annu Rev Phytopathol* 44:235–260.
 111. **Morales FJ, Anderson PK.** 2001. The emergence and dissemination of whitefly-transmitted geminiviruses in Latin America. *Arch Virol* 146:415–441.
 112. **Seal SE, Jeger MJ, Van den Bosch F.** 2006. Begomovirus evolution and disease management. *Adv Virus Res* 67:297–316.
 113. **Gibbs A, Gibbs M, Ohshima K, García-Arenal F.** 2008. More about plant virus evolution: past, present, and future, p. 229–250. *In* *Origin and Evolution of Viruses* (Second Edition). Elsevier.
 114. **Jeger MJ, Seal SE, Van den Bosch F.** 2006. Evolutionary epidemiology of plant virus disease. *Adv Virus Res* 67:163–203.
 115. **Bhat AI, Hohn T, Selvarajan R.** 2016. Badnaviruses: the current global scenario. *Viruses* 8:177.
 116. **Polston JE, Anderson PK.** 1997. The emergence of whitefly-transmitted geminiviruses in tomato in the western hemisphere. *Plant Dis* 81:1358–1369.
 117. **Moriones E, Navas-Castillo J.** 2000. Tomato yellow leaf curl virus, an emerging virus complex causing epidemics worldwide. *Virus Res* 71:123–134.
 118. **Morales FJ.** 2006. History and current distribution of begomoviruses in Latin America. *Adv Virus Res* 67:127–162.
 119. **Borah BK, Sharma S, Kant R, Johnson AMA, Saigopal DVR, Dasgupta I.** 2013. Bacilliform DNA-containing plant viruses in the tropics: commonalities within a genetically diverse group. *Mol Plant Pathol* 14:759–771.
 120. **Mahy BWJ, Van Regenmortel MH V.** 2008. *Encyclopedia of virology*. Academic Press.
 121. **Zhang Y.** 2016. Characterization of grapevine vein clearing virus expression strategy and development of caulimovirus infectious clones. University of Missouri--Columbia.
 122. **Su L.** 2018. Assessment of Resistance to *Botrytis Cinerea* in *Arabidopsis* Expressing Grapevine STS Genes and Analysis of New Grapevine Vein Clearing Virus Isolates.

123. **Ryabova LA, Hohn T.** 2000. Ribosome shunting in the cauliflower mosaic virus 35S RNA leader is a special case of reinitiation of translation functioning in plant and animal systems. *Genes Dev* 14:817–829.
124. **Fütterer J, Kiss-László Z, Hohn T.** 1993. Nonlinear ribosome migration on cauliflower mosaic virus 35S RNA. *Cell* 73:789–802.
125. **Su L, Gao S, Huang Y, Ji C, Wang D, Ma Y, Fang R, Chen X.** 2007. Complete genomic sequence of *Dracaena mottle virus*, a distinct badnavirus. *Virus Genes* 35:423–429.
126. **Kalischuk ML, Fusaro AF, Waterhouse PM, Pappu HR, Kawchuk LM.** 2013. Complete genomic sequence of a *Rubus* yellow net virus isolate and detection of genome-wide pararetrovirus-derived small RNAs. *Virus Res* 178:306–313.
127. **Cheng C-P, Lockhart BEL, Olszewski NE.** 1996. The ORF I and II Proteins of *Commelina Yellow Mottle Virus* Are Virion-Associated. *Virology* 223:263–271.
128. **Jacquot E, Hagen LS, Jacquemond M, Yot P.** 1996. The open reading frame 2 product of cacao swollen shoot badnavirus is a nucleic acid-binding protein. *Virology* 225:191–195.
129. **Medberry SL, Lockhart BEL, Olszewski NE.** 1990. Properties of *Commelina yellow mottle virus*'s complete DNA sequence, genomic discontinuities and transcript suggest that it is a pararetrovirus. *Nucleic Acids Res* 18:5505–5513.
130. **Hohn T, Fütterer J, Hull R.** 1997. The proteins and functions of plant pararetroviruses: knowns and unknowns. *CRC Crit Rev Plant Sci* 16:133–161.
131. **Hagen LS, Jacquemond M, Lepingle A, Lot H, Tepfer M.** 1993. Nucleotide sequence and genomic organization of cacao swollen shoot virus. *Virology* 196:619–628.
132. **Hohn T, Rothnie H.** 2013. Plant pararetroviruses: replication and expression. *Curr Opin Virol* 3:621–628.
133. **Pfeiffer P, Hohn T.** 1983. Involvement of reverse transcription in the replication of cauliflower mosaic virus: a detailed model and test of some aspects. *Cell* 33:781–789.
134. **Schoelz JE, Wintermantel WM.** 1993. Expansion of viral host range through complementation and recombination in transgenic plants. *Plant Cell* 5:1669–1679.
135. **Luo GX, Taylor J.** 1990. Template switching by reverse transcriptase during DNA synthesis. *J Virol* 64:4321–4328.

136. **Dixon L, Nyffenegger T, Delley G, Martinez-Izquierdo J, Hohn T.** 1986. Evidence for replicative recombination in cauliflower mosaic virus. *Virology* 150:463–468.
137. **Bell SM, Bedford T.** 2017. Modern-day SIV viral diversity generated by extensive recombination and cross-species transmission. *PLoS Pathog* 13:e1006466.
138. **Poirier EZ, Vignuzzi M.** 2017. Virus population dynamics during infection. *Curr Opin Virol* 23:82–87.
139. **Geering ADW, Maumus F, Copetti D, Choisine N, Zwickl DJ, Zytnicki M, McTaggart AR, Scalabrin S, Vezzulli S, Wing RA.** 2014. Endogenous florendoviruses are major components of plant genomes and hallmarks of virus evolution. *Nat Commun* 5:5269.
140. **Chabannes M, Iskra-Caruana M-L.** 2013. Endogenous pararetroviruses—a reservoir of virus infection in plants. *Curr Opin Virol* 3:615–620.
141. **Chen S, Liu R, Koyanagi KO, Kishima Y.** 2014. Rice genomes recorded ancient pararetrovirus activities: Virus genealogy and multiple origins of endogenization during rice speciation. *Virology* 471:141–152.
142. **Gayral P, Iskra-Caruana M-L.** 2009. Phylogeny of Banana streak virus reveals recent and repetitive endogenization in the genome of its banana host (*Musa* sp.). *J Mol Evol* 69:65–80.
143. **Zhang Y, Singh K, Kaur R, Qiu W.** 2011. Association of a novel DNA virus with the grapevine vein-clearing and vine decline syndrome. *Phytopathology* 101:1081–1090.
144. **Singh K, Kaur R, Qiu W.** 2012. New virus discovery by deep sequencing of small RNAs, p. 177–191. *In* RNA Abundance Analysis. Springer.
145. **Beach S, Kovens M, Hubbert L, Honesty S, Guo Q, Pap D, Dai R, Kovacs L, Qiu W.** 2016. Genetic and Phenotypic Characterization of Grapevine vein clearing virus from Wild *Vitis rupestris*. *Phytopathology* 107:138–144.
146. **Guo Q, Honesty S, Xu ML, Zhang Y, Schoelz J, Qiu W.** 2014. Genetic diversity and tissue and host specificity of Grapevine vein clearing virus. *Phytopathology* 104:539–547.
147. **Zhang Y, Angel CA, Valdes S, Qiu W, Schoelz JE.** 2015. Characterization of the promoter of Grapevine vein clearing virus. *J Gen Virol* 96:165–169.

148. **Petersen SM. 2016.** Discover And Analysis Of Grapevine Vein-Clearing Virus In *Ampelopsis Cordata*.
149. **Howard S, Qiu W. 2017.** Viral small RNAs reveal the genomic variations of three grapevine vein clearing virus quasispecies populations. *Virus Res* 229:24–27.
150. **Kumar S, Nei M. 2000.** *Molecular evolution and phylogenetics*. Oxford University Press New York.
151. **Nei M. 1987.** *Molecular evolutionary genetics*. Columbia university press.
152. **Drummond AJ, Bouckaert RR. 2015.** *Bayesian evolutionary analysis with BEAST*. Cambridge University Press.
153. **Hein J, Schierup M, Wiuf C. 2004.** *Gene genealogies, variation and evolution: a primer in coalescent theory*. Oxford University Press, USA.
154. **Kingman JFC. 1982.** The coalescent. *Stoch Process their Appl* 13:235–248.
155. **Nei M, Tajima F. 1981.** Genetic drift and estimation of effective population size. *Genetics* 98:625–640.
156. **Hartl DL, Clark AG, Clark AG. 1997.** *Principles of population genetics*. Sinauer associates Sunderland.
157. **Kimura M. 1983.** *The neutral theory of molecular evolution*. Cambridge University Press.
158. **Hasegawa M, Kishino H, Yano T. 1985.** Dating of the human-ape splitting by a molecular clock of mitochondrial DNA. *J Mol Evol* 22:160–174.
159. **Jukes TH, Cantor CR. 1969.** Evolution of protein molecules. *Mamm protein Metab* 3:132.
160. **Muller HJ. 1932.** Some genetic aspects of sex. *Am Nat* 66:118–138.
161. **Fraile A, Pagán I, Anastasio G, Sáez E, García-Arenal F. 2010.** Rapid genetic diversification and high fitness penalties associated with pathogenicity evolution in a plant virus. *Mol Biol Evol* 28:1425–1437.
162. **de la Iglesia F, Elena SF. 2007.** Fitness declines in tobacco etch virus upon serial bottleneck transfers. *J Virol* 81:4941–4947.
163. **Domingo E, Holland JJ. 1997.** RNA virus mutations and fitness for survival. *Annu Rev Microbiol* 51:151–178.

164. **Kimura M.** 1980. A simple method for estimating evolutionary rates of base substitutions through comparative studies of nucleotide sequences. *J Mol Evol* 16:111–120.
165. **Uzzell T, Corbin KW.** 1971. Fitting discrete probability distributions to evolutionary events. *Science* (80-) 172:1089–1096.
166. **Arbogast BS.** 2001. Phylogeography: the history and formation of species. *Am Zool* 41:134–135.
167. **Hickerson MJ, Carstens BC, Cavender-Bares J, Crandall KA, Graham CH, Johnson JB, Rissler L, Victoriano PF, Yoder AD.** 2010. Phylogeography's past, present, and future: 10 years after Avise, 2000. *Mol Phylogenet Evol* 54:291–301.
168. **De Maio N, Wu C-H, O'Reilly KM, Wilson D.** 2015. New routes to phylogeography: a Bayesian structured coalescent approximation. *PLoS Genet* 11:e1005421.
169. **Kühnert D, Wu C-H, Drummond AJ.** 2011. Phylogenetic and epidemic modeling of rapidly evolving infectious diseases. *Infect Genet Evol* 11:1825–1841.
170. **Lemey P, Suchard M, Rambaut A.** 2009. Reconstructing the initial global spread of a human influenza pandemic: a Bayesian spatial-temporal model for the global spread of H1N1pdm. *PLoS Curr* 1.
171. **Bourhy H, Reynes J-M, Dunham EJ, Dacheux L, Larrous F, Huong VTQ, Xu G, Yan J, Miranda MEG, Holmes EC.** 2008. The origin and phylogeography of dog rabies virus. *J Gen Virol* 89:2673–2681.
172. **Abubakar Z, Ali F, Pinel A, Traore O, N'Guessan P, Notteghem J-L, Kimmins F, Konate G, Fargette D.** 2003. Phylogeography of Rice yellow mottle virus in Africa. *J Gen Virol* 84:733–743.
173. **Cuevas JM, Delaunay A, Visser JC, Bellstedt DU, Jacquot E, Elena SF.** 2012. Phylogeography and molecular evolution of Potato virus Y. *PLoS One* 7:e37853.
174. **Kumar S, Stecher G, Tamura K.** 2016. MEGA7: molecular evolutionary genetics analysis version 7.0 for bigger datasets. *Mol Biol Evol* 33:1870–1874.
175. **Thompson JD, Higgins DG, Gibson TJ.** 1994. CLUSTAL W: improving the sensitivity of progressive multiple sequence alignment through sequence weighting, position-specific gap penalties and weight matrix choice. *Nucleic Acids Res* 22:4673–4680.
176. **Martin DP, Murrell B, Golden M, Khoosal A, Muhire B.** 2015. RDP4: Detection and analysis of recombination patterns in virus genomes. *Virus Evol* 1.

177. **Schierup MH, Hein J.** 2000. Consequences of recombination on traditional phylogenetic analysis. *Genetics* 156:879–891.
178. **Rambaut A, Lam TT, Max Carvalho L, Pybus OG.** 2016. Exploring the temporal structure of heterochronous sequences using TempEst (formerly Path-O-Gen). *Virus Evol* 2:vew007.
179. **Smith MD, Wertheim JO, Weaver S, Murrell B, Scheffler K, Kosakovsky Pond SL.** 2015. Less is more: an adaptive branch-site random effects model for efficient detection of episodic diversifying selection. *Mol Biol Evol* 32:1342–1353.
180. **Drummond AJ, Rambaut A.** 2007. BEAST: Bayesian evolutionary analysis by sampling trees. *BMC Evol Biol* 7:214.
181. **Tavaré S.** 1986. Some probabilistic and statistical problems in the analysis of DNA sequences. *Lect Math life Sci* 17:57–86.
182. **Bielejec F, Rambaut A, Suchard MA, Lemey P.** 2011. SPREAD: spatial phylogenetic reconstruction of evolutionary dynamics. *Bioinformatics* 27:2910–2912.
183. **Drummond AJ, Nicholls GK, Rodrigo AG, Solomon W.** 2002. Estimating mutation parameters, population history and genealogy simultaneously from temporally spaced sequence data. *Genetics* 161:1307–1320.
184. **Hillis DM.** 1995. Approaches for assessing phylogenetic accuracy. *Syst Biol* 44:3–16.
185. **Posada D, Crandall KA.** 2002. The effect of recombination on the accuracy of phylogeny estimation. *J Mol Evol* 54:396–402.
186. **Holmes EC.** 2011. The evolution of endogenous viral elements. *Cell Host Microbe* 10:368–377.
187. **Feschotte C, Gilbert C.** 2012. Endogenous viruses: insights into viral evolution and impact on host biology. *Nat Rev Genet* 13:283.
188. **Murray GGR, Wang F, Harrison EM, Paterson GK, Mather AE, Harris SR, Holmes MA, Rambaut A, Welch JJ.** 2016. The effect of genetic structure on molecular dating and tests for temporal signal. *Methods Ecol Evol* 7:80–89.
189. **Duchêne D, Duchêne S, Ho SYW.** 2015. Tree imbalance causes a bias in phylogenetic estimation of evolutionary timescales using heterochronous sequences. *Mol Ecol Resour* 15:785–794.

190. **Jones AT, McGavin WJ, Geering ADW, Lockhart BEL.** 2001. A new badnavirus in *Ribes* species, its detection by PCR, and its close association with gooseberry vein banding disease. *Plant Dis* 85:417–422.
191. **BaSSO MF, FAJARDO TV, SalDaReIII P.** 2017. Grapevine virus diseases: economic impact and current advances in viral prospection and management. *Rev Bras Frutic* 39.
192. **Hubbert LC.** 2014. New Isolate of Grapevine Vein Clearing Virus Found in Grapevine in Native Habitat and Commercial Vineyard.
193. **Koch R.** 1884. An address on cholera and its bacillus. *Br Med J* 2:453.
194. **Yanagi M, Purcell RH, Emerson SU, Bukh J.** 1997. Transcripts from a single full-length cDNA clone of hepatitis C virus are infectious when directly transfected into the liver of a chimpanzee. *Proc Natl Acad Sci* 94:8738–8743.
195. **Rizzo TM, Palukaitis P.** 1990. Construction of full-length cDNA clones of cucumber mosaic virus RNAs 1, 2 and 3: generation of infectious RNA transcripts. *Mol Gen Genet MGG* 222:249–256.
196. **López-Moya JJ, García JA.** 2000. Construction of a stable and highly infectious intron-containing cDNA clone of plum pox potyvirus and its use to infect plants by particle bombardment. *Virus Res* 68:99–107.
197. **Huang Q, Hartung JS.** 2001. Cloning and sequence analysis of an infectious clone of Citrus yellow mosaic virus that can infect sweet orange via *Agrobacterium*-mediated inoculation. *J Gen Virol* 82:2549–2558.
198. **Huang Q, Hartung JS.** 2008. Construction of infectious clones of double-stranded DNA viruses of plants using citrus yellow mosaic virus as an example, p. 525–533. *In Plant Virology Protocols.* Springer.
199. **Hay JM, Jones MC, Blakebrough ML, Dasgupta I, Davies JW, Hull R.** 1991. An analysis of the sequence of an infectious clone of rice tungro bacilliform virus, a plant pararetrovirus. *Nucleic Acids Res* 19:2615–2621.
200. **NRCS U.** Plant Database.

Table 1: Number of samples collected over the previous years. “W” denotes wild and “C” denotes cultivated.

Year	Species	Total sampled	Positive sampled	Percent (%)
Before 2016	<i>A. cordata</i>	2	2	100
Before 2016	<i>V. spp.</i>	W-35 C*-42	W-2 C*- 35	W- 5.7 C- 83
2016	<i>A. cordata</i>	111	35	31.5
2016	<i>V. spp.</i>	W-14 C-19	W-0 C-4	W-0.0 C- 21.1
2017	<i>A. cordata</i>	257	85	33.1
2017	<i>V. spp.</i>	W-69	W-10	W-13.8
Total	<i>A. cordata</i>	370	122	33
Total	<i>V. spp.</i>	W-118 C-61	W-12 C-39	W-10.2 C-63.9

*: Samples were collected from only symptomatic vines.

Table 2: Primer list. Used in *Grapevine vein clearing* detection, ORF II amplification, sequencing, and construction of infectious clone.

Primer Name	Sequence (5'-3')
16s F	tgettaacacatgcaagtcgga
16s R	agccgtttccagctgttgtc
M13 F	gtttcccagtcacgac
M13 R	caggaaacagctatgac
697 F	gctgctgaatacactgtacg
963 F	tccatcacagatctaacggca
1101 F	ctgaaaggtagatgtccacg
1179 R	gccacgtggacatctacct
1634 R	caaggtagcgggcacgag
1935 R	tcggtgtagcactgtattct
4363 F	atctgctcaatttctgaaggagaag
4804 R	ggaatgcattgtgctcgtag

Table 3: Molecular clock rates of sequences and R² values.

ID	Rate (changes per site, per year)	R ²
<i>Badnavirus</i>	4.8 E ⁻³	7.49 E ⁻²
GVCV	1.0 E ⁻³	0.682
GVCV -ORF II	4.6 E ⁻³	7.43 E ⁻²

Table 4: Restriction enzyme list used in construction of clone.

Restriction Enzyme	Recognition Sequence (5'-3')
Sal I	GTCGAC
Rsr II	CGGWCCG
Avr II	CCTAGG
BsrG I	TGTACA
Hpa I	GTTAAC
Dra I	TTTAAA

Table 5: Table of plasmids and restriction enzymes used in the first step of clone construction. Note the similar sizes of the produced fragments of GVCV DNA and the pCR8/GW/TOPO backbone.

Plasmid	Restriction Enzymes	GVCV Fragment size	Plasmid Backbone size
pCR8/1179	Sal I and Avr II	3,429	3,903
pCR8/1179	Sal I and Rsr II	3,893	3,439
pCR8/4804	Rsr II and Sal I	3,853	3,072

Vitis rupestris Scheele
sand grape

Show All



General Information	
Symbol:	VIRU2
Group:	Dicot
Family:	Vitaceae
Duration:	Perennial
Growth Habit:	Shrub Vine
Native Status:	L48 N
Data Source and Documentation	

About our new maps

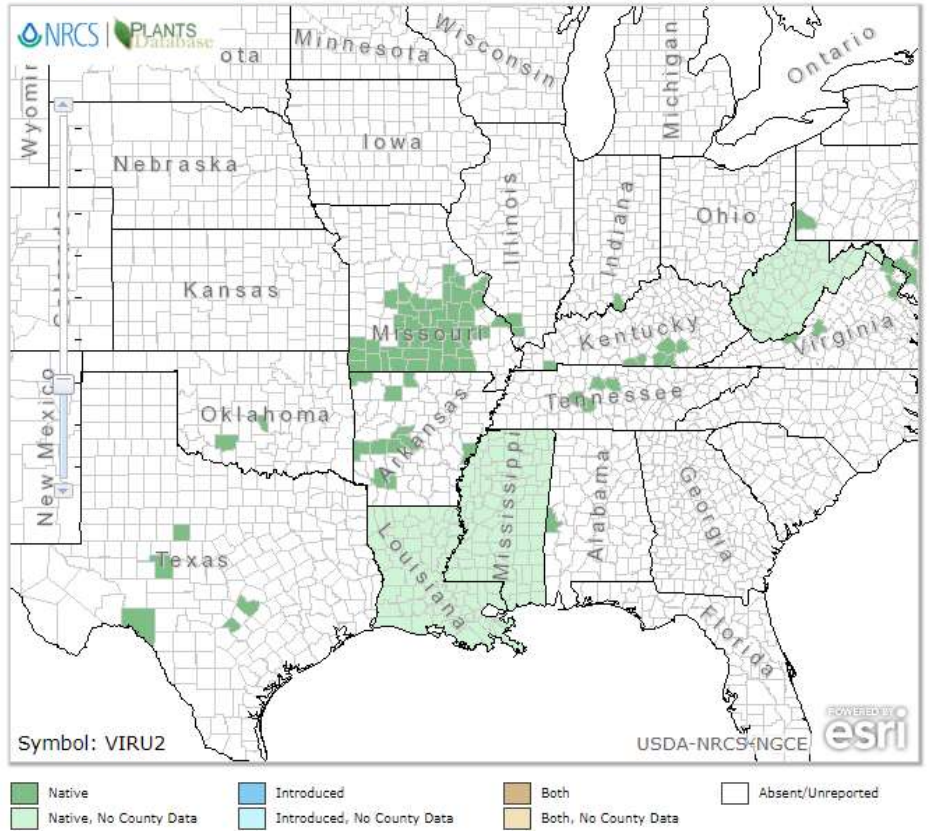


Figure 1: Native range of *Vitis rupestris*. Courtesy of USDA-NRCS (200).

Vitis riparia Michx.
riverbank grape

Show All



General Information	
Symbol:	VIRI
Group:	Dicot
Family:	Vitaceae
Duration:	Perennial
Growth Habit:	Vine
Native Status:	CAN N L48 N
Characteristics	
Data Source and Documentation	

About our new maps

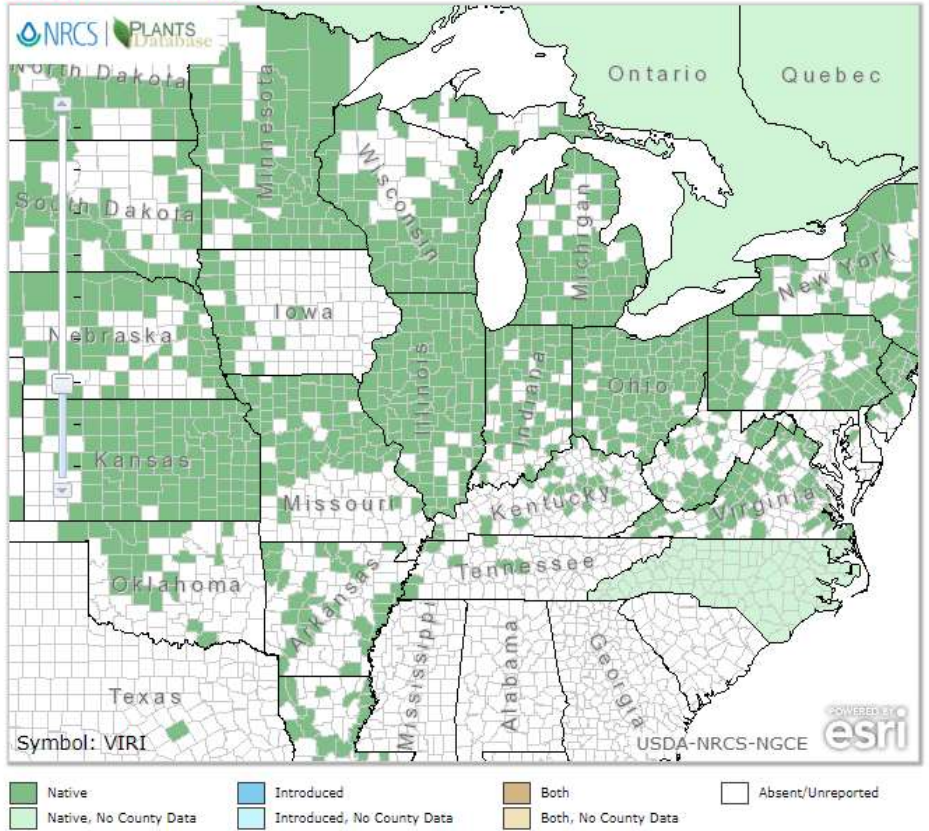


Figure 2: Native range of *Vitis riparia*. Courtesy of USDA-NRCS (200).

Ampelopsis cordata Michx.
heartleaf peppervine

Show All



General Information	
Symbol:	AMCO2
Group:	Dicot
Family:	Vitaceae
Duration:	Perennial
Growth Habit:	Vine
Native Status:	L48 N
Characteristics	
Data Source and Documentation	

About our new maps

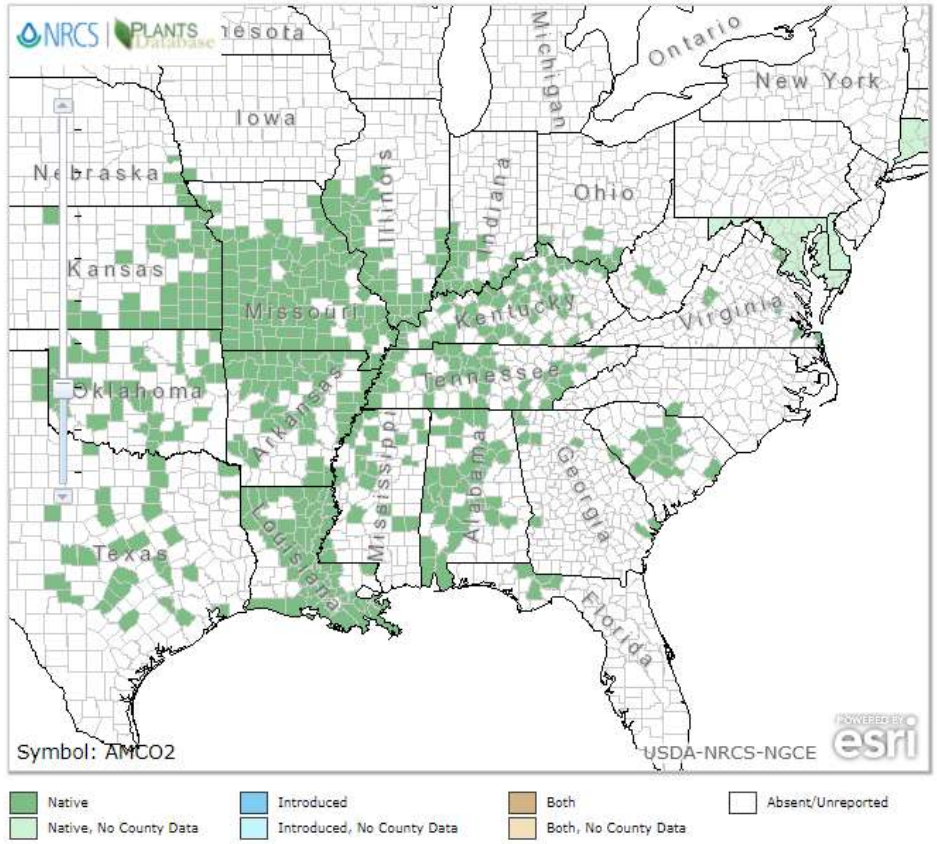


Figure 3: Native range of *Ampelopsis cordata*. Courtesy of USDA-NRCS (200).

Vitis cinerea (Engelm.) Engelm. ex Millard
graybark grape

Show All



General Information	
Symbol:	VICI2
Group:	Dicot
Family:	Vitaceae
Duration:	Perennial
Growth Habit:	Vine
Native Status:	L48 N
Characteristics	
Data Source and Documentation	

About our new maps

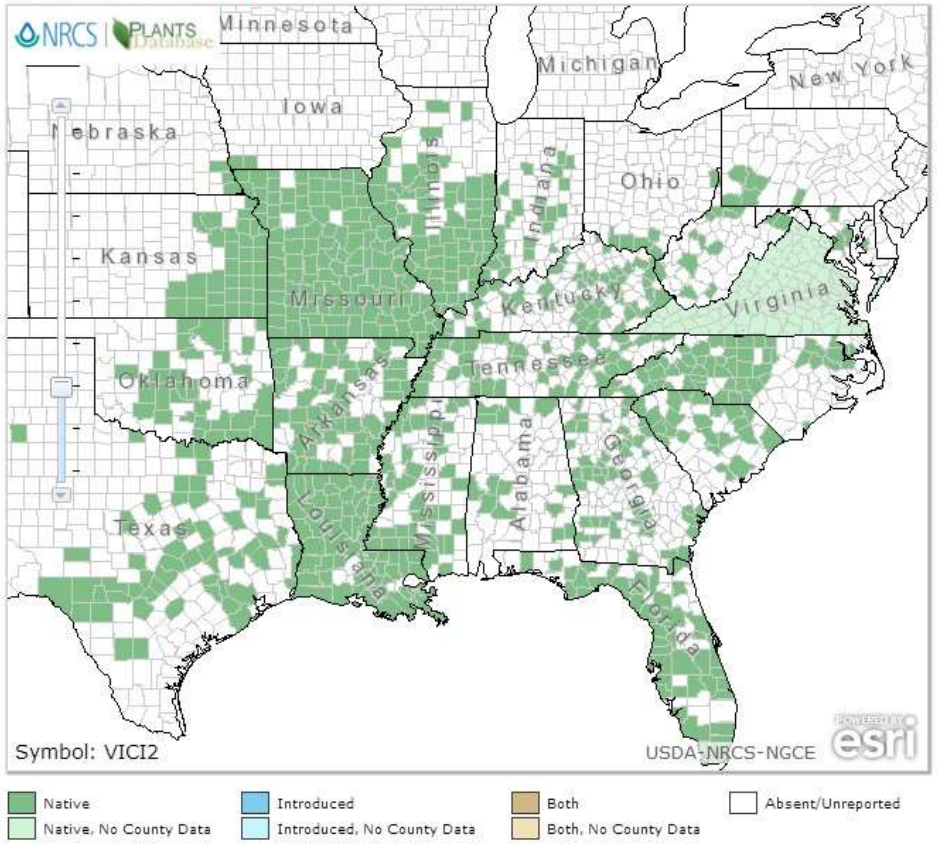


Figure 4: Native range of *Vitis cinerea*. Courtesy of USDA-NRCS (200).

Vitis vulpina L.
frost grape

Show All



General Information	
Symbol:	VIVU
Group:	Dicot
Family:	Vitaceae
Duration:	Perennial
Growth Habit:	Vine
Native Status:	CAN N L48 N
Characteristics	
Data Source and Documentation	

About our new maps

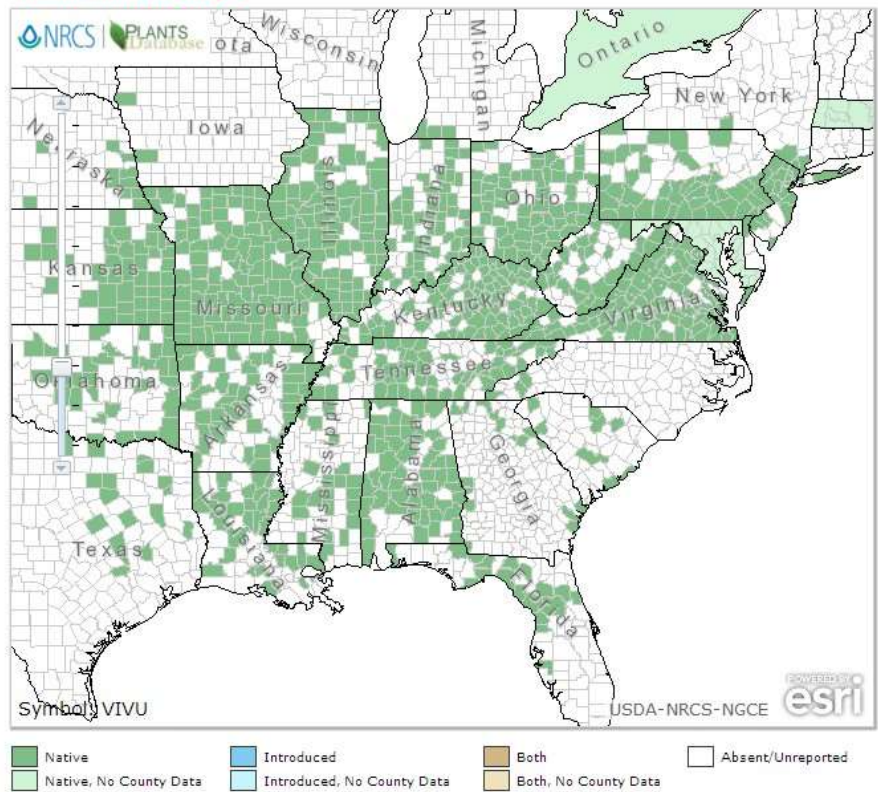


Figure 5: Native range of *Vitis vulpina*. Courtesy of USDA-NRCS (200).

Vitis L.
grape



[Show All](#)

General Information	
Symbol:	VITIS
Group:	Grass
Family:	Vitaceae
Duration:	
Growth Habit:	
Native States:	CA, IL, IN, MI, OH, PA, VA, WI, WY

Data Source and Documentation

About our new maps



Symbol: VITIS

USDA-NRCS-NCCE

Native
 Native, No County Data
 Introduced
 Introduced, No County Data
 Both
 Both, No County Data
 Unknown/Unrecorded

Vitis L.
grape



[Show All](#)

General Information	
Symbol:	VITIS
Group:	Grass
Family:	Vitaceae
Duration:	
Growth Habit:	
Native States:	CA, IL, IN, MI, OH, PA, VA, WI, WY

Data Source and Documentation

About our new maps



Symbol: VITIS

USDA-NRCS-NCCE

Native
 Native, No County Data
 Introduced
 Introduced, No County Data
 Both
 Both, No County Data
 Unknown/Unrecorded

Vitis L.
grape



[Show All](#)

General Information	
Symbol:	VITIS
Group:	Grass
Family:	Vitaceae
Duration:	
Growth Habit:	
Native States:	CA, IL, IN, MI, OH, PA, VA, WI, WY

Data Source and Documentation

About our new maps



Symbol: VITIS

USDA-NRCS-NCCE

Native
 Native, No County Data
 Introduced
 Introduced, No County Data
 Both
 Both, No County Data
 Unknown/Unrecorded

Figure 6: Native range of *Vitis* Spp. Courtesy of USDA-NRCS. Insets are the county distribution of the east and west coasts (200).

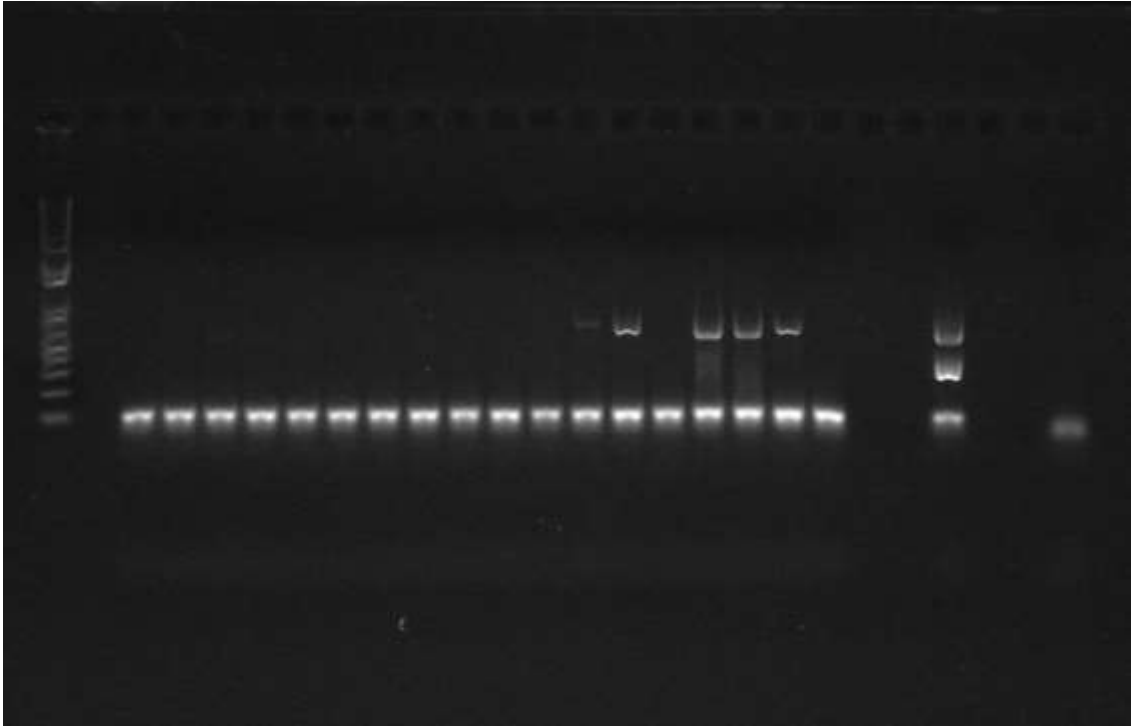


Figure 7: Example of triplex PCR diagnostic to test for *Grapevine vein clearing virus*.



Figure 8: Locations of *Grapevine vein clearing virus*-infected samples in from 2016 and 2017.

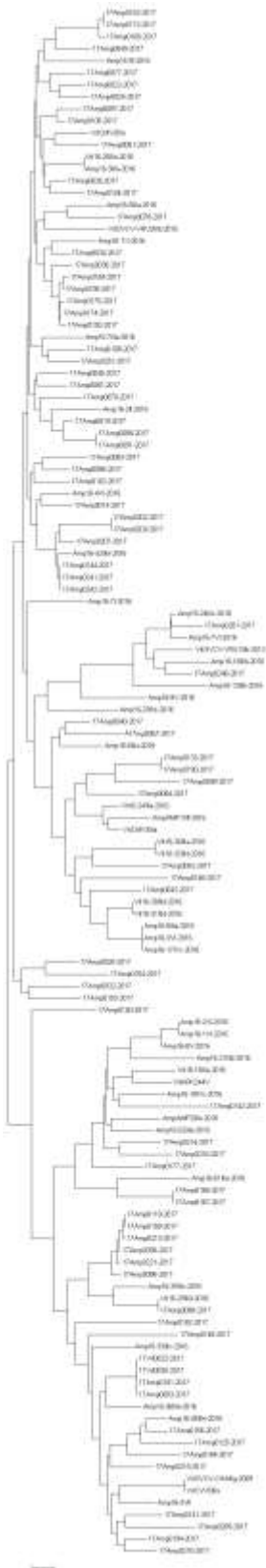


Figure 9: Neighbor-joining tree of GVCV ORF II sequences. Used for estimation of molecular clock.

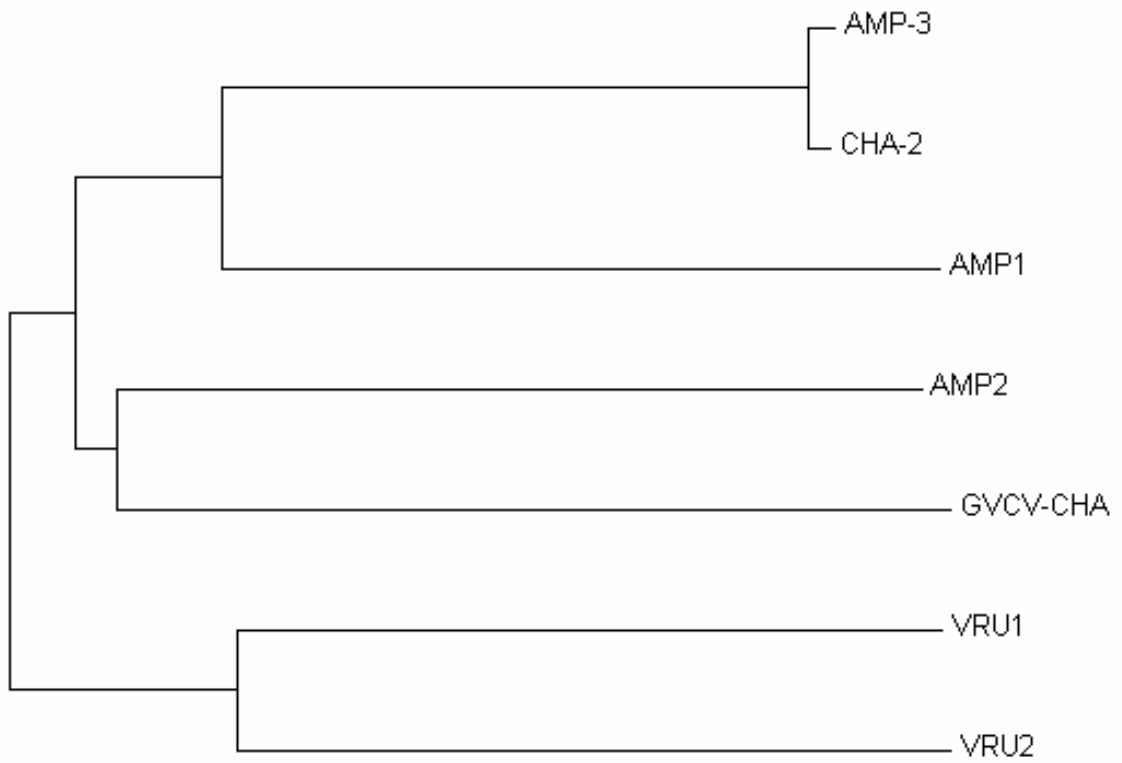


Figure 10: Neighbor-joining tree of *Grapevine vein clearing virus* genomes. It is used for estimation of molecular clock.

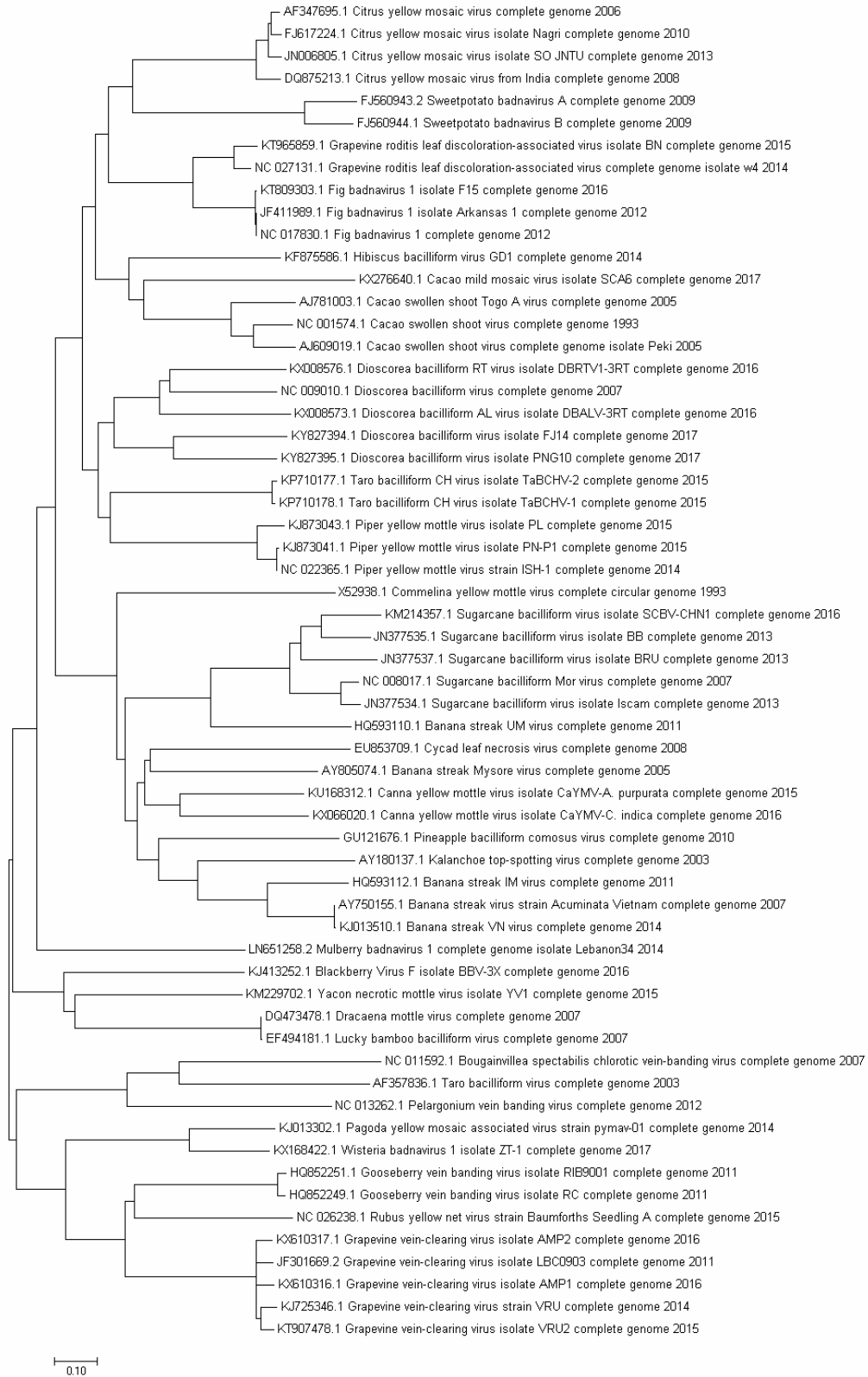


Figure 11: Neighbor-joining tree of *Badnavirus* genomes, that is used for estimation of molecular clock.

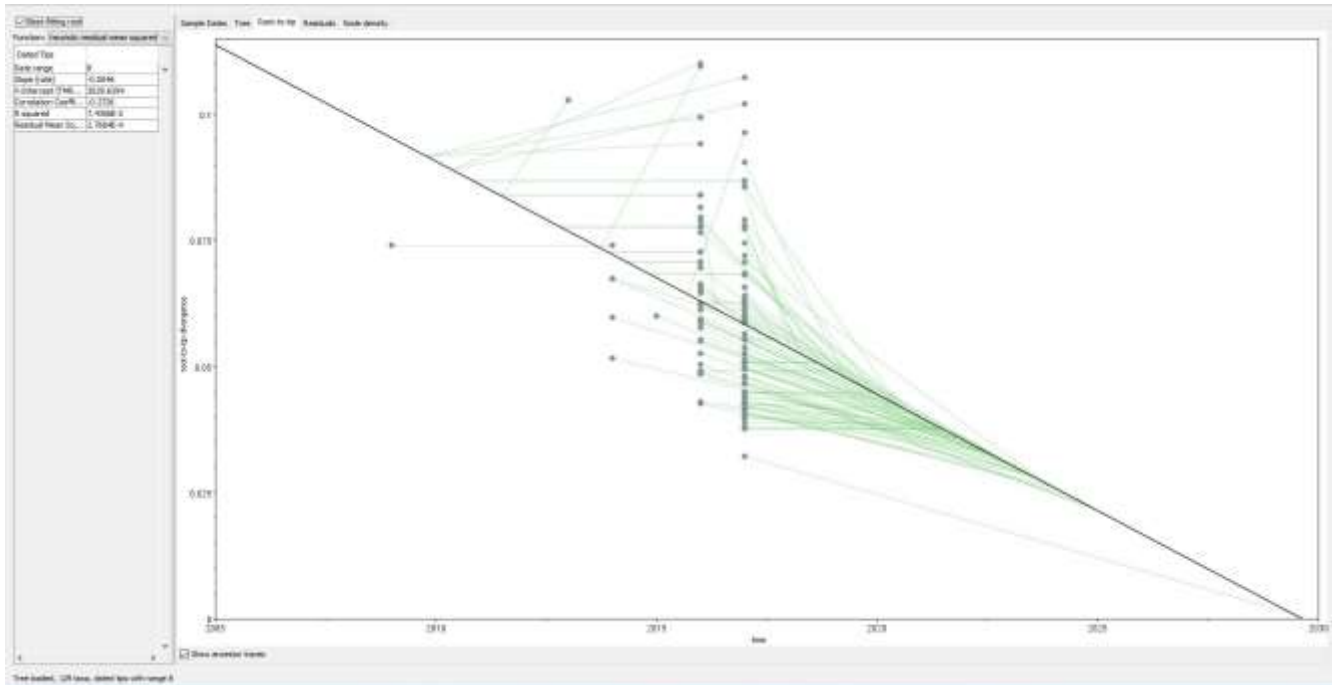


Figure 12: Linear regression of evolutionary distance and time of GVCV based on ORF II sequences. Statistics are in the table at the upper left-hand corner.

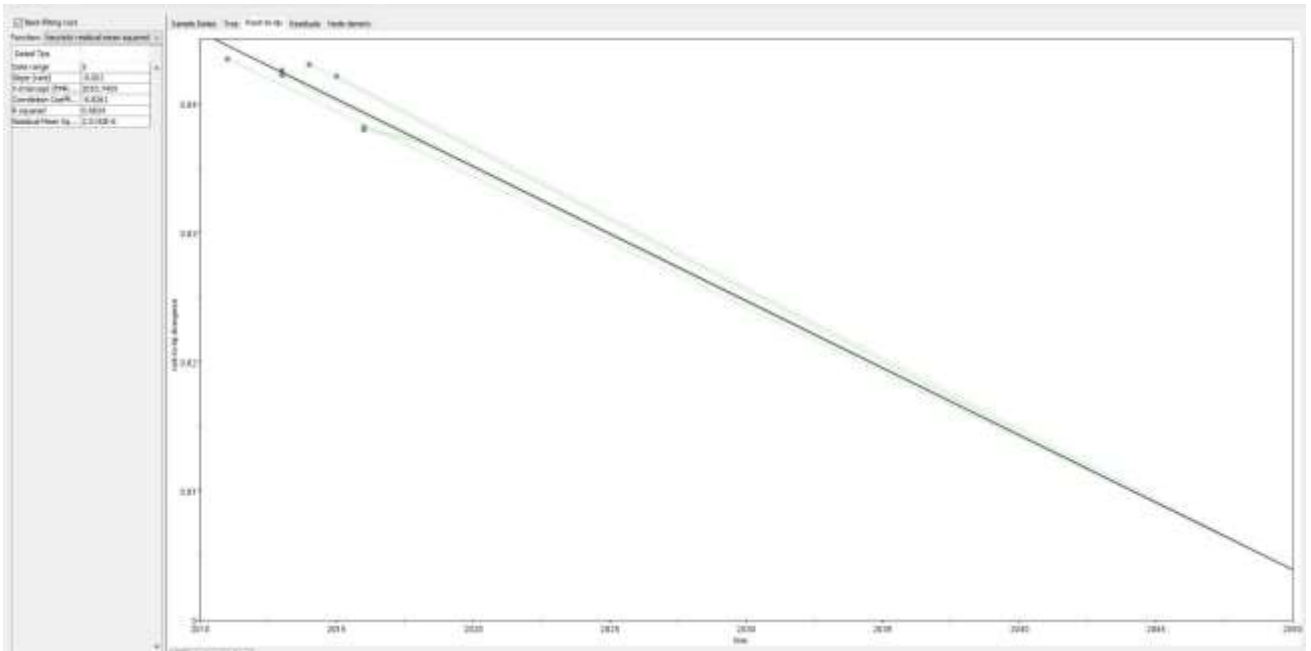


Figure 13: Linear regression of evolutionary distance and time of *Grapevine vein clearing virus* based on the genome sequences. Statistics are in the table at the upper left-hand corner.

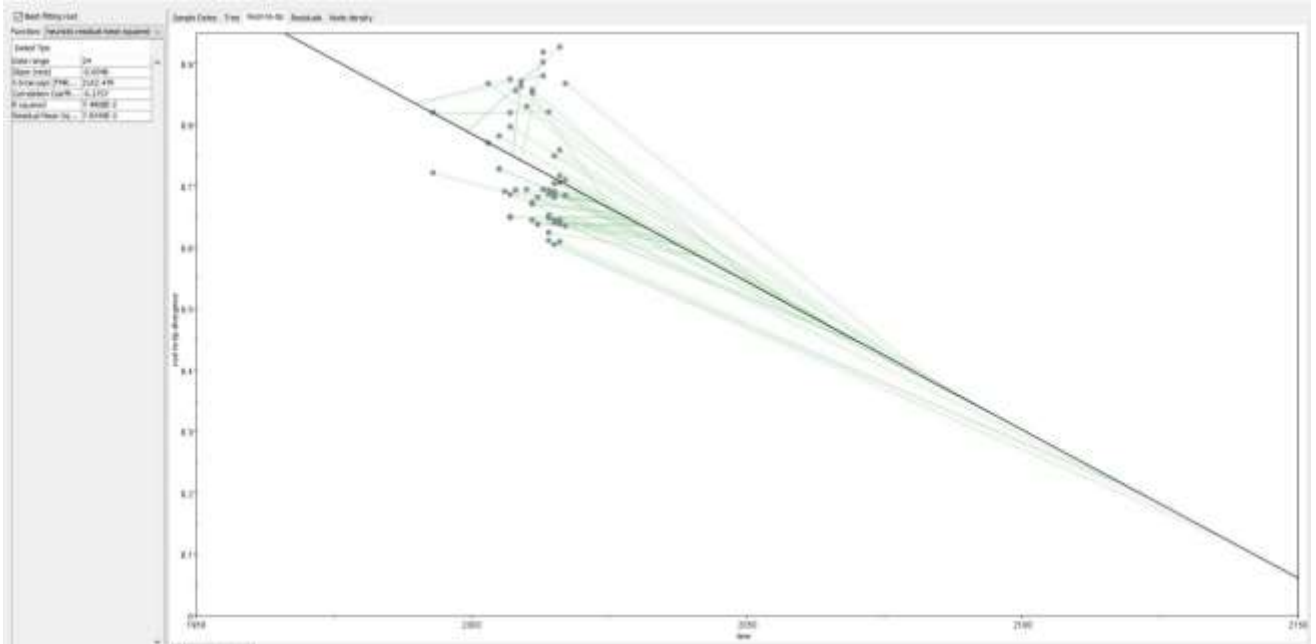


Figure 14: Linear regression of evolutionary distance and time of *Badnaviruses* based on the genome sequences. Statistics are in the table at the upper left-hand corner.

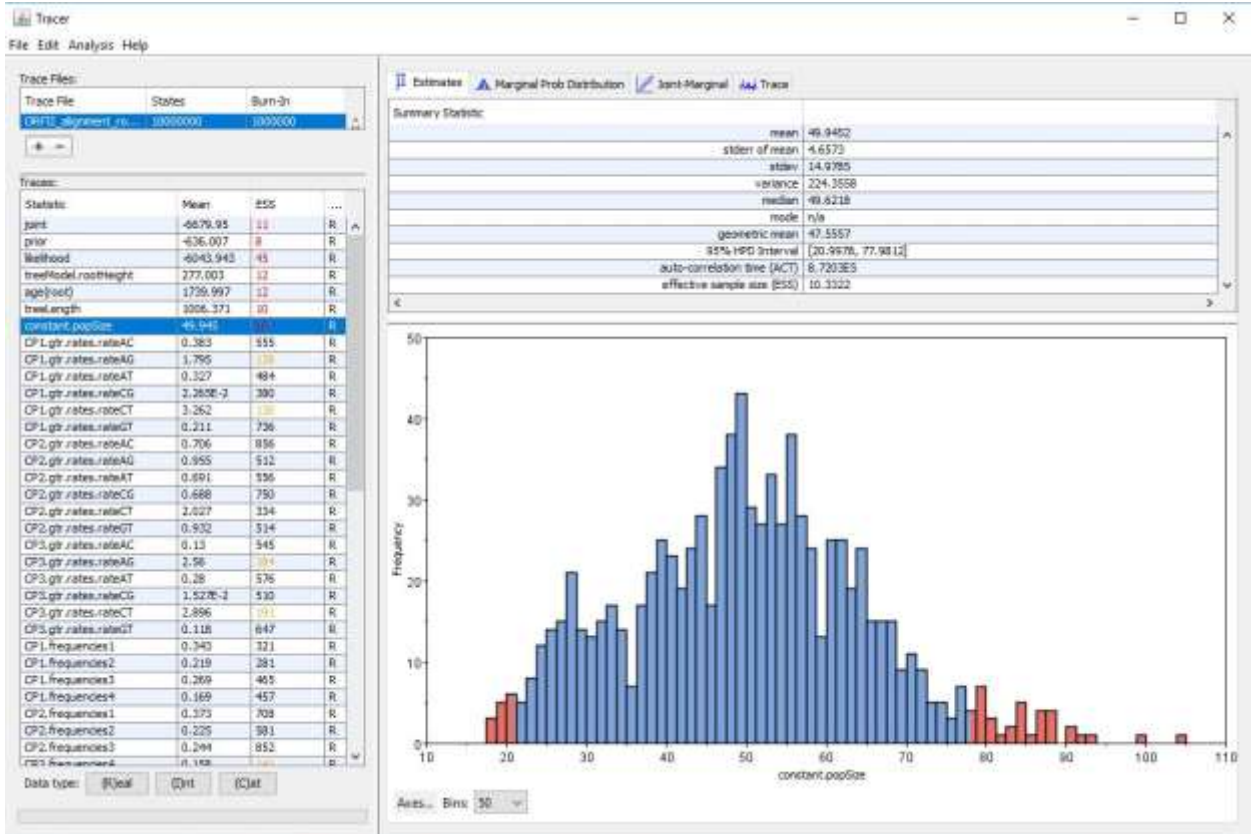


Figure 16: Screenshot from Tracer of ESS values and 95% HPD interval. Relative constant population size range and frequency distribution is graphed.

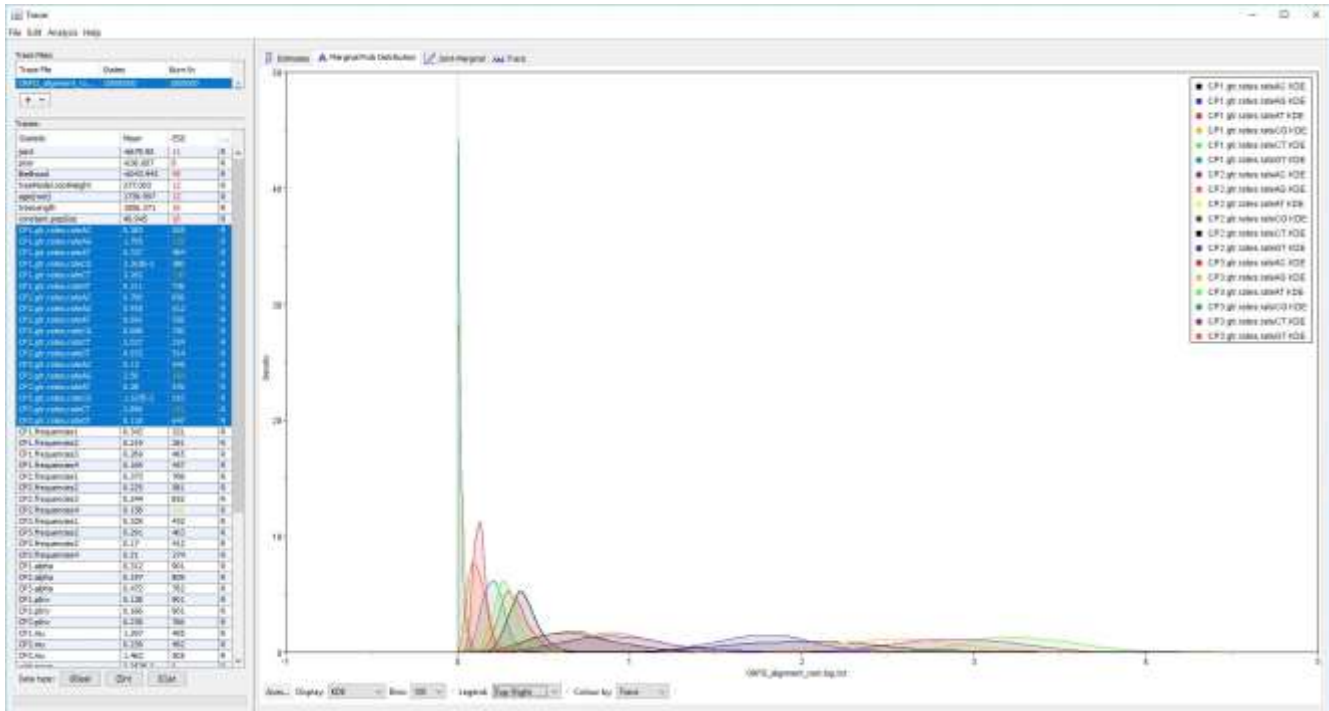


Figure 17: Screenshot from Tracer showing ESS values for the GTR gamma distribution for rates. Each codon position is highlighted. The gamma distribution of the substitution density and frequency of changes is graphed.

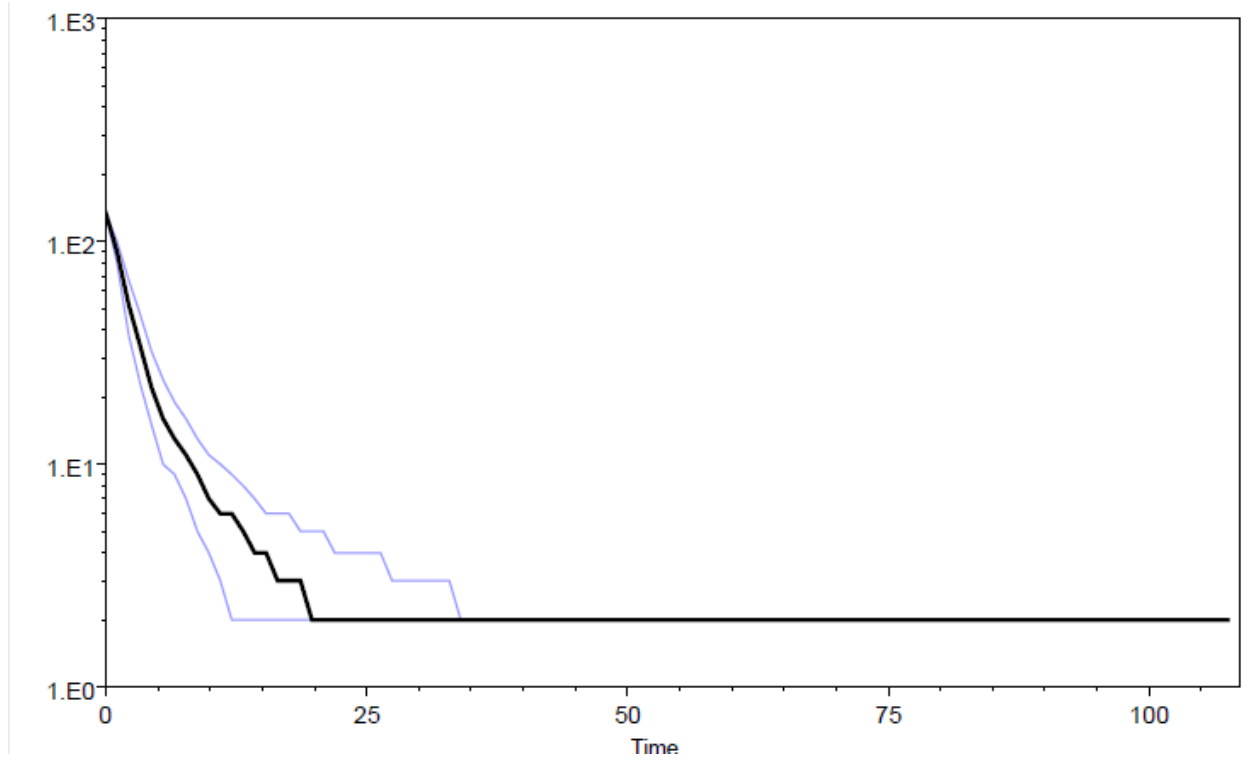


Figure 18: Divergence time and relative effective population size of *Grapevine vein clearing virus* estimated using ORF II sequence data.

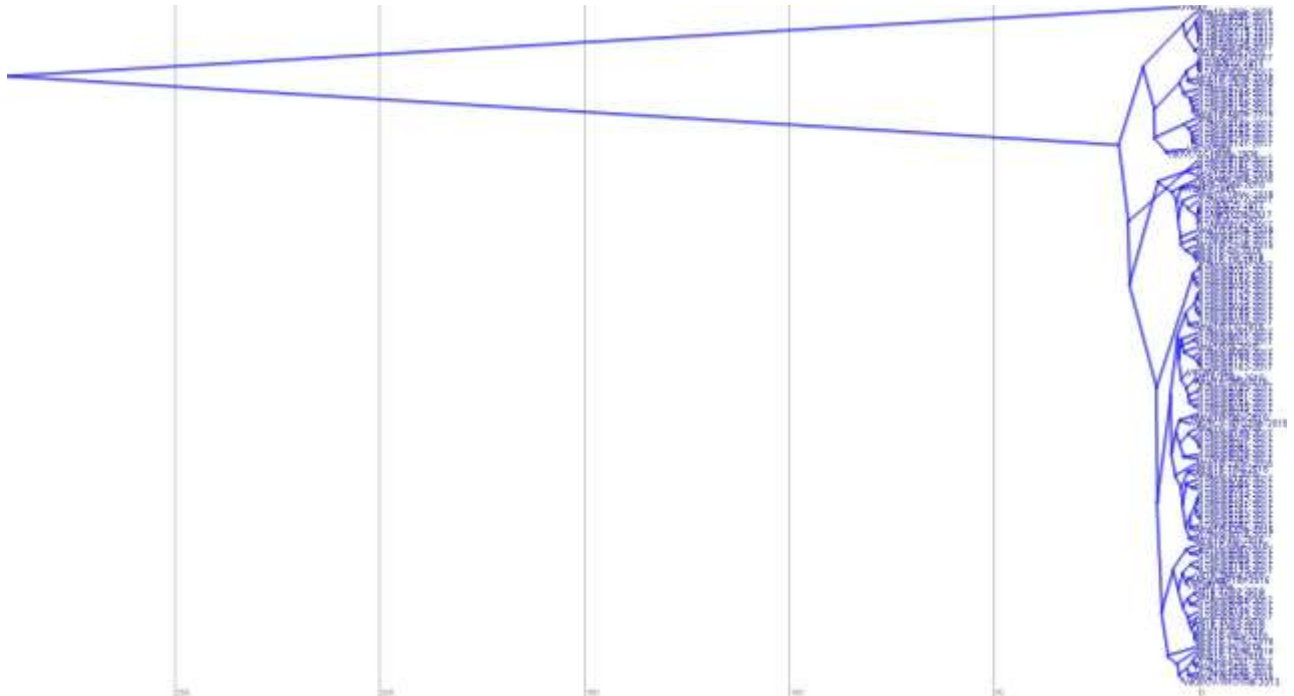


Figure 19: Maximum clade credibility tree of ORF II isolates evolution through time. *Gooseberry vein banding associated virus* is used as a root at the top. Times are in years before present.

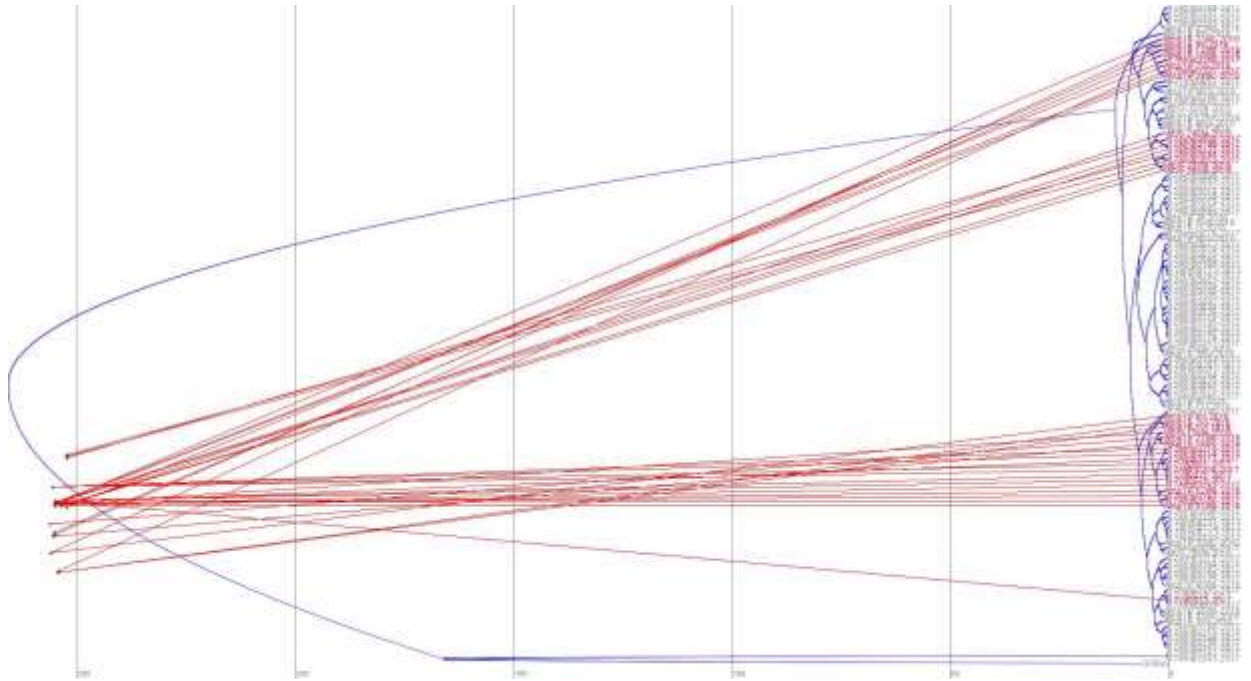


Figure 20: Maximum clade credibility tree of GVCV isolates based on ORF II sequences evolution through time. The red lines highlight ORF II sequences that contain the 9-bp indel and are traced back to relative geographic points.

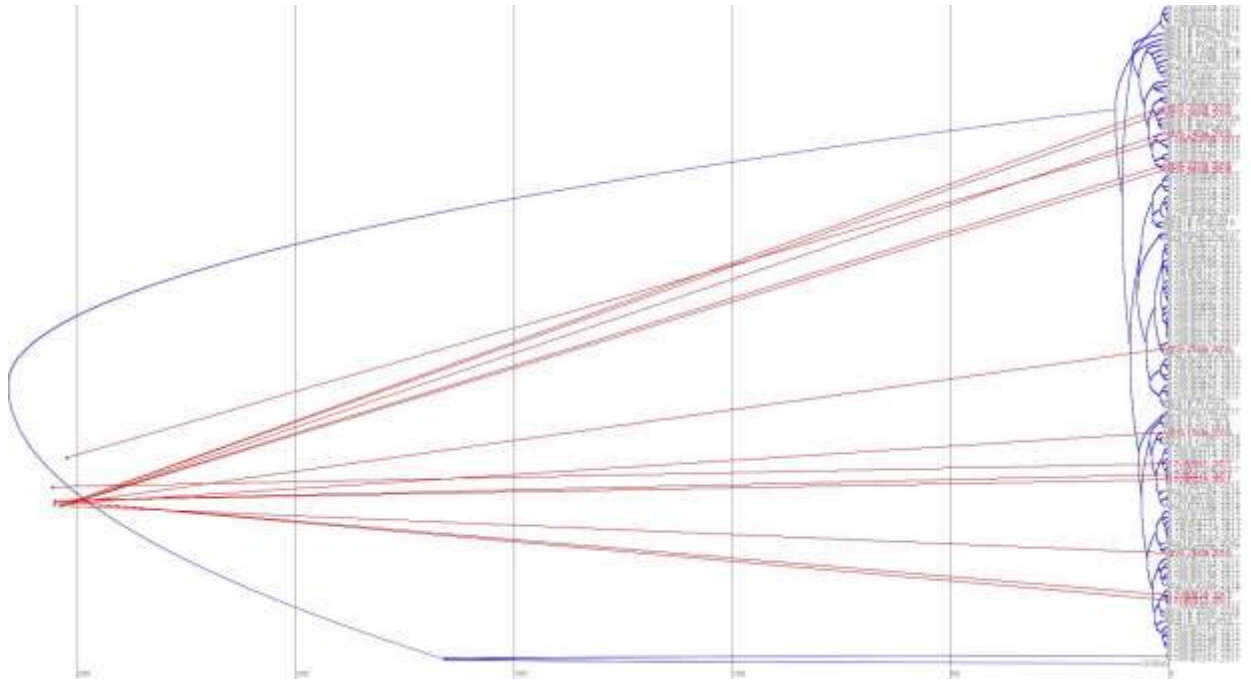


Figure 21: Maximum clade credibility tree of ORF II isolates evolution through time. The red lines highlight ORF II sequences that were isolated from *Vitis* spp. and are traced back to relative geographic points with the top point being the most northerly.

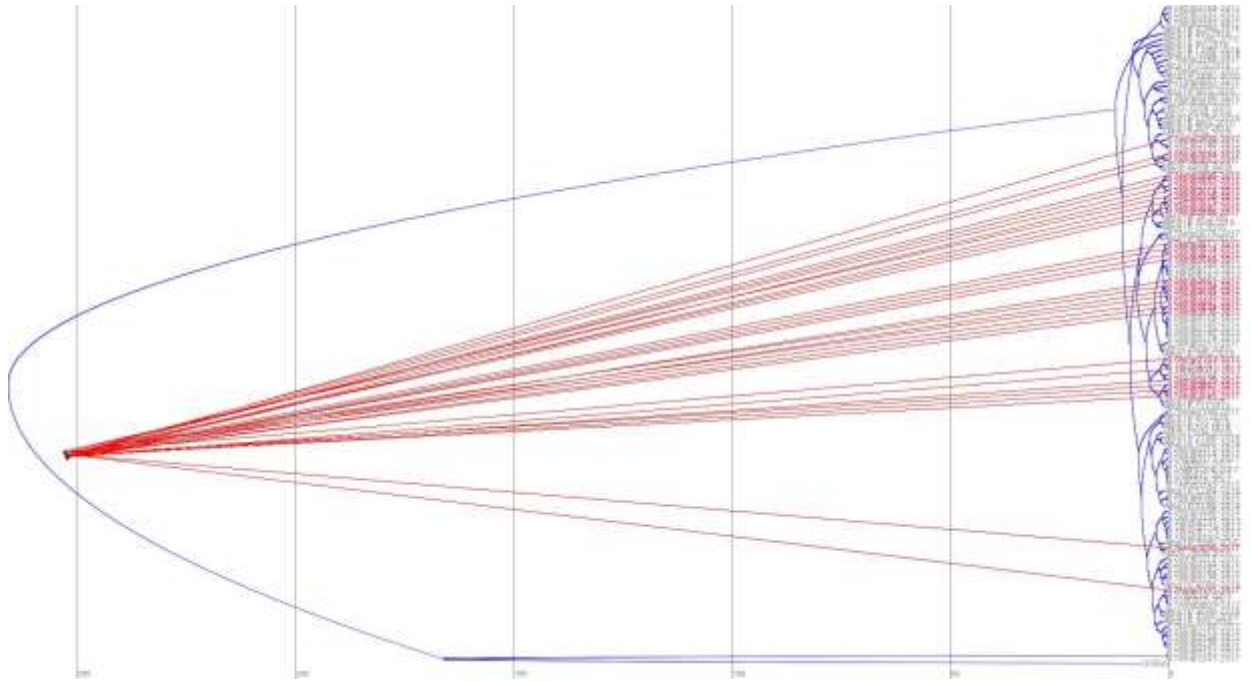


Figure 22: Maximum clade credibility tree of GVCV isolates based on ORF II sequences through time. The red lines highlight GVCV isolates from samples collected from the Herman and Augusta wine producing regions and are traced back to relative geographic points.

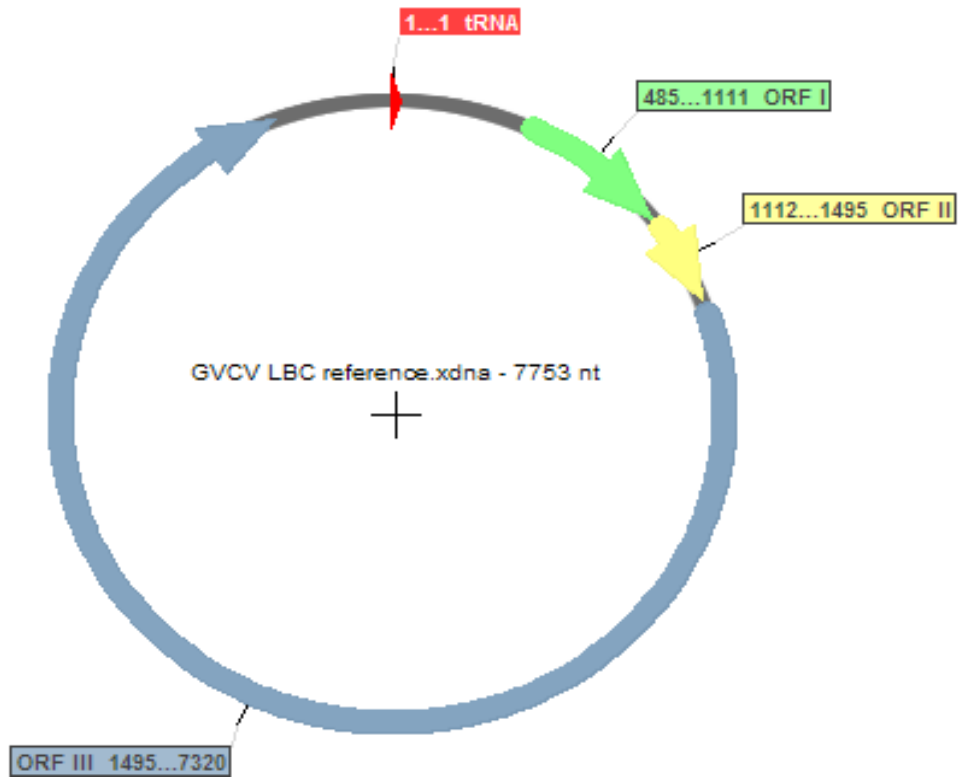


Figure 23: Genome arrangement of GVCV-CHA reference. The tRNA binding site, and three open reading frames (ORF) are highlighted and nucleotide positions are listed.

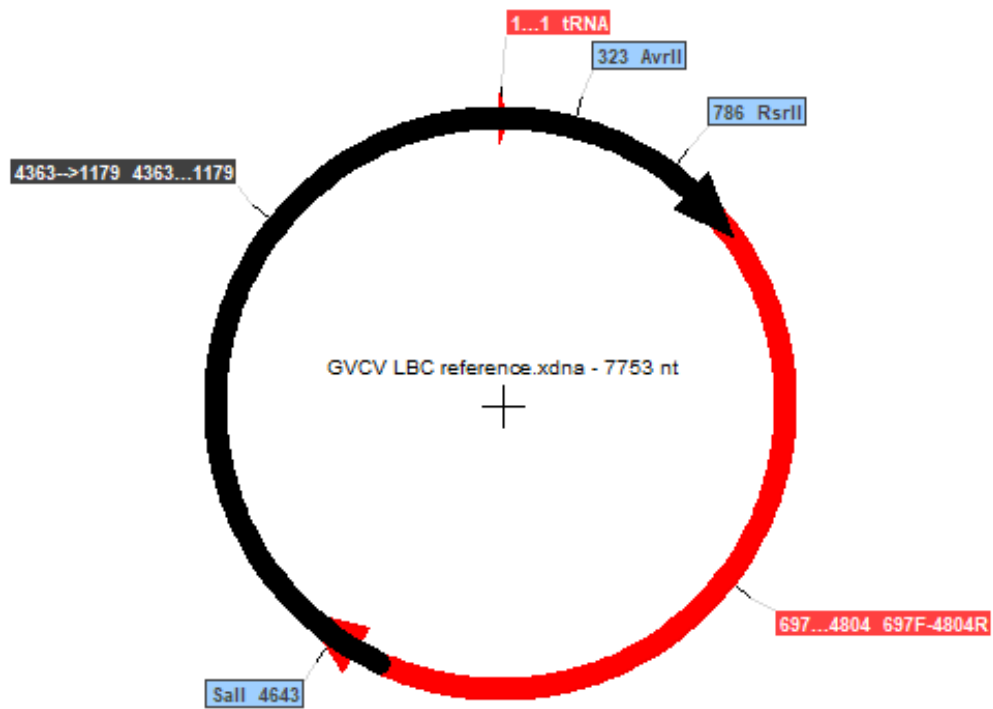


Figure 24: GVCV genome with overlapping PCR fragments. Overlapping fragments are highlighted and GVCV unique restriction sites are shown.

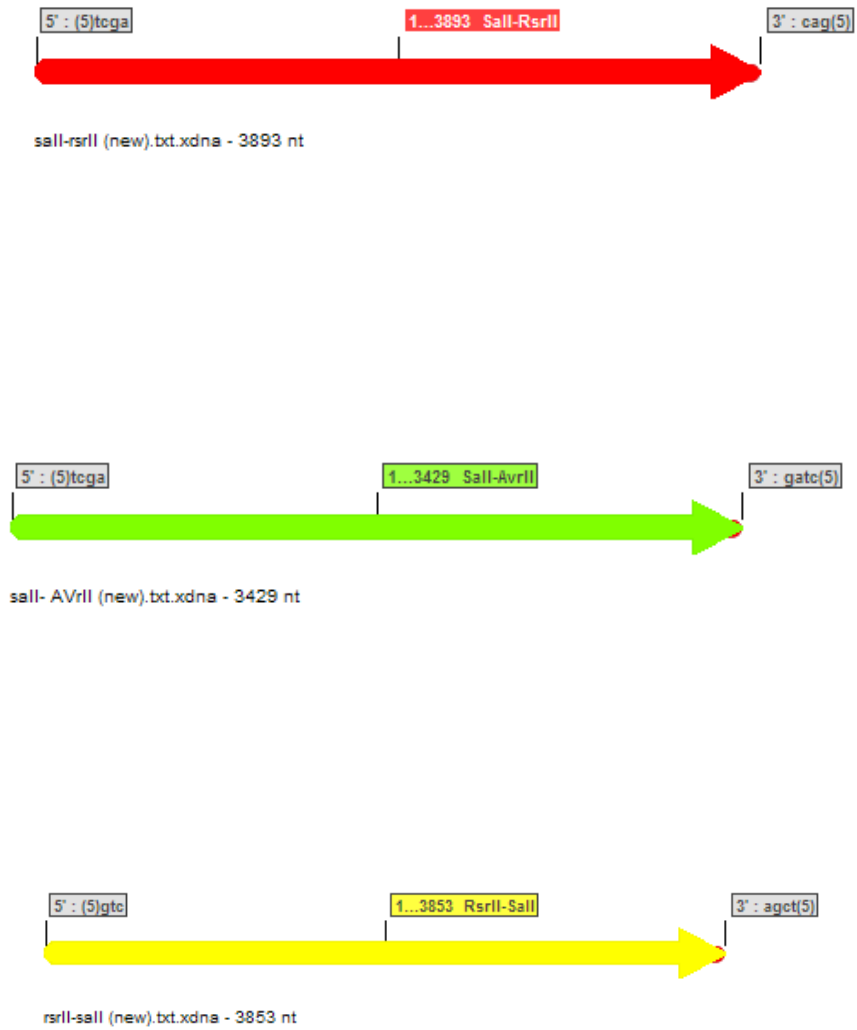


Figure 25: Restriction enzyme digested fragments from PCR products.



Figure 26: Fragments from Figure 3 ligated in correct orientation

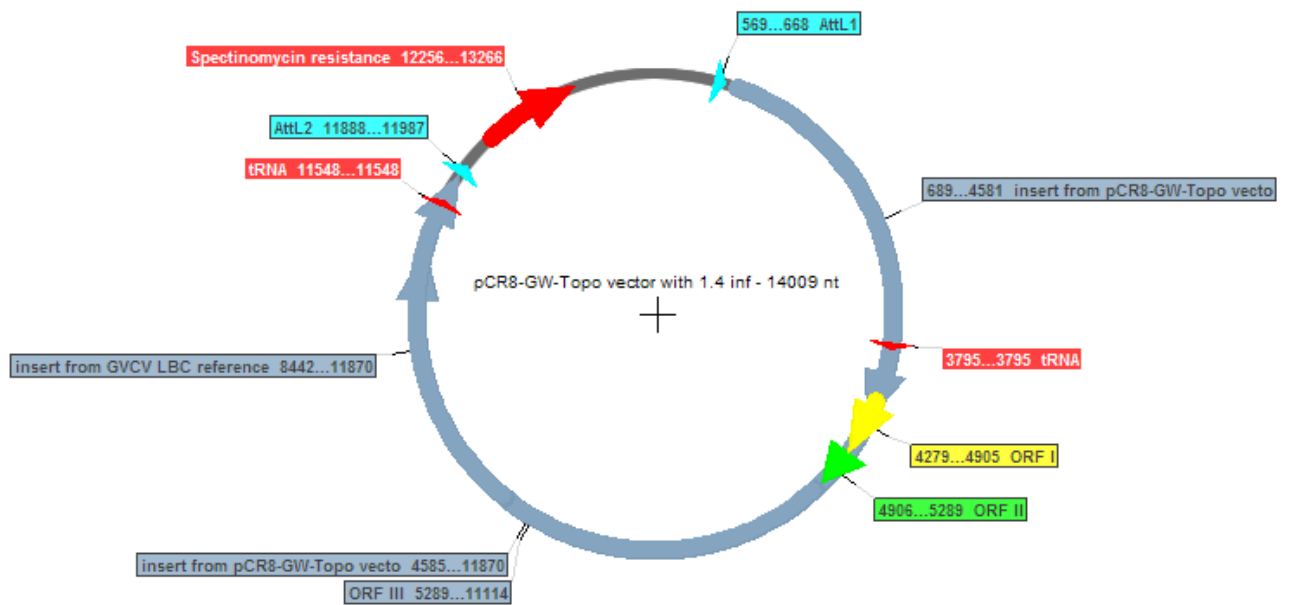


Figure 27: pCR8/GVCV. The 1.4 length GVCV genome is highlighted in blue. The pCR8/GW/TOPO backbone is shown in grey. Features of interest are highlighted and genome positions are delineated.

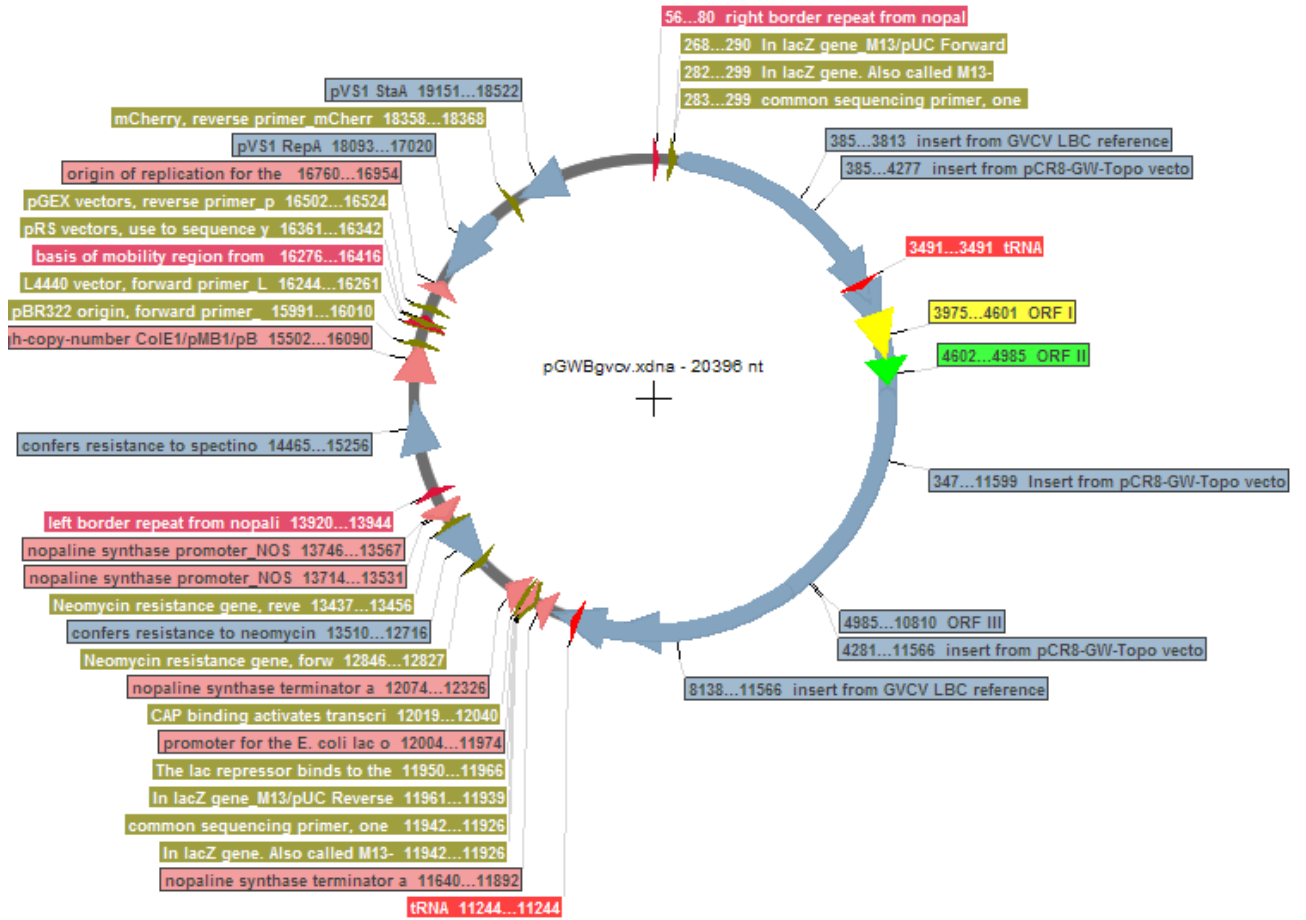


Figure 28: pGWB/GVCV. The 1.4 length GVCV genome is highlighted in blue. The pGWB 401 backbone is shown in grey. Features of interest are highlighted and genome positions are delineated.

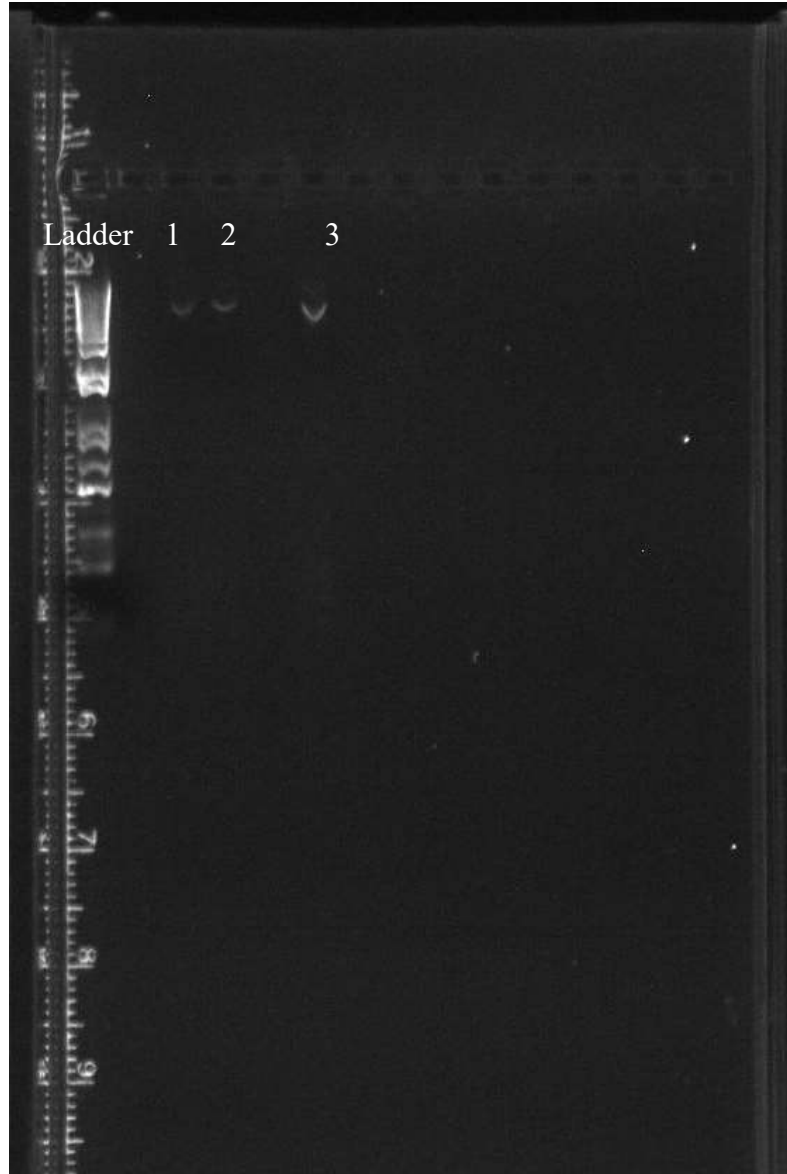


Figure 29: Ligation of fragments “RsrII-Sall” and “Sall-AvrII” to make fragment “RsrII-AvrII” consisting of 7,286 bps. All lanes contain the ligated fragment.

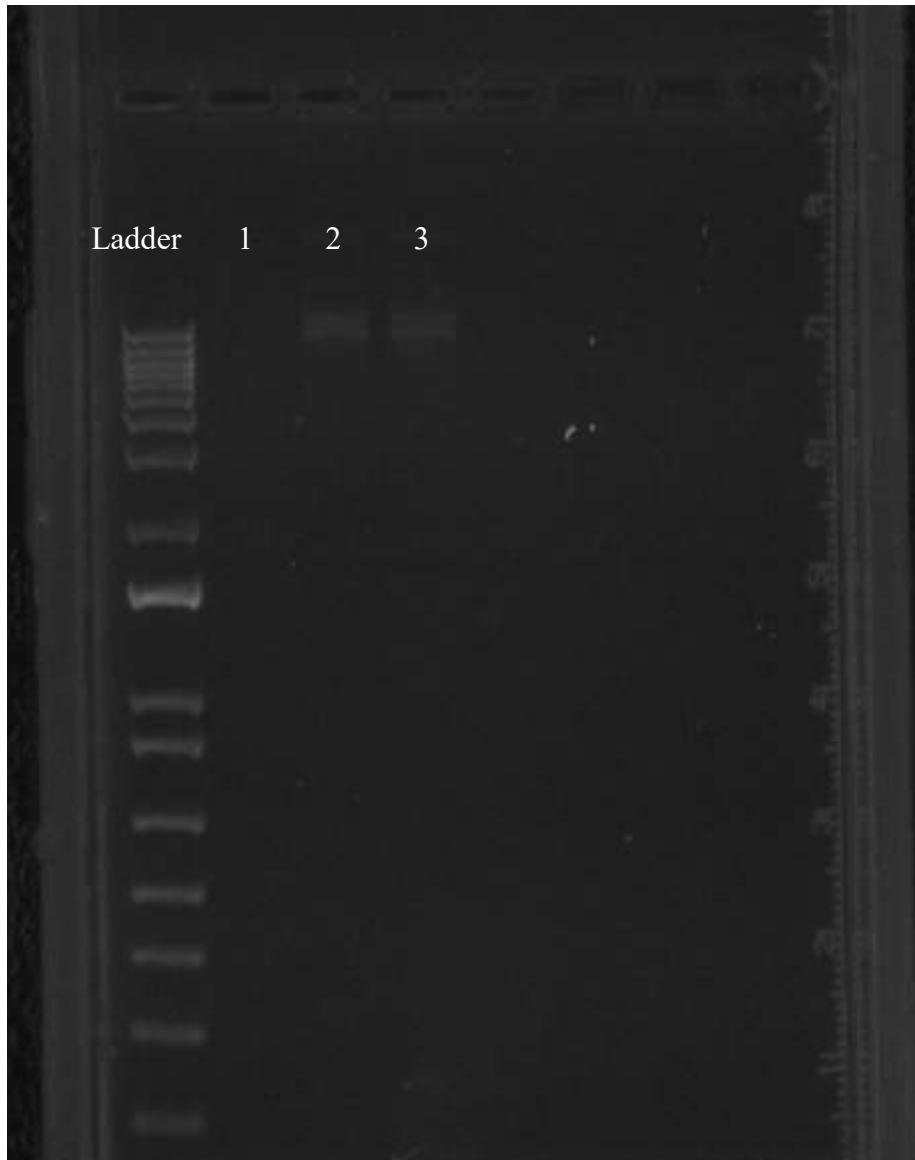


Figure 30: Ligation of “1.4 genome” into pGWB 401 to make pGWB/GVCV. Lanes 2 and 3 have an expected band size at 20,396 bps. The top bar on the ladder corresponds to 20,000 bps.

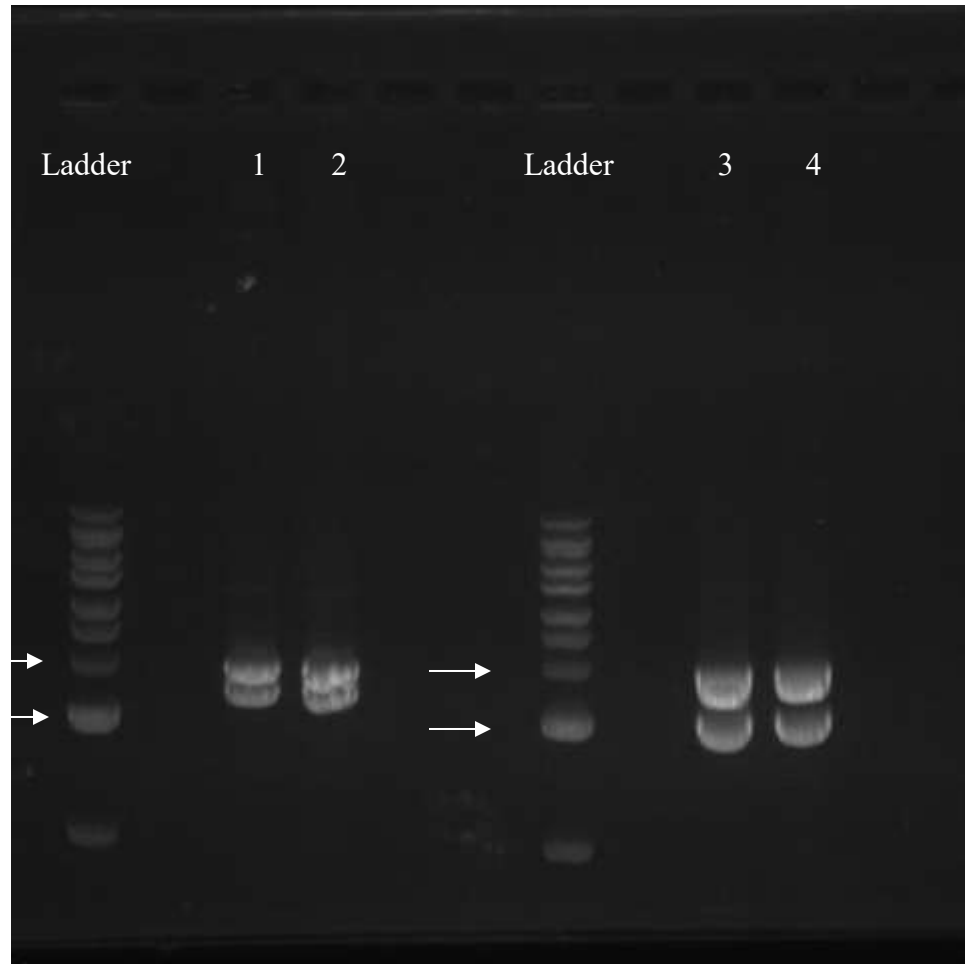


Figure 31: Restriction digest of pCR8/1179 and pCR8/4804. Gel ran for two hours. Lanes 1 and 2 have pCR8/1179 digested with Sal I and Avr II to produce two fragments at sizes 3,429 bps and 3,903 bps. Lanes 3 and 4 have pCR8/4804 digested with Rsr II and Sal I to produce two fragments at sizes 3,853 bps and 3,072 bps. The top arrow on the ladder corresponds to 4,000 bps and the bottom corresponds to 3,000 bps.

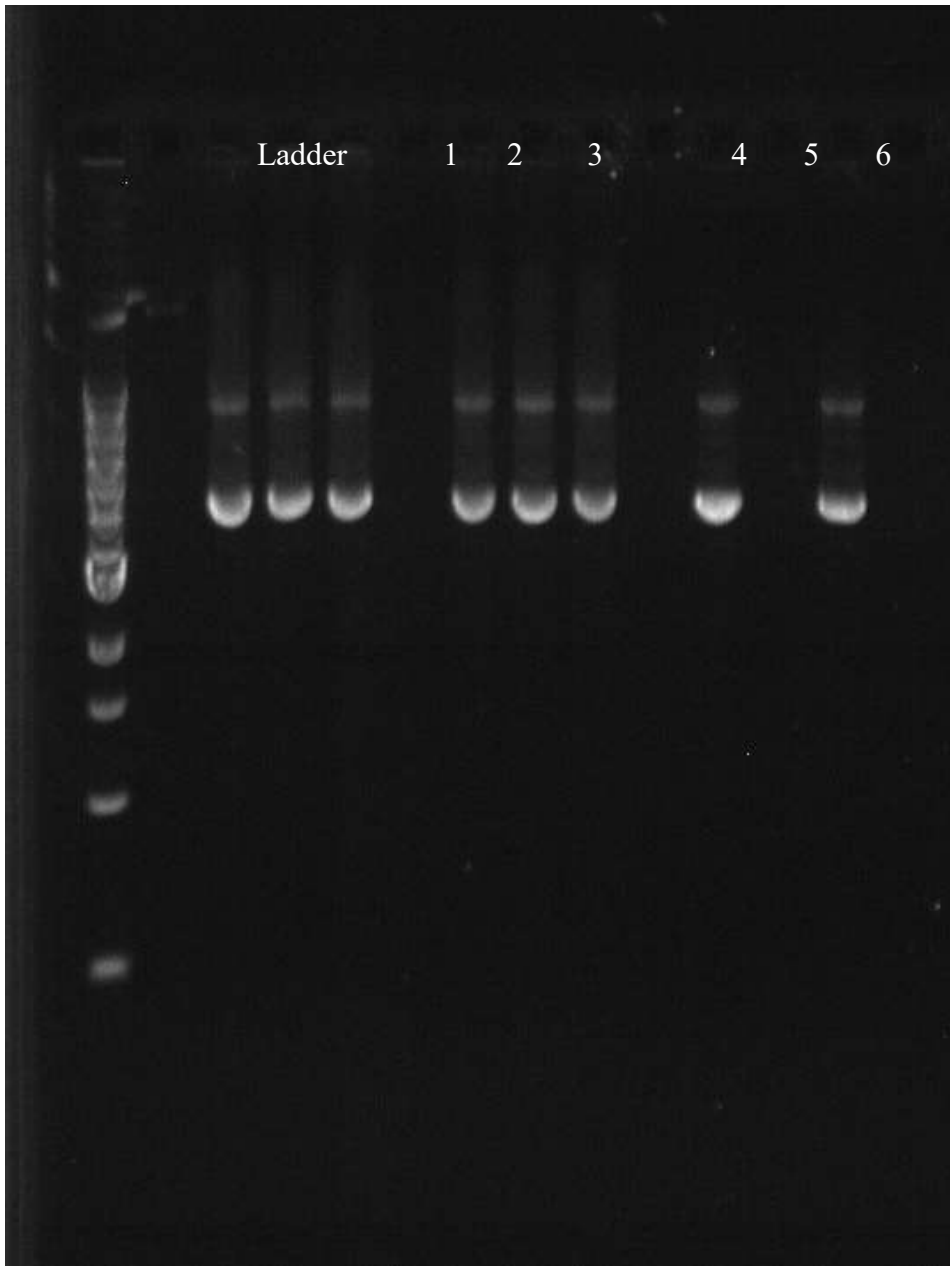


Figure 32: Gel image of multiple pCR8/GVCV plasmids to check for contamination. No restriction enzyme was used, so only one band should be present, the upper band, corresponding to 14,009 bps. The lower band is at position 5,000 bps, and is an unknown contaminant.

Appendix

Appendix A

17Vitis0009	37.15	-93.05
17Vitis0021	37.15	-93.05
17Vitis0022	37.15	-93.05
17Vitis0025	37.15	-93.05
17Vitis0027	37.15	-93.05
17Vitis0030	37.15	-93.05
17Vitis0045	37.15	-93.05
17Vitis0047	37.15	-93.05
17Vitis0051	37.6093	-93.4191
17Vitis0052	37.6092	-93.4189
17Amp0003	37.1948	-93.6479
17Amp0009	38.5429	-90.9954
17Amp0014	38.5408	-90.9854
17Amp0019	38.5445	-90.9752
17Amp0022	38.5618	-91.0173
17Amp0024	38.5643	-91.0257
17Amp0025	38.564	-91.0256
17Amp0029	38.5637	-91.0264
17Amp0030	38.5631	-91.0279
17Amp0032	38.5623	-91.0277
17Amp0034	38.562	-91.0278
17Amp0035	38.5619	-91.0279
17Amp0040	38.6044	-91.0011
17Amp0042	38.6053	-91.0026
17Amp0045	38.6061	-91.0038
17Amp0049	38.5938	-90.9838
17Amp0051	38.5864	-90.968
17Amp0052	38.5829	-90.9644
17Amp0067	38.594	-90.8873
17Amp0070	38.5865	-90.8947
17Amp0077	38.6163	-91.0406
17Amp0078	38.6164	-91.0409
17Amp0083	38.6312	-91.0646
17Amp0084	38.631	-91.0643
17Amp0086	38.6299	-91.0635
17Amp0087	38.6348	-91.0494
17Amp0088	38.6273	-91.0516
17Amp0091	38.6272	-91.0515
17Amp0096	38.6293	-91.1074
17Amp0097	38.6444	-91.1833
17Amp0098	38.6443	-91.1836
17Amp0101	38.6444	-91.1851
17Amp0102	38.6967	-91.44
17Amp0103	38.6969	-91.4397
17Amp0104	38.7018	-91.4378
17Amp0105	38.7018	-91.4379
17Amp0108	38.7492	-91.4512
17Amp0119	37.0667	-93.0167
17Amp0125	37.0667	-93.0167
17Amp0133	37.0667	-93.0167
17Amp0140	37.0833	-93.0333

17Amp0141	37.0833	-93.0333
17Amp0142	37.0667	-93.05
17Amp0144	37.0833	-93.0333
17Amp0146	37.0672	-93.05
17Amp0148	37.0667	-93.0333
17Amp0156	37.0833	-93.0333
17Amp0154	37.0833	-93.0333
17Amp0156	37.0833	-93.0333
17Amp0158	37.15	-93.05
17Amp0159	37.15	-93.05
17Amp0160	37.15	-93.05
17Amp0162	37.15	-93.05
17Amp0164	37.1	-93.05
17Amp0166	37.1	-93.05
17Amp0167	37.1	-93.05
17Amp0172	37.1	-93.05
17Amp0174	37.1	-93.05
17Amp0175	37.1	-93.0667
17Amp0177	37.1	-93.05
17Amp0180	37.1	-93.05
17Amp0182	37.1	-93.05
17Amp0184	37.1	-93.05
17Amp0190	37.0833	-93.05
17Amp0192	37.0833	-93.05
17Amp0194	37.0833	-93.05
17Amp0195	37.0833	-93.05
17Amp0201	37.0833	-93.05
17Amp0202	37.0833	-93.05
17Amp0203	37.0833	-93.05
17Amp0207	37.6094	-93.4191
17Amp0208	37.6093	-93.4191
17Amp0209	37.6092	-93.4191
17Amp0210	37.6091	-93.4192
17Amp0213	37.6082	-93.419
17Amp0214	37.608	-93.419
17Amp0215	37.6071	-93.4187
17Amp0218	37.605	-93.4185
17Amp0221	37.6051	-93.4184
17Amp0241	39	94.0167
17Amp0242	39	94.0167
17Amp0246	36.9505	-90.9922
17Amp0251	36.9959	-91.013
17Amp0254	36.0167	-93.05
17Amp0256	38.6312	-91.0646
17Amp0257	38.6312	-91.0646
Vit16-15III	37.0356	-93.1516
Vit16-24III	37.1014	-90.0192
Vit16-25III	37.0836	-90
Vit16-26III	37.1019	-90.0019
Vit16-29III	37.0017	-92.0833
Vit16-30III	37.0017	-92
Vit16-31III	37.0017	-92.0833
Vit16-32III	37.0017	-92.0833
Amp16-7I	38.0022	-91.0333
Amp16-9I	38.0017	-91.1333
Amp16-11I	38.0172	-91.1017

Amp16-3IIIa	37.0836	-90
Amp16-5IIIa	37.0836	-90.0019
Amp16-6IIIa	37.1019	-90.0019
Amp16-7IIIa	37.1019	-90.0019
Amp16-8IIIa	37.1019	-90.0019
Amp16-13IIIb	36.0692	-93.0524
Amp16-17IIIb	36.1357	-93.1336
Amp16-18IIIb	36.1357	-93.1336
Amp16-21IIIb	36.4231	-93.8422
Amp16-23IIIc	37.0354	-93.1513
Amp16-24IIIc	37.0384	-93.1516
Amp16-25IIIc	37.0355	-93.1515
Amp16-33IIIc	37.0345	-93.0023
Amp16-36IIIe	37	-93.15
Amp16-42IIIe	37.0014	-93.15
Amp16-45IIIe	37.0019	-93.0344
Amp16-51IIIe	37.0006	-93.0839
Amp16-52IIIe	37.0356	-93.1516
AMP2IIIe	37.0008	-93.1503
AMP1III f	38.0432	-92.7142
Amp16-17IVc	36.0204	-93.3567
Amp16-18IVc	36.0204	-93.3567
Amp16-8V	35.4712	-93.8109
Amp16-9V	35.4703	-93.8103
Amp16-1VI	34.8516	-92.4832
Amp16-2VI	34.8513	-92.4835
Amp16-3VI	34.8512	-92.4836
Amp16-4VI	34.9041	-92.4481
Amp16-7VI	34.9053	-92.4477
Amp16-1VII	35.1019	-98.0183
Amp16-3VII	35.1019	-98.0183

Appendix B

Codon	dS	dN	dN-dS	P-value
1	0	0	0	N/A
2	1	4.001384818	3.001384818	0.142959599
3	1	0	-1	1
4	0	0	0	N/A
5	0	0	0	N/A
6	5.348465017	0	-5.348465017	1
7	4	0	-4	1
8	2	0	-2	1
9	3	0	-3	1
10	1	0.5	-0.5	0.888888889
11	10.33560478	0	-10.33560478	1
12	1.337070414	0	-1.337070414	1
13	10.52619562	0	-10.52619562	1
14	15.45176937	1.70357158	-13.74819779	0.999994144
15	4.750799062	2.854810645	-1.895988417	0.872656224
16	3	0	-3	1
17	3.885740644	0	-3.885740644	1
18	10.632716	3.566783559	-7.065932438	0.990899824
19	17	0	-17	1
20	5	0	-5	1
21	1.048671897	1.978949592	0.930277695	0.486392159
22	8	0	-8	1
23	7	0	-7	1
24	10	0	-10	1
25	24.02168734	0	-24.02168734	1
26	0	0	0	N/A
27	7.972544882	0	-7.972544882	1
28	5.690498738	0	-5.690498738	1
29	11	0.500215677	-10.49978432	0.999998112
30	1	0	-1	1
31	16	0	-16	1
32	19.54454151	0	-19.54454151	1
33	22	0	-22	1
34	5.477592218	0	-5.477592218	1
35	10	0	-10	1
36	0	0	0	N/A
37	5.436934154	0	-5.436934154	1
38	12.58332593	0	-12.58332593	1
39	19.18857439	0	-19.18857439	1
40	1	0	-1	1
41	26.83346937	0	-26.83346937	1
42	5.637952591	3.388986506	-2.248966086	0.881539136
43	5.148672983	0	-5.148672983	1
44	0	0	0	N/A
45	5	0	-5	1
46	10.18901587	0	-10.18901587	1
47	12.35013488	0	-12.35013488	1
48	8.852121258	0	-8.852121258	1
49	12.68454686	0	-12.68454686	1
50	5.34139973	0	-5.34139973	1

51	10.25704497	0	-10.25704497	1
52	1.28921662	0	-1.28921662	1
53	16	0	-16	1
54	5.783427403	0	-5.783427403	1
55	4.015387781	0	-4.015387781	1
56	9.06450081	0	-9.06450081	1
57	7.024176796	0	-7.024176796	1
58	8.200218651	0	-8.200218651	1
59	5.080021403	0.496092729	-4.583928673	0.998752906
60	2.548371665	4.233757008	1.685385343	0.396101734
61	0	2.5	2.5	0.131687243
62	0	1.038503643	1.038503643	0.433588707
63	0	4.533723679	4.533723679	0.046156937
64	0	0.500053562	0.500053562	0.698743294
65	0	1	1	0.444444444
66	0	7.070505927	7.070505927	0.003268459
67	0	0.999532627	0.999532627	0.444860179
68	1.960925031	5.103525034	3.142600003	0.164533324
69	0	5.79976085	5.79976085	0.011582408
70	0	7.400456182	7.400456182	0.005661323
71	0	0	0	N/A
72	0	0	0	N/A
73	0	1.998025677	1.998025677	0.198312772
74	1.004884804	1.995150727	0.990265923	0.464109918
75	0	3.999550372	3.999550372	0.039438971
76	1.185074634	1.731123111	0.546048477	0.535788729
77	8.014866335	5.494903903	-2.519962432	0.855199913
78	0	1.892883087	1.892883087	0.297297905
79	0	9.689675583	9.689675583	0.000335811
80	0	9.27349736	9.27349736	0.001146213
81	1.119524055	9.600655299	8.481131244	0.005570597
82	1.181475219	14.43103572	13.2495605	1.34844E-05
83	0	2.130001694	2.130001694	0.179152257
84	0	4	4	0.039018442
85	1.125078402	0.473670312	-0.651408089	0.91222074
86	0	1.794757095	1.794757095	0.137976818
87	0	7.767242901	7.767242901	0.047080068
88	0	0	0	N/A
89	0	3.315004304	3.315004304	0.085595084
90	0	5.221639798	5.221639798	0.034389266
91	0	1.99857173	1.99857173	0.198738599
92	0	3.552828148	3.552828148	0.053123924
93	0	6.994244109	6.994244109	0.003465165
94	12.49380507	1.887180873	-10.60662419	0.999927827
95	0	0.509590012	0.509590012	0.654291191
96	1.084022115	0.515441379	-0.568580737	0.896149188
97	0	8.718463919	8.718463919	0.000905455
98	0	2.697845482	2.697845482	0.165988325
99	0	12.13710937	12.13710937	9.94129E-06
100	0	6.556923415	6.556923415	0.010564957
101	0	3.423506631	3.423506631	0.068391576
102	0.606275831	2.584429094	1.978153263	0.314276423
103	0	8.738959838	8.738959838	0.001142327
104	0	2.0609688	2.0609688	0.209539858
105	7	5	-2	0.828143294
106	0	0	0	N/A

107	2.005047005	1.556023335	-0.44902367	0.778690165
108	0	3.694745582	3.694745582	0.108107945
109	0	0.515634194	0.515634194	0.677547526
110	0	0.5	0.5	0.666666667
111	0	1	1	0.444444444
112	0	0	0	N/A
113	1.001167236	7.500915403	6.499748167	0.01376568
114	0	0.499696352	0.499696352	0.667071777
115	0	0	0	N/A
116	0	0	0	N/A